Neuron-Microdevice Connections

Thesis by

Wade G. Regehr

In Partial Fullfillment of the Requirements

for the Degree of

Doctor of Philosophy

California Institute of Technology,

Pasadena, California

1988

(Submitted March 25, 1988.)

TO MY PARENTS AND GRANDPARENTS

Acknowledgements

I am grateful to have had the opportunity to work on a very interesting project, and in the course of my research to have worked with many excellent people. I am fortunate to have had Jerry Pine and Dave Rutledge for advisors. They provided the environment necessary for the success of such an interdisciplinary project. In addition to providing scientific guidance, they were understanding and encouraging. This was never more apparent than their realization that a trip around the world would be an excellent opportunity for me. I would like to thank the members of Dave and Jerry's groups, both past and present. Not only did they teach me a great deal, we had some good times along the way. In particular I would like to thank Dean Neikirk who taught me integrated circuit fabrication. Lastly, I would like to thank my family and friends for their support. Michelle...thankyou.

Abstract

A new method for long-term recording and stimulation applicable to cultured neurons has been developed. Silicon-based microelectrodes have been fabricated using integrated-circuit technology and micromachining. The chronic connection is made by positioning the electrode tip into contact with the cell body, and gluing the device to the bottom of the culture dish. These "diving-board electrodes" consist of an insulated lead exposed only at the tip sealed to the cell body of a cultured neuron. A two-way electrical connection to *Helisoma* B19 neurons has been established for up to four days. Preliminary experiments with cultured superior cervical ganglion neurons indicate diving-board electrodes can be used with cultured neurons larger than 20 μm in diameter.

In a related technique *Helisoma* neurons grown on special dish containing a multielectrode array were found to seal to the dish electrodes, establishing similar long-term connections. This capability will make it possible to conduct experiments with either diving-board electrodes or dishes that cannot be performed using conventional techniques.

Table of Contents

Chapter 1

Introduction

A primary goal of neurobiology is to learn how the nervous system works by determining how neurons communicate with each other, how they are put together to form a functioning nervous system, and the means by which a system of neurons learns based on experience. Many different approaches are required to begin to understand the nervous system. While it is possible to study neurons in intact animals, such systems are complex and experiments can be difficult to interpret. Another approach is to simplify the nervous system and study single cells and then small networks of neurons. Technological advances will allow many interesting experiments to be performed on such systems.

Cell-culture techniques, in which neurons are grown in the artificial environment of a tissue culture dish, provide a powerful tool for answering fundamental neurobiological questions. A great variety of neuronal cell types can be grown in cell culture providing: (1) the neurons are removed from the animal at the appropriate time, (2) culture dishes are prepared to provide a place for the neurons to attach, and (3) the culture medium provides a correct balance of biologically necessary molecules [1]. In addition to the many types of embryonic neurons that have been cultured, recently it has been possible to culture adult identified neurons from various invertebrates, including the leech [2], *Helisoma* [3], and *Aplysia* [4]. While most of these large neurons have been characterized *in vivo*, the *in vitro* preparations make it possible to study neurite outgrowth and synapse formation under experimentally controlled conditions. Stimulating and recording from neurons is greatly simplified because the individual cells are visible and accessible, the biochemical environment is easily manipulated, and the nervous system can be greatly simplified. However there are a number of

interesting questions that remain unanswered because experiments are difficult or impossible to perform since a long-term, two-way electrical contact is not available.

There are several ways to make electrical contact to a cell. A method that provides an excellent signal-to-noise ratio is to insert a glass electrode with a submicron tip into a cell. Another way to make electrical contact is to whole-cell patch to the cell [5]. A glass pipette several microns in diameter is brought up against a cell and a seal of several gigohms is obtained by applying suction. It is possible to break down the membrane beneath the patch and get inside the cell. However, these techniques have several disadvantages: it is difficult to maintain such connections for more than a few hours, they are invasive methods usually damaging the cell, and it is not generally practical to use more than two electrodes simultaneously.

Another approach is to use extracellular electrodes to stimulate and record from cultured neurons. Cells have been grown on specially prepared dishes with a multielectrode array pattern [6]–[10]. Such methods are noninvasive, and have been used successfully to stimulate neurons [7]–[9], and to record action potentials from cultured neurons for periods of weeks [6]. However, this technique is not sensitive to subthreshold signals, it is often difficult to interpret recordings since it is possible to record from several cells simultaneously, and a current pulse passed through an electrode may stimulate more than one cell.

It is also possible to measure the intracellular voltage of cultured neurons using voltage-sensitive dyes. When these dyes are bound to a cell membrane they respond linearly to changes in the intracellular potential either by changing their fluorescence or their absorption [11],[12]. This change follows the potential change recorded by an intracellular electrode. By having an array of detectors it

is possible to record from many cells simultaneously. However, there are drawbacks in the use of such dyes: illumination breaks down the dye molecules into toxic byproducts limiting the total exposure time and the number of measurements; signals are small, and shot noise results in poor signal-to-noise ratios; an appropriate dye must be found for each preparation; a complicated array of detectors and amplifiers, and a data acquisition system is required; and some means of stimulating cells are required [13], [14]. While voltage-sensitive dyes are promising for long-term recording, limitations of this technique warrant searching for other solutions to the problem of long-term recording and stimulating.

It is also possible to stimulate and record by a loose-patch method [15] that does not break down the membrane (Figure 1.1a). Chapter 2 deals with experiments using glass pipettes and cultured *Helisoma* snail neurons and cultured rat superior cervical ganglion neurons (SCG's), demonstrating the feasibility of a loose-patch type connection for stimulating and recording. Two types of experiments were performed: one-electrode experiments with 10 μm–12 μm diameter patch pipettes; and two electrode experiments with an intracellular microelectrode used as well, to stimulate the neuron and compare the intracellular potential with the loose-patch electrode potential. However, it is difficult to maintain the connection for long periods and to communicate with more than two cells simultaneously due to the large manipulators needed to position the electrodes.

The diving-board electrode is a silicon microdevice used in a manner similar to a loose-patch electrode (Figure 1.1b), but without the need to be held in place by manipulators. Each electrode is positioned and is then glued to the bottom of the tissue culture dish. A seal is made between the lower surface of the electrode and the cell in the same way that a seal is made to the bottom of a glass pipette, although suction cannot be applied when using this device. This establishes

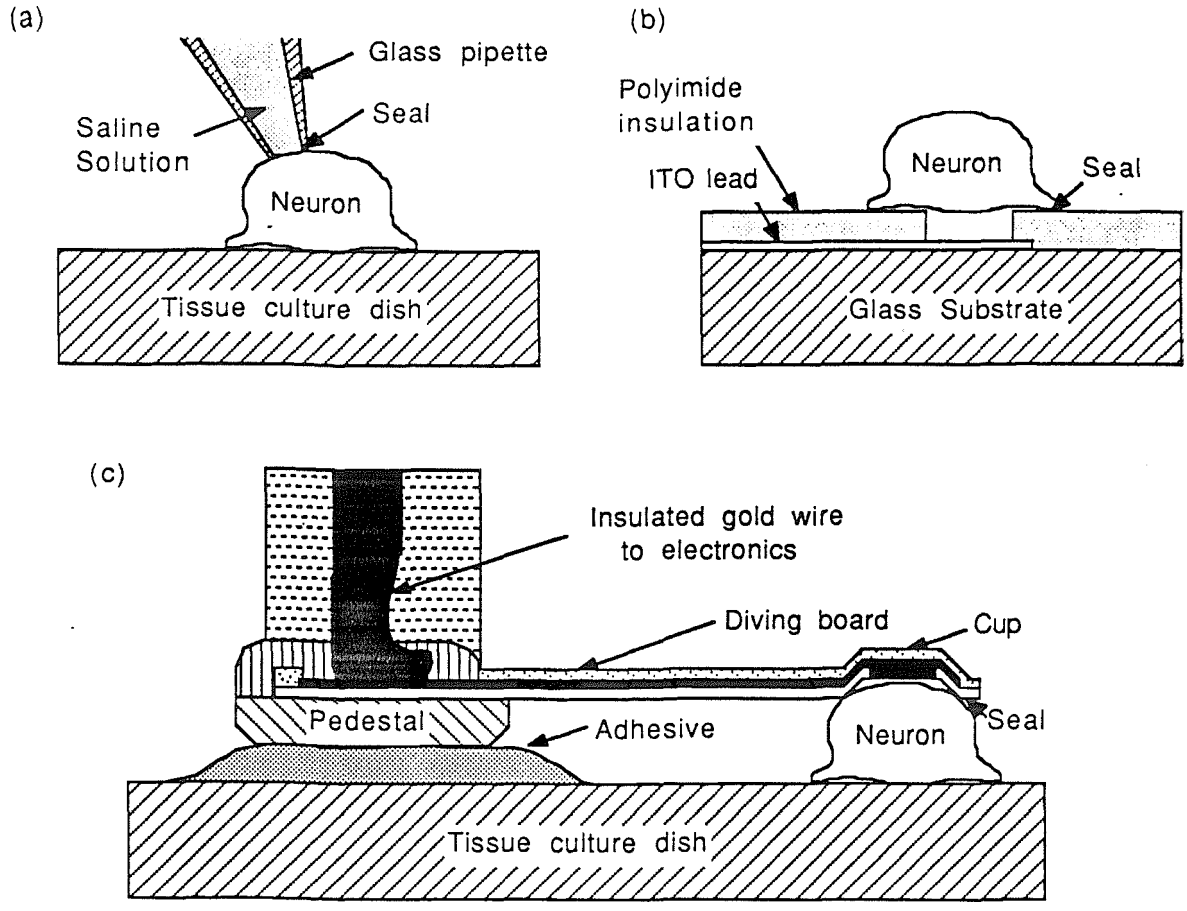

Figure 1.1. (a) Schematic view of a conventional glass micropipette patch electrode being used to record from a cell. (b) Neuron sealed to an electrode in the bottom of a dish. (c) Diving-board electrode in contact with a cell.

a one-to-one connection between a device and a cell for both stimulating and recording. An insulated gold wire extends vertically from the device out of the solution to connect to the electronics.

Integrated circuit-technology and micromachining of silicon provide powerful tools to fabricate such microelectrodes [16]. Chapter 3 begins with an introduction to silicon micromachining techniques, illustrating the capabilities and limitations of such techniques, and motivating the diving-board electrode

fabrication procedure. Also, insulating layers available for use in saline environments are reviewed to explain the choice of passivation layers used in the diving-board electrode. Next the electrode fabrication procedure is outlined, with a more detailed treatment given in Appendix A.

Glass loose-patch electrodes, diving-board electrodes, and sealed dish electrodes improve recording and stimulation capabilities by sealing to a neuron. Chapter 4 discusses the principles of operation of such devices by starting with an appropriate equivalent circuit, and then considering stimulating and recording.

Diving-board electrodes were tested on identified *Helisoma* neurons, and on SCG's. First, a procedure for manipulating the electrodes into place and gluing them down under water was developed. Then it was necessary to determine the biocompatibility of the glue, the gluing process, and the electrodes. Once the biocompatibility was established electrophysiological tests of the device were performed, including simultaneous recording with an intracellular electrode and long-term studies. These results are presented in Chapter 5.

Another approach to obtain a chronic two-way connection is to use multielectrode dishes in a manner similar to the loose-patch method by growing a neuron over an electrode to form a stable seal between the cell and the electrode [9]. Such a technique is practical only with large invertebrate neurons such as *Helisoma* neurons, but is not effective for smaller vertebrate neurons such as SCG's. Chapter 6 deals with the use of such multielectrode arrays, beginning with their fabrication and moving on to electrode tests using *Helisoma* neurons.

The results obtained with diving-board electrodes and neuron-capped electrode dishes as presented in this thesis are promising, but can be thought of as a first step. While the capability of chronic stimulation and long term recording

of action potentials has been demonstrated, the techniques must be improved if subthreshold signals are to be chronically recorded. Integrated circuit techniques and micromachining of silicon have yet to significantly impact the field of neurobiology. However, the potential exists for innovative solutions to difficult biological problems using such technologies. Chapter 7 is a discussion of ways in which the operation of multielectrode dishes and multielectrode arrays might be improved, and applications of such devices. Other devices with biological applications that could be fabricated using such techniques are discussed.

References

[1] P. G. Nelson, and M. Lieberman ed., *Excitable Cells in Tissue Culture*, Plenum Press, New York, 1981.

[2] D. F. Ready, and J. F. Nicholls, "Identified neurons isolated from the leech CNS make selective connections in cell culture,"*Nature*, vol. 182, pp. 67-69.

[3] R. G. Wong, R. D. Hadley, S. B. Kater and G. Hauser, "Neurite outgrowth in molluscan organ and cell cultures: The role of conditioning factor(s)", *J. Neuroscience*, vol. 1, p. 1008, 1981.

[4] D. Dagan, and I. B. Levitan, "Isolated identified *Aplysia* neurons in cell culture," *J. Neurosci.*, vol. 1, pp. 736-740, 1981.

[5] A. Marty, and E. Neher, "Tight-seal whole-cell recording," in *Single Channel Recording*, ed. B. Sakmann, and E. Neher, Plenum Press, New York, pp. 107–122, 1983.

[6] G. W. Gross, A. N. Williams, and J. H. Lucas, "Recording of spontaneous activity with photoetched microelectrode surfaces from spinal cord neurons in culture," *J. Neurosc. Methods*, vol. 5, pp. 13–22, 1982.

[7] J. Pine, "Recording action potentials from cultured neurons with extracellular microcircuit electrodes," *J. Neurosc. Methods*, vol. 2, pp. 19–31, 1980.

[8] C. A. Thomas, Jr., P. A. Springer, G. E. Loeb, Y. Berwald-Netter, and L. M. Okun, "A miniature microelectrode array to monitor the bioelectric activity of cultured cells," *Exp. Cell Res.*, vol. 74, pp. 61–66, 1972.

[9] D. W. Tank, C. S. Cohan, and S. B. Kater, "Cell body capping of array electrodes improves measurements of extracellular voltages in micro–cultures of invertebrate neurons," *IEEE Conference on Synthetic Microstructures*, Airlie, 1986.

[10] D. A. Israel, W. H. Barry, D. J. Edell, and R. G. Mark, "An array of microelectrodes to stimulate and record from cardiac cells in culture," *Am. J. Physio.*, vol. 247, *Am. J. Physio.*, vol. 247, pp. H669–H674, 1984.

[11] A. Grinvald,"Real-time optical imaging of neuronal activity," *TINS*, pp. 143-150, 1984.

[12] B. M. Salzberg, "Optical recording of electrical activity in neurons using molecular probes, in *Cellular Mechanisms of Neurobiology,* vol. 3, 1982.

[13] H. Rayburn, J. Gilbert, C-B .Chien, and J. Pine, Noninvasive techniques for long term monitoring of synaptic connectivity in cultures of superior ganglion cells, *Soc. of Neurosci. 14th Annual Meeting,* Abstract 171.1, 1984.

[14] C-B. Chien, W. D. Crank, J. Pine, "Noninvasive techniques for measurement and long–term monitoring of synaptic connectivity in microcultures of sympathetic neurons," *Soc. of Neurosci. 17th Annual Meeting*, Abstract 393.14, 1987.

[15] W. Stuhmer, W. M. Roberts, and W. Almers, "The loose patch clamp," in *Single Channel Recording*, ed. B. Sakmann, and E. Neher, Plenum Press, New York, pp. 123–132, 1983.

[16] K. E. Peterson, "Silicon as a mechanical material," *Proc. IEEE*, vol. 70, no. 5, pp. 420–457, 1982.

[17] W. G. Regehr, S. B. Kater, J. Pine, "A chronic *in vitro* microdevice–neuron connection," *Soc. of Neurosci.*, 17th Annual Meeting, Abstract 393.15, 1987.

Chapter 2

Stimulating and Recording from Cultured Neurons with Glass Loose-Patch Electrodes

2.1 Background

Preliminary experiments were performed with glass patch-pipettes to determine what seals and electrode diameters would be required for (1) recording action potentials with good signal-to-noise ratios, (2) stimulating, (3) verifying the stimulus with the same electrode, and (4) recording subthreshold post synaptic potentials. Patch electrodes were used in a method that combines features from the loose-patch clamp [1], and extracellular stimulation and recording techniques that have been used both *in vivo* and *in vitro*.

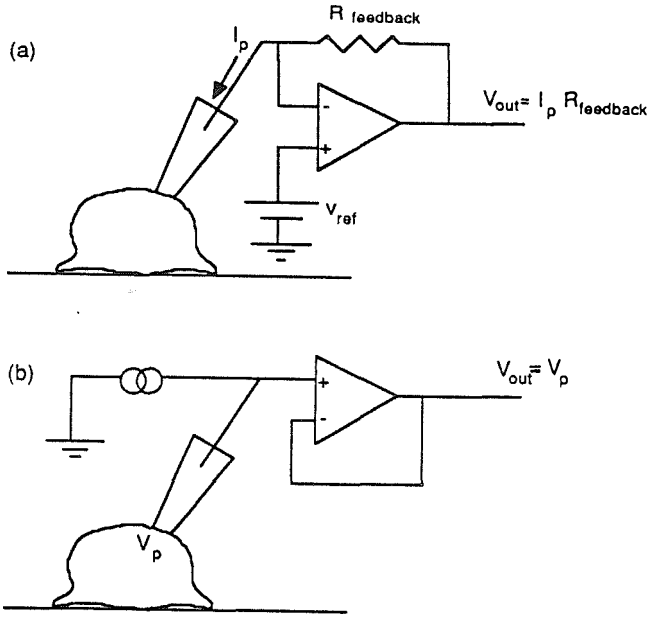

Figure 2.1. Loose-patch electrode in (a) voltage-clamp (b) current-clamp

The loose-patch clamp method was developed to map the channel distributions in cells without requiring large seal resistances. Glass pipettes are brought

i contact with the cell membrane until a seal of 1–3 MΩ is obtained. The pipette is operated in voltage-clamp mode as in Figure 2.1 (a). Voltage steps are applied to the pipette, the potential of the patch membrane is changed, and current flows through channels in the patch. Using large diameter glass electrodes to record from a 50-200 μm^2 patch containing thousands of channels, the resulting membrane currents are large enough to record with good signal-to-noise, without requiring gigaohm seals. A combination of analog and digital techniques is used to correct for current lost through the seal resistance. The loose patch clamp has been used primarily to map channel distributions on muscles [2]–[4].

We used patch electrodes of comparable diameters and had seal resistances in a similar range to those of loose patch clamping. However, our primary goal is to record the intracellular potential and to stimulate cells. Also, the final electrode design utilizes metal electrodes, precluding voltage clamping the patch membrane (see Chapter 4). Consequently current clamping as in Figure 2.1(b) was used rather than voltage clamping which is used in conventional loose-patch recording.

Tests with glass electrodes were performed on both *Helisoma* neurons and SCG's: to measure typical seal resistances that could be attained without applying suction; to determine breakdown voltage of the cell membrane and the maximum amplitude of the stimulus current pulse that could be passed through the electrode, without damaging the cell; to compare the intracellular potential to the signal recorded using the patch electrode; to determine appropriate stimulus paradigms; and to investigate the seals required for whole-cell recording, breaking down the cell membrane with a current pulse, and reversibly breaking down the cell membrane as an approach to obtaining improved signal-to-noise ratios for subthreshold events.

2.2 Cultured Identified Helisoma Neurons

Identified *Helisoma* snail neurons were used for initial electrode tests since they are large (cell bodies are about 50 μm in diameter), robust, and have been studied extensively both *in vivo* and *in vitro* [5]. Neurons were taken from the buccal ganglia which innervates the muscles of the buccal mass and controls feeding activity. Based on their size and location in the ganglia it is possible to identify individual neurons in the ganglia. Electrode tests were performed on two types of neurons: neuron B5 whose axons branch extensively over the foregut, and neuron B19 which provides chemical excitatory input to a large muscle in the buccal mass. Each neuron type has its own distinct physiology, and morphology, and forms unique connections with other neurons.

2.21 Culture Techniques

Animals from inbred stocks of *Helisoma trivolvis* were dissected under sterile conditions and their buccal ganglia were removed [10]. Buccal ganglia were treated with 0.2% trypsin (Sigma III) for 30 minutes followed by a 15 minute rinse in trypsin inhibitor. Trypsin softened the connective tissue within the ganglion and in the outer ganglionic sheath. Ganglia were pinned to a Sylgard dish and identified neurons B5 and B19 were exposed by making an incision in the ganglionic sheath with a tungsten microknife. Then, while observing through a dissecting scope at a magnification of about 90X, neurons were removed using a micrometer-drive syringe and a micropipette controlled by a micromanipulator.

Identified neurons were placed in polylysine-coated 35 mm *Falcon* dishes containing conditioned medium [7]-[9], which contains factor(s) necessary for process outgrowth in isolated neurons. It is produced by incubating two adult *Helisoma* brains/ml of *Helisoma* defined medium for 72 hours prior to cell plating. *Helisoma* defined medium consists of 50% Leibowitz L-15 medium without inor-

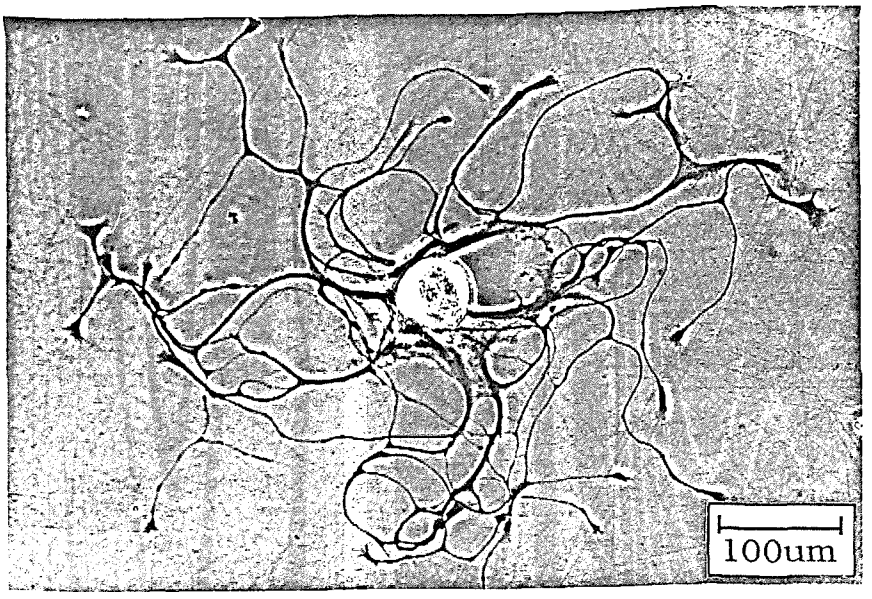

Figure 2.2. *Helisoma* B19 neuron after 3 days in culture.

ganic salts, and 50% salt, buffer, and antibiotic solution in distilled water with an osmolarity of 130 mOsm. The final concentrations are 40 mM NaCl, 1.7 mM KCl, 4.1 mM $CaCl_2$, 1.5 mM $MgCl_2$, 5 mM Hepes, with 50 μg/ml gentamycin sulfate. *Helisoma* saline consists of 51.3 mM NaCl, 1.7 mM KCl, 4.1 mM $CaCl_2$, 1.5 mM $MgCl_2$, and 5 mM Hepes (pH 7.3) distilled water. Antibiotic saline was made by autoclaving *Helisoma* saline, and adding gentamycin sulfate to a final concentration of 150 μmg/ml.

Normal cell growth is shown in Figure 2.2. Initially the cell is simply a sphere that has had all of its processes removed. After several hours in culture cells "veil" and grow processes. Growth continues for several days and then stops and the cell is said to be stable state, as indicated by "phase bright" growth cones.

2.22 Electrophysiology of Cultured B5 and B19 Neurons

Morphologically and electrophysiologically *Helisoma* B5 and B19 neurons differ both *in vivo* and *in vitro* [6],[10]. B5 neurons have a larger total neu-

rite outgrowth, higher growth rate, and more filopodia per growth cone than B19 neurons. Serotonin applied to the growth cones of B19 neurons causes them to retract, while having no effect on the growth cones of B5 neurons [11]. Levels of serotonin as low as 1μM cause B19 neurons to fire and cease growing, while having no effect on B5 neurons. The action potential half-width for cultured neurons is 15.6 ± 5.8 msec for B5's and 6.7 ± 1.2 msec for B19's [6]. Figure 2.3 shows action potentials typical of B5 and B19 neurons. The half-width of action potentials of cultured neurons increases with their time in culture.

2.3 Cultured Rat Superior Cervical Ganglion Neurons (SCG's)

Cultured SCG's provide an excellent preparation for initial studies [12]–[13]: (1) the well defined trophic factor necessary for long-term growth, nerve growth factor (NGF), is readily available, (2) ganglia are discrete, easily obtainable containers filled with a large number of relatively homogeneous neurons, (3) they are relatively immature at birth, facilitating dissociation and culturing, (4) they have been extensively studied and characterized both *in vivo* and *in vitro*, and (5) the study of such mammalian neurons compliments the study of *Helisoma* invertebrate neurons.

2.31 Culture Techniques

Neonatal rats less than one day old were decapitated just above the arms and the superior cervical ganglia were removed, cleaned of surrounding tissue, and placed in a dish containing 4 ml of sterile Hanks solution. $200\,\mu$l of 2.5% trypsin was added, and it was allowed to incubate at 37°C in 5% CO_2 for 30 minutes. Then the ganglia were removed from the trypsin medium, placed in a dish containing serum, and each ganglia was pulled apart with tweezers. The contents of the dish were transferred to a 15 ml centrifuge, triturated 30–50 times, and

(a)

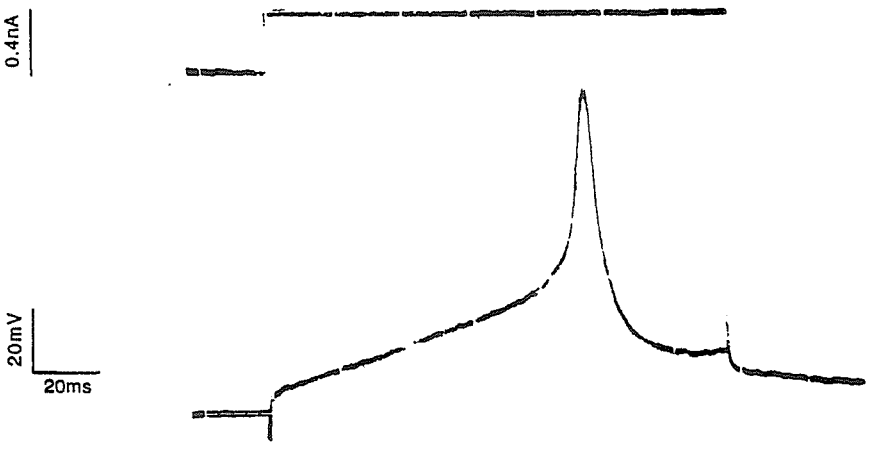

(b)

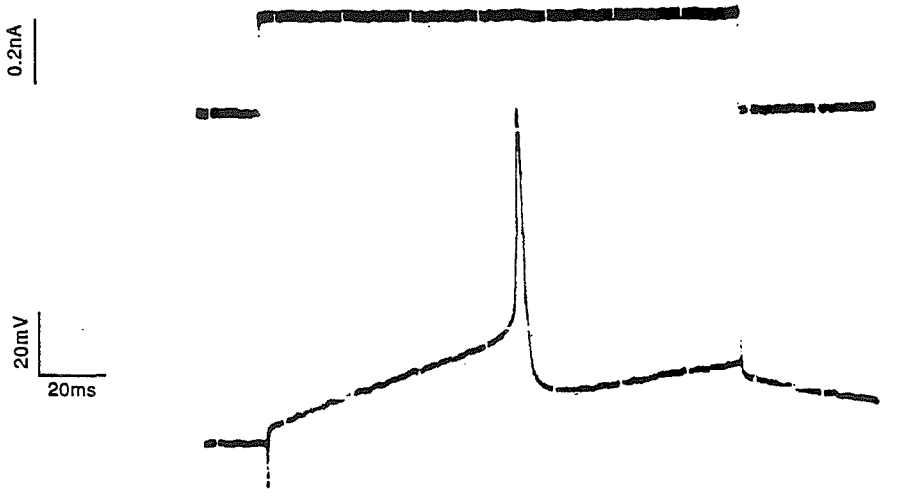

Figure 2.3. Electrophysiology of cultured *Helisoma* (a) B5 and (b) B19 neurons.

filtered through a 44 μm nylon filter. After spinning at 1400 r.p.m. the supernatant was removed and the cells suspended in plating medium at a density of 3×10^4 cells/ml. Cells were then added dropwise inside glass rings in culture dishes containing complete growth medium.

The dishes used to culture the neurons were 35 mm *Falcon* dishes. Two different surfaces were used: polylysine, or extracellular matrix from bovine en-

dothelial cells [14]. The culture medium used has been described elsewhere [15]. Figure 2.4 is an example of a mass culture of SCG's.

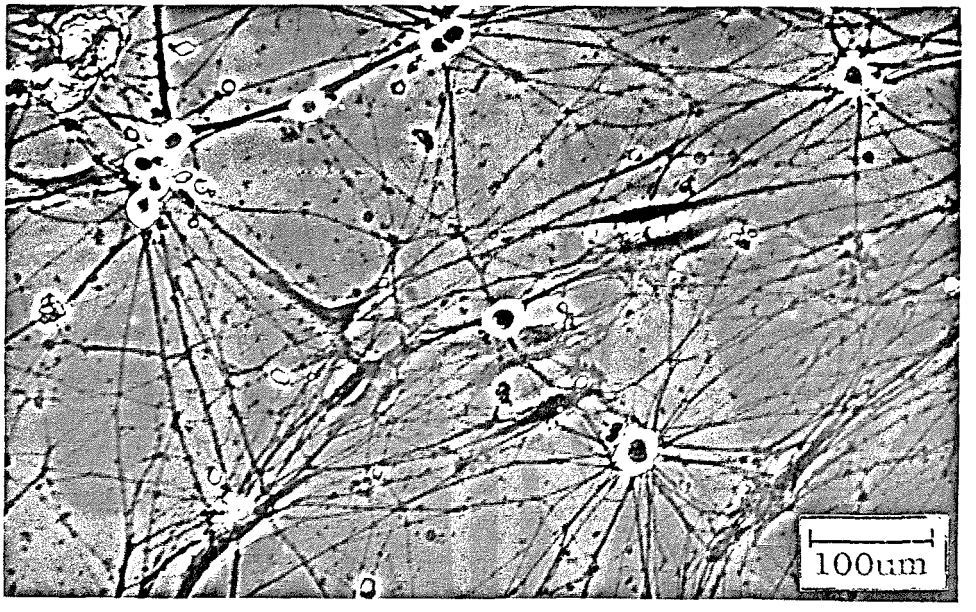

Figure 2.4. Normal growth of a mass culture of SCG neurons.

2.32 Electrophysiology of Cultured SCG's Neurons

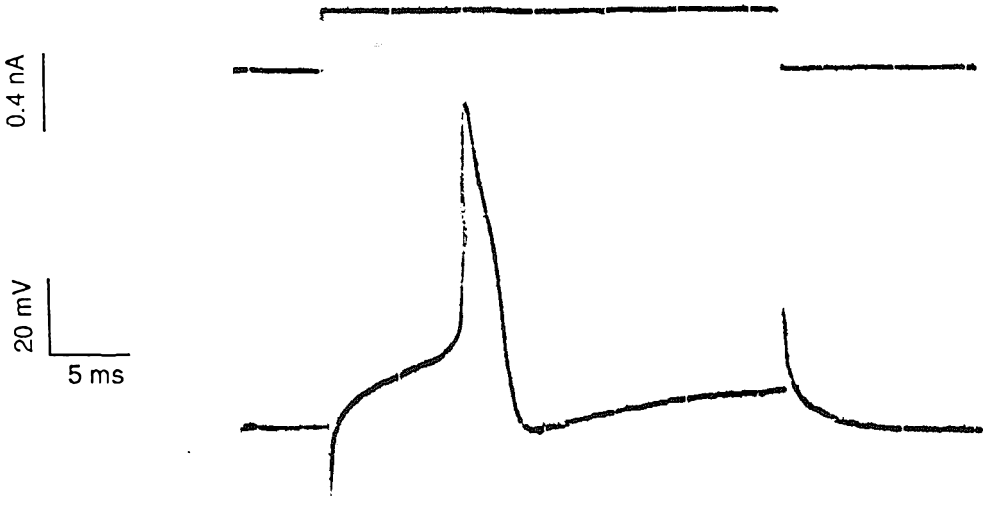

Figure 2.5. Intracellular electrophysiology of cultured SCG's.

SCG's has been studied extensively in cell culture. Two weeks after plating the cells are large enough to reliably penetrate with an intracellular electrode as shown in Figure 2.5. The whole-cell patch can be used with younger cells [16], but with time in culture in a serum containing medium the cells become more difficult to seal to as the surfaces become coated with material from the medium. Membrane currents have been studied using a two-electrode voltage clamp [17]. While SCG's rarely interconnect in intact animals, they form extensive connections in dissociated cell culture [18].

2.4 Patch Electrode Tests

Patch electrodes were made from soda-lime glass (*Kimble* 73811). Electrode diameters were varied by changing the heat on the second pull. Pipettes were filled with extracellular salts that had been filtered to 0.2 μm . These solutions were used to closely replicate the solution between the electrode and the cell for diving-board and dish electrodes. Intracellular electrodes were pulled on a *Brown and Flaming* P77 pipette puller using 1.0 mm o.d. omega dot borosilicate glass (*WPI* 1B100F-4). Electrode and seal resistances were determined by injecting a current pulse of known amplitude, and measuring the resulting voltage drop.

As expected the seal resistance varied roughly as the inverse of the electrode diameter, and resistances were in the range 1–3 MΩ for a 10 μm diameter pipette tip, for SCG's and 2–6 MΩ for *Helisoma* neurons. Due to higher resistivity extracellular solution the electrode and seal impedances were larger for the *Helisoma* studies. The resistivity of media used for SCG's is approximately 100 ohm-cm, and for *Helisoma* neurons approximately 300 ohm-cm.

Next the breakdown voltage of the patch beneath the membrane was determined. First the electrode impedance and then the seal resistance was measured. Then current pulses of progressively larger amplitude were applied. An intracel-

lular electrode was used to determine when the cell membrane was broken down. For positive going 2 msec pulses the breakdown voltage was determined to be 400 mV ±50 mV (n=8) for SCG's, with similar results obtained for *Helisoma* neurons. There was not a large dependence of breakdown voltage on polarity or on pulse length for pulse lengths of 0.2 msec–50 msec.

Next, the intracellular potential was compared to the patch electrode signal. This necessitated an intracellular electrode in addition to the loose-patch electrode. The patch pipette was pressed against the cell body to obtain a stable seal, then an intracellular electrode was used to penetrate the cell. The intracellular electrode was used both to stimulate the cell, and to record the resulting action potential. This intracellular response was compared to that recorded with the loose-patch pipette. Signals recorded on the patch electrode were essentially derivatives of the action potentials (see Chapter 4). For each cell type, *Helisoma* B19, *Helisoma* B15, or SCG, the magnitude and duration of the signal recorded on the patch pipette was very different. This can be attributed to the fact that both the channels contained within the patch and the rate of rise of an action potential are very cell dependent. As seen in Figure 2.6, patch signals recorded from *Helisoma* B19 neurons are larger than for *Helisoma* B5 neurons, due to the faster rate of rise of a B19 action potential.

In the next experiment a cell was stimulated with a patch pipette and an intracellular electrode was used to verify the stimulus. Using patch electrodes with a diameter of 10 μm facilitated stimulating neurons without breaking down the cell membrane. If significantly smaller pipettes were used stimulation through the patch was not possible without breaking down the cell membrane. Many different types of stimuli were used to fire neurons. Although stimulation with long pulses could be accomplished easily, primarily short stimuli were used since

(a) *Helisoma* B19

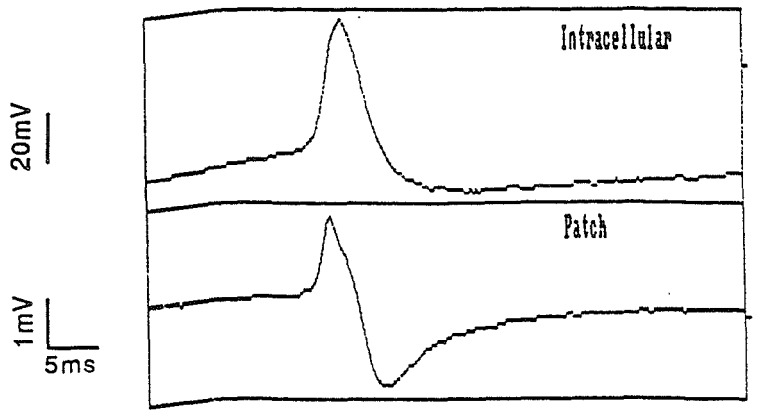

(b) *Helisoma* B5

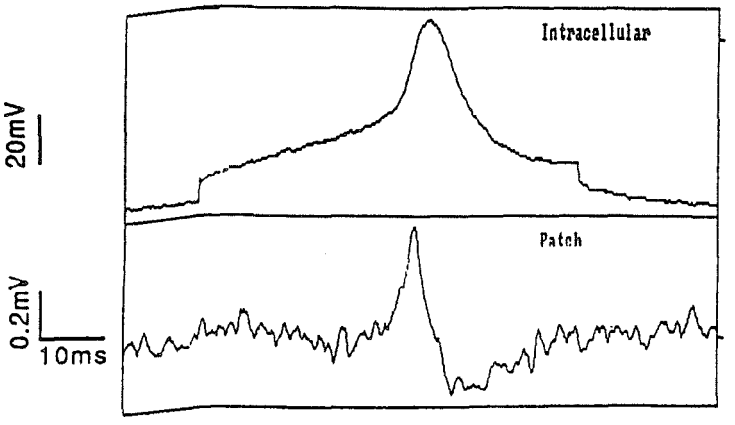

(c) Rat SCG

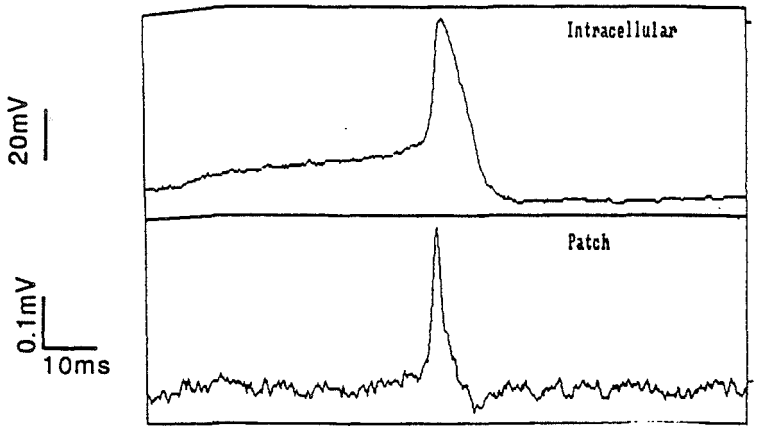

Figure 2.6. Neurons stimulated with a current pulse passed through an intracellular electrode (40–50 MΩ), and the response of the cell recorded with the intracellular electrode, and the loose-patch electrode (diameter $\approx 10\,\mu$m). (a) *Helisoma* B19 neuron ($R_{seal} = 3.5\,$MΩ, bandwidth 10 Hz–1 kHz). (b) A *Helisoma* B5 neuron ($R_{seal} = 4.0\,$MΩ, bandwidth 10 Hz–1 kHz). (c) SCG neuron ($R_{seal} = 3.0\,$MΩ, bandwidth 10 Hz–1 kHz).

when using a metal electrode, such as the diving-board or dish electrodes, long voltage pulses will charge up the electrode to potentials large enough to produce gas. Figure 2.7 shows an example of some of the many stimulus experiments that were done using SCG's, and *Helisoma* B19 and B5 neurons. In 7 (a) a 1 msec long pulse is used to stimulate a *Helisoma* B19 neuron, with four traces superimposed. In 2.7 (b) a 2 msec long pulse is used to stimulate a *Helisoma* B5 neuron. This is an example of near-threshold stimulation. If the amplitude of the stimulus were increased slightly a more reliable stimulus as in 2.7 (a) would be obtained. However, if the amplitude were further increased by more than about 30% then the potential would be sufficient to break down the cell membrane. Figure 2.7 (c) is an experiment in which an SCG is stimulated. Four successively larger stimuli were used: the first two resulted in no discernible intracellular response, the third resulted in a 5 msec depolarization, and the fourth stimulated the neuron. This demonstrates that the response is all or none, as an action potential should be. Based on these experiments it is possible to reliably stimulate neurons, even using fairly short stimulus pulses.

In addition to the stimulus experiments of Figure 2.7 negative stimulus pulses were used. Such negative pulses could be used to reliably stimulate SCG neurons, but not *Helisoma* neurons. Figure 2.8 is an example of a patch electrode stimulating an SCG, recording the resulting action potential with the same electrode, and using an intracellular electrode to verify the response. This is promising because it suggests that using the same electrode for both stimulation and verification of stimulation is possible. However, the diving-board electrode and dish electrode are metal, with a complex impedance that has a time constant extending the stimulus artifact for many milliseconds after the stimulus current pulse. If the same electrode is to be used for both stimulating and recording

the resulting action potential a combination of digital and analog, techniques similar to those employed in the loose patch clamp, must be used to remove the stimulus artifact.

In order to improve the signal-to-noise ratio and obtain essentially an intracellular connection using a patch electrode it is possible to break down the membrane and get inside the cell as in whole cell patching [19]. But there is a problem: if seals are only of the order of several megohms and a hole is put into the cell beneath the patch electrode then the cell becomes very leaky, the resting potential of the cell deteriorates, and the cell dies. However, if very short current pulses of appropriate amplitude are used, the membrane can be reversibly broken down, leaving a $50\,\mu m^2$ patch with a resistive leak of about $200\,M\Omega$ [20]–[21]. An illustration of the impressive signal-to-noise ratio that can be obtained with a seal resistance of $3\,M\Omega$ is given in Figure 2.9. At time $t = 0$ a 0.5 msec current pulse of 225 nA was passed through the patch electrode, resulting in a 400 mV drop across the patch and breaking the membrane down. Five seconds later the intracellular signal is essentially an intracellular signal that has been attenuated by a factor of 50, with R_{seal} and R_{patch} forming a voltage divider so that $V_{out} \approx R_{seal}/(R_{patch} + R_{seal})$ (see Chapter 4 for a detailed explanation). Based on this, at $t = 5\,sec$ $R_{seal} \approx 150\,M\Omega$. At time $t = 2\,min.$ the signal recorded by the patch electrode is much smaller, indicating that the hole in the patch has begun to seal ($R_{seal} \approx 750\,M\Omega$). By $t = 4\,min.$ the patch has essentially sealed and only a small differentiated signal is recorded by the patch electrode.

The results of such experiments suggest a technique allowing even electrodes with seals as low as several megohms to record essentially intracellular signals; it would be possible to peak inside a cell and record from it for a short time, let the patch seal, and then come back at a later time and repeat the process

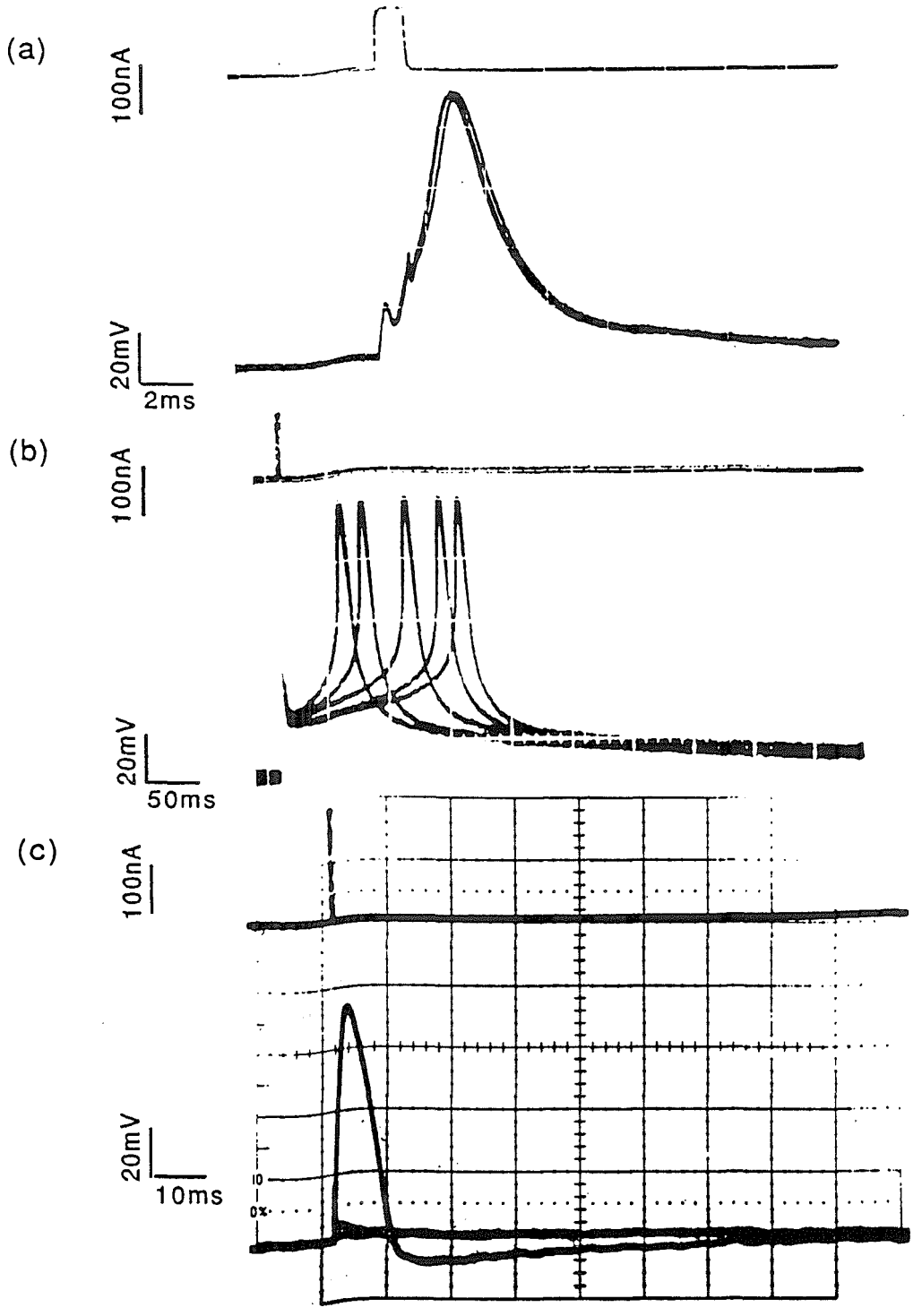

Figure 2.7. Stimulation of neurons using a current pulse passed through a loose-patch electrode (diameter $\approx 10\,\mu$m). to stimulate and recording using an intracellular electrode. (a) *Helisoma* B19 neuron, $\Delta t_{stim} = 1$ msec, $I_{stim} = 100$ nA, $R_{seal} = 3\,\mathrm{M}\Omega$. (b) *Helisoma* B5 neuron, $\Delta t_{stim} = 2$ msec, $I_{stim} = 100$ nA, $R_{seal} = 3\,\mathrm{M}\Omega$, stimulated at 0.1 Hz. (c) SCG neuron, $\Delta t_{stim} = 0.5$ msec, $I_{stim} = 100$ nA, $R_{seal} = 2\,\mathrm{M}\Omega$.

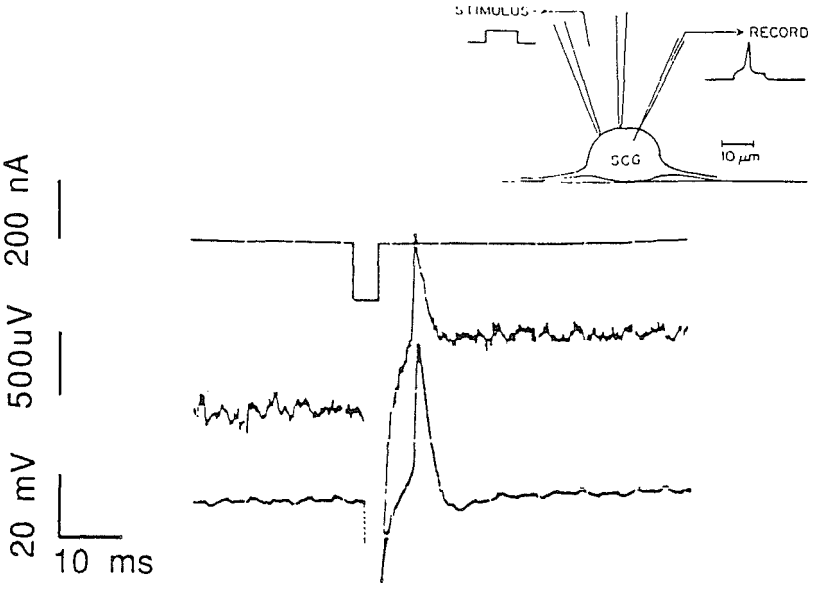

Figure 2.8. Stimulation of neurons using a current pulse passed through a loose patch electrode to stimulate and record, and using an intracellular electrode to record. $\Delta t_{stim} = 2\,\text{msec}$, $I_{stim} = -200\,\text{nA}$, $R_{seal} = 1.5\,\text{M}\Omega$, $V_{patch} = -300\,\text{mV}$.

when desired. However, for large diameter pipettes even a hole put in a cell by this reversible breakdown technique is large enough to seriously damage the cell; calibrating the signals recorded through a patch membrane with variable seal resistance is difficult; and the range of membrane voltages resulting in reversible breakdown is small and it is easy to exceed this range and damage the cell. For these reasons the approach adopted for the diving-board electrode was to try to get large seals to facilitate whole-cell recording. This is a reasonable approach, since gigaohm seals have been obtained in some preparations using glass patch pipettes without providing suction. Failing this it would still be possible to noninvasively record action potentials and stimulate neurons with the diving-board electrode, with the use of reversible-breakdown existing as a backup technique.

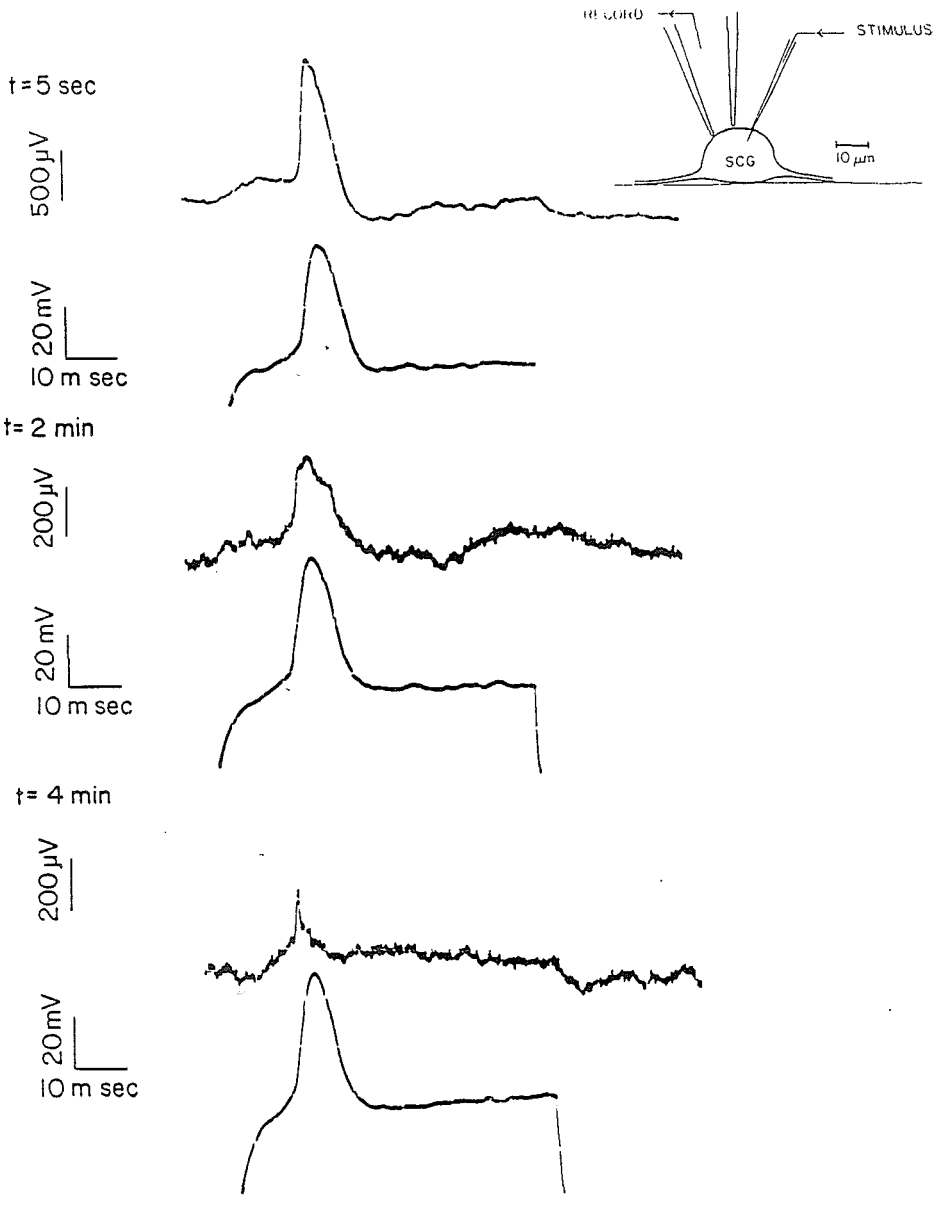

Figure 2.9. Rat SCG neuron stimulated with a current pulse passed through an intracellular electrode, and the response of the cell recorded with the intracellular electrode, and the loose-patch electrode at times $t = 5\,\text{sec}$, $t = 2\,\text{min}$, $t = 4\,\text{min}$. ($R_{seal} = 3.0\,\text{M}\Omega$, $d_{patch} = 7\,\mu\text{m}$, at time $t = 0$ patch membrane broken down with a +130 nA, 0.5 msec, current pulse, bandwidth 10 Hz–1 kHz, resistance of intracellular electrode 140 MΩ.

References

[1] W. Stuhmer, W. M. Roberts, and W. Almers, "The loose patch clamp," in *Single Channel Recording*, ed. B. Sakmann, and E. Neher, Plenum Press, New York, pp. 123–132, 1983.

[2] J. H. Caldwell, D. T. Campbell, and K. G. Beam, "Na channel distribution in vertebrate skeletal muscle," *J. Gen. Physiology*, vol. 87, pp. 907-932, June 1986.

[3] W. Almers, W. M. Roberts, and R. L. Ruff, "Voltage clamp of rat and human skeletal muscle: measurements with an improved loose-patch technique," J. Physiol., vol. 307, pp. 751-768, 1984.

[4] R. E. Weiss, W. M. Roberts, W. Stuhmer, and W. Almers, "Mobility of voltage-dependent ion channels and lectin receptors in the sarcolemma of frog skeletal muscle," *J. Gen. Physiol*, vol. 87, pp. 955-983, June 1986,.

[5] S. B. Kater, "Dynamic regulators of neuronal form and connectivity in the adult snail *Helisoma*," in *Model Neural Networks and Behavior,* Plenum publishing Corp., 1985.

[6] C. S. Cohan, P. G. Haydon, and S. B. Kater, "Single channel activity differs in growing and nongrowing growth cones of isolated identified neurons of *Helisoma*," *J. Neurosci. Res.*, vol. 13, 1985.

[7] D. L. Barker, R. G. Wong, and S. B. Kater, "Separate factors produced by the CNS of the snail *Helisoma* stimulate neurite outgrowth and choline metabolism in cultured neurons, *J. Neurosci. Res.*, vol. 8, pp.419–432, 1982.

[8] R. G. Wong, R. D. Hadley, S. B. Kater, and G. Hauser, "Neurite outgrowth in molluscan organ and cell cultures: the role of conditioning factor(s)," *J. Neurosci.*, vol. 1, pp. 1008–1021, 1981.

[9] R. G. Wong, D. L. Barker, and D. A. Bodnar, "Nerve growth-promoting factor produced in cultured media conditioned by specific CNS tissues of snail *Helisoma*, *Brain Res.*, vol. 292, pp. 81–91, 1984.

[10] P. G. Haydon, C. S. Cohan, D. P. McCobb, H. R. Miller, and S. B. Kater, "Neuron-specific growth cone properties as seen in identified neurons of *Helisoma*," *J. Neurosci. Res.*, vol. 13, pp. 135-147, 1985.

[11] P. G. Haydon, D. P. McCobb, and S. B. Kater, " Serotonin selectivity inhibits growth cone motility and synaptogenisis of specific identified neurons," *Science*, vol. 226, pp. 561–564, 1984.

[12] S. C. Landis, "Environmental influences on the development of sympathetic neurons," in *Cell Culture in the Neurosciences*, eds. J. E. Bottenstein and G. Sato, Plenum Press, New York, pp. 169-192, 1985.

[13] H. Burton, and R. P. Bunge, "The expression of cholinergic and adrenergic properties by autonomic neurons in tissue culture," in *Excitable Cells in Tissue Culture,* eds. P. G. Nelson, and M. Lieberman, Plenum Press, New York, pp. 1–29, 1981.

[14] D. K. MacCallum, J. H. Lillie, L. J. Scaletta, J. C. Occhino, W. G. Frederick, and S. R. Ledbetter, "Bovine corneal endothelium *in vitro*: elaboration and

organization of a basement membrane," *Exp. Cell Res.*, vol. 139, pp. 1–13, 1982.

[15] R. E. Mains, and P. H. Patterson, "Primary cultures of dissociated sympathetic neurons. I. Establishment of long-term growth in culture and studies of differentiated properties, *J. Cell Biol.*, vol. 59, no. 329, 1973.

[16] J. M. Nerbonne, A. M. Gurney, and H. B. Rayburn, "Development of the fast, transient outward K^+ current in embryonic sympathetic neurons," *Brain Research*, vol. 378, pp. 197-202, 1986.

[17] J. E. Freschi, "Membrane currents of cultured rat sympathetic neurons under voltage clamp," *Journal of Neurophysiology*, vol. 50, no. 6, Dec. 1983.

[18] C.-P. Ko, H. Burton, M. I. Johnson, and R. P. Bunge, "Synaptic transmission between rat superior cervical ganglion neurons in dissociated cell cultures," *Brain Research*, vol. 117, pp. 461-485, 1976.

[19] A. Marty, and E. Neher, "Tight-seal whole-cell recording," in *Single Channel Recording*, ed. B. Sakmann, and E. Neher, Plenum Press, New York, pp. 107–122, 1983.

[20] U. Zimmerman, "Electric field-mediated fusion and related electrical phenomena," *Biochimica et Biophysica Acta*, vol 694, pp. 227-277, 1982.

[21] U. Zimmerman, and J. Vieken, "Electric field-induced cell-to-cell fusion," *J. Membrane Biol.*, vol. 67, pp. 165-182, 1982.

Chapter 3

Diving-Board Electrode Fabrication

3.1 The Idea

The diving-board electrode as shown in Figure 2.1 is a silicon microdevice used in a manner similar to a loose-patch electrode. Each electrode is manipulated into place and is then glued to the bottom of the tissue culture dish. A seal is made between the lower surface of the electrode and the cell in the same way that a seal is made to the bottom of a glass pipette, although suction cannot be applied when using this device. This establishes a one-to-one connection between a device and a cell for both stimulating and recording.

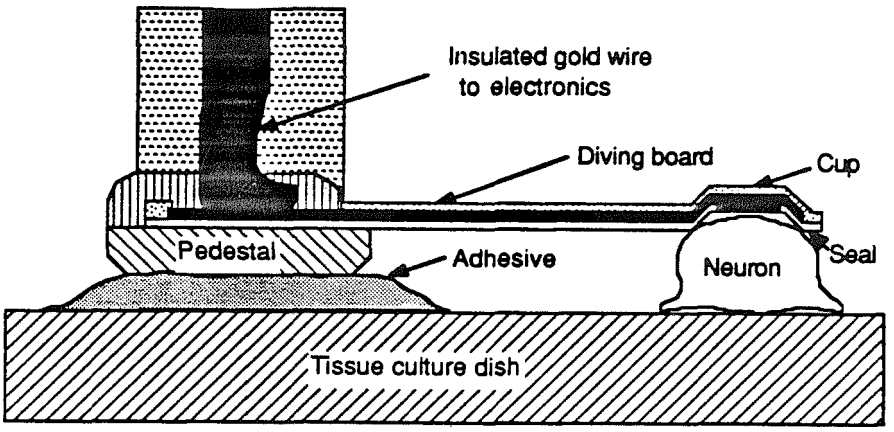

Figure 3.1. Schematic of a diving-board electrode in contact with a cell.

A long flexible arm makes gentle contact with a cell, while its silicon support pedestal is permanently mounted to the bottom of the culture dish. A gold strip sandwiched between two insulating layers leads to a cup-shaped structure at the end of the diving board. Here the diving board makes a seal to the

neuron and electrical contact is made by a platinized gold electrode. An insulated gold wire extends vertically from the device out of the solution to connect to the electronics. In principal diving-board electrodes can be placed on many neurons simultaneously, and after doing so the micromanipulators are free for conventional physiology.

3.2 Micromachining of Silicon

Integrated circuit-technology and micromachining of silicon provide powerful tools to fabricate very small three-dimensional structures with well defined mechanical properties [1]-[4], such as the diving-board electrode. These methods have the advantage of being well established for use in the semiconductor industry, and allow batch fabrication of many devices on one wafer with feature sizes down to a micron.

In order to build such three-dimensional structures wet-etching techniques are indispensable. Figure 3.2 shows the characteristic etching of several such techniques. Figure 3.2(a) and 3.2(b) show a wafer first patterned by etching a SiO_2 masking layer, and then etched by an isotropic etchant. HF/HNO_3 $/CH_3COOH$ [5] is an example of such an isotropic etch: one with an etch rate unaffected by crystal orientation.

There are also anisotropic etches that etch along different crystal planes at very different etch rates. This orientation-dependent etching can be explained by considering the lower order crystal planes of silicon, which is crystallized in the diamond structure. Ethylene-diamine/pyrocatechol/water (EDP) etch [6],[7] has several properties that make it indispensable in the fabrication of many micromechanical devices: the etch rates in the (100):(110):(111) directions are about 50:30:1 μm/hour; and the relative etch rate of gold, SiO_2, Si_3N_4, and heavily doped boron regions is extremely small. Figures 3.2(c) and 3.2(d) show EDP

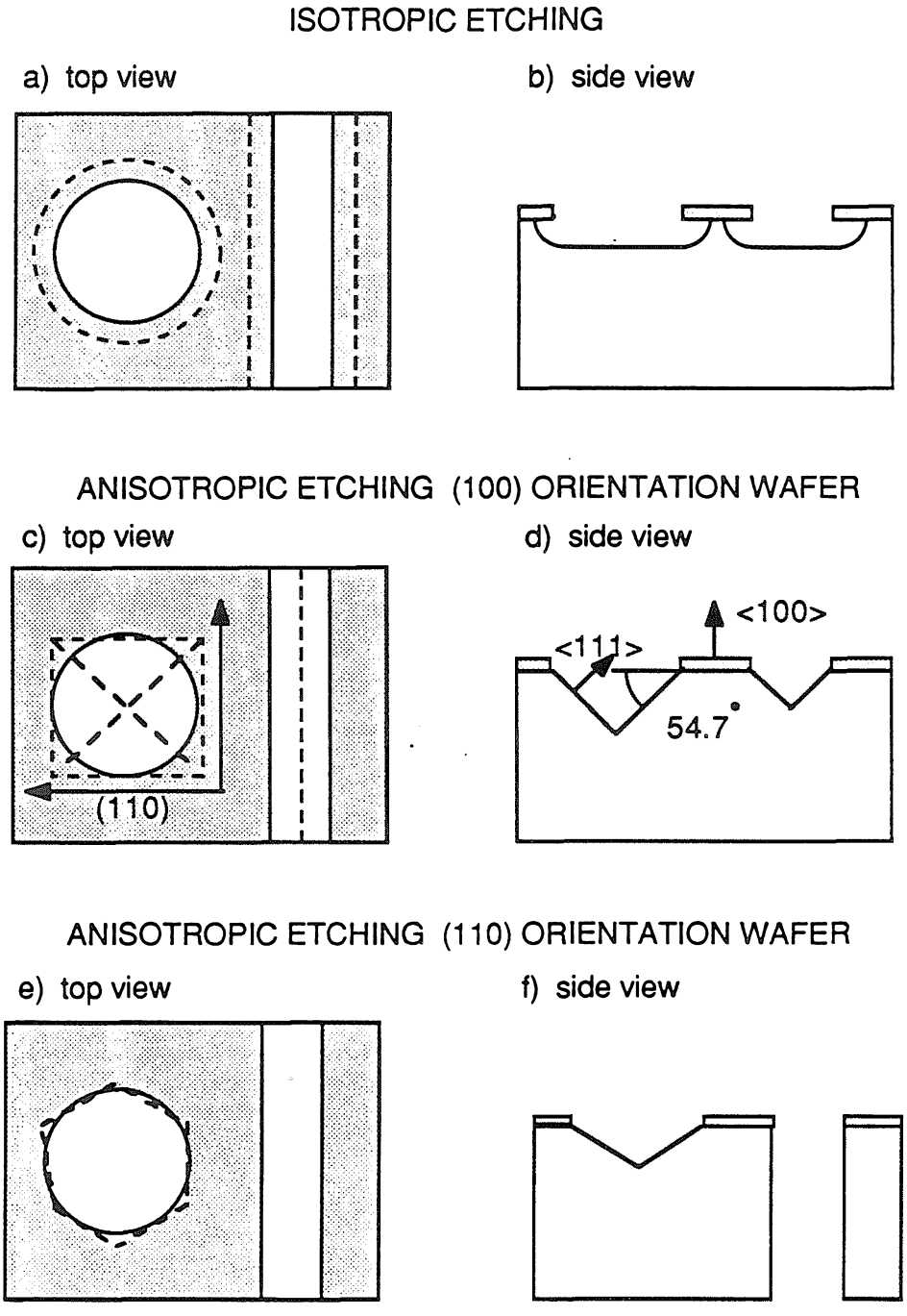

Figure 3.2. Isotropic etching of silicon using an etchant such as HF-Nitric-Acetic (a) top-view (b) side view. Anisotropic etching on (100) surfaces using EDP, (c) top view (d) side view. Anisotropic etching on (110) surface using KOH/H_2O (e) top view (f) side view.

etching (100) orientation silicon that has a SiO_2 mask. EDP etches down until a (111) plane is reached which serves as an etch stop. Even when the opening in the oxide is circular the resulting etching pattern is an inverted pyramid with the (111) planes making an angle of approximately 54.7° with the (100) surface which it intersects in perpendicular (110) planes.

There are also orientation-dependent etches that are used on (110) silicon wafers as shown in Figures 3.2 (e) and (f). KOH/H_2O [8] is the primary etchant used in such applications. It etches silicon in the 100:110:111 directions at rates of 60:400:1 μm/hour [9]. Such etches attack thermal SiO_2 masks at 0.2 μm/hour, therefore Si_3N_4 which is attacked extremely slowly, is used as a mask. As is seen in Figure 3.2 using a circle for a mask will result in a structure as shown, with (111) planes serving as etch stops. However, if a properly oriented mask is used it is possible to etch vertical grooves completely through the wafer, bounded by (111) planes.

While the mechanisms responsible for orientation-dependent etching have not been studied extensively they can be qualitatively understood. The etching of silicon by any etch proceeds via essentially the same course: (1) Si is oxidized to Si^+; (2) OH^- attaches to the positively charged group; (3) hydrated silicon reacts with complexing agents; and (4) reaction products dissolve into solution. There are two principle ways in which differences in crystal planes can affect these reaction rates. First, different crystal planes have different atomic densities and water effectively screens reactive species much better for high atomic densities. Since the atomic packing densities of the different crystal planes are (111) > (100) > (110), one would expect (111) to etch more slowly. Second, the energy to move an atom is dependent upon orientation and the number of dangling bonds. On this basis the (111) orientation, with only one dangling bond, is expected

to etch much more slowly than either the (100) or the (110) orientations, which both have two dangling bonds.

The dopant dependence of etching is also poorly understood. When silicon is doped to boron concentrations in excess of 5×10^{19} cm^{-3} the etch rate is reduced in EDP by a factor of 50 [7], and similarly reduced in KOH/H_2O. But for"Dash" etch [10], a mixture of $HF/HNO_3/CH_3COOH$ the etch rate is actually increased by a factor of 20 for such heavily doped regions. There are two factors that could affect the etch rate: first, such heavily doped regions are in strong tension with the smaller boron atom replacing the larger silicon atom, increasing the binding energy, and increasing the etch rate as is seen in the case of EDP and KOH/H_2O; and second, the availability of holes would tend to make the reaction proceed more quickly as in the case of "Dash" etch. Qualitatively such different etch-rate effects can be explained by different steps being the rate-limiting steps for different etchants.

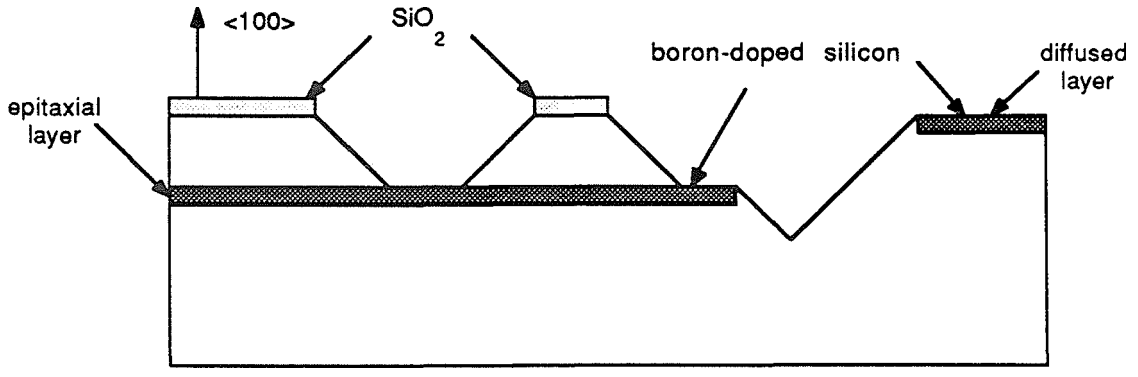

Figure 3.3. Etching of (100) silicon with heavily boron-doped regions.

In the fabrication of the diving-board electrode the anisotropic etch of choice was EDP used on (100) orientation wafers. The fabrication required an etch

that would attack insulators such as thermal SiO_2 and SiO_xN_y very slowly; would not etch heavily boron-doped regions; and had a well defined undercut rate. Figure 3.3 demonstrates how the etch resistance of boron diffusion can be exploited. A heavily boron-doped epitaxial region followed by a layer with lower doping levels serves as an etch-stop layer and surface doping defines regions that aren't etched by EDP.

Figures 3.4(a),(b) show how it is possible with a system such as EDP on (100) orientation wafers to define a free standing cantilever structure. The convex corner of the diving board is readily attacked by EDP; only (111) planes that intersect in concave corners are protected from EDP. However, atoms at convex corners are exposed and readily attacked by EDP. Figure 3.4(c) shows the undercut proceeding along the (331) planes, with

. (rate of undercut)/(etch rate in the (100) direction) ≈ 0.6 [10].

Wet chemical etching techniques with great selectivity, are extremely easy to use. While useful anisotropic etching methods have been obtained using such techniques as reactive-ion etching, such methods tend to have much slower etch rates and their use is generally limited to smaller geometries.

3.3 Insulators for Saline Environments

A necessary fabrication requirement is a means of insulating the electrode lead that is both biocompatible and capable of standing up to saline for the duration of the experiment. In addition it may be necessary to pattern the passivation layer. Such long-term passivation of sensors remains a difficult problem [11] without a standard solution. Choosing an insulation is a compromise between equipment availability, cost, fabrication time, and film properties.

The available insulating layers can be grouped into polymers and dielectrics such as oxides and nitrides. The success of polymer encapsulants requires that

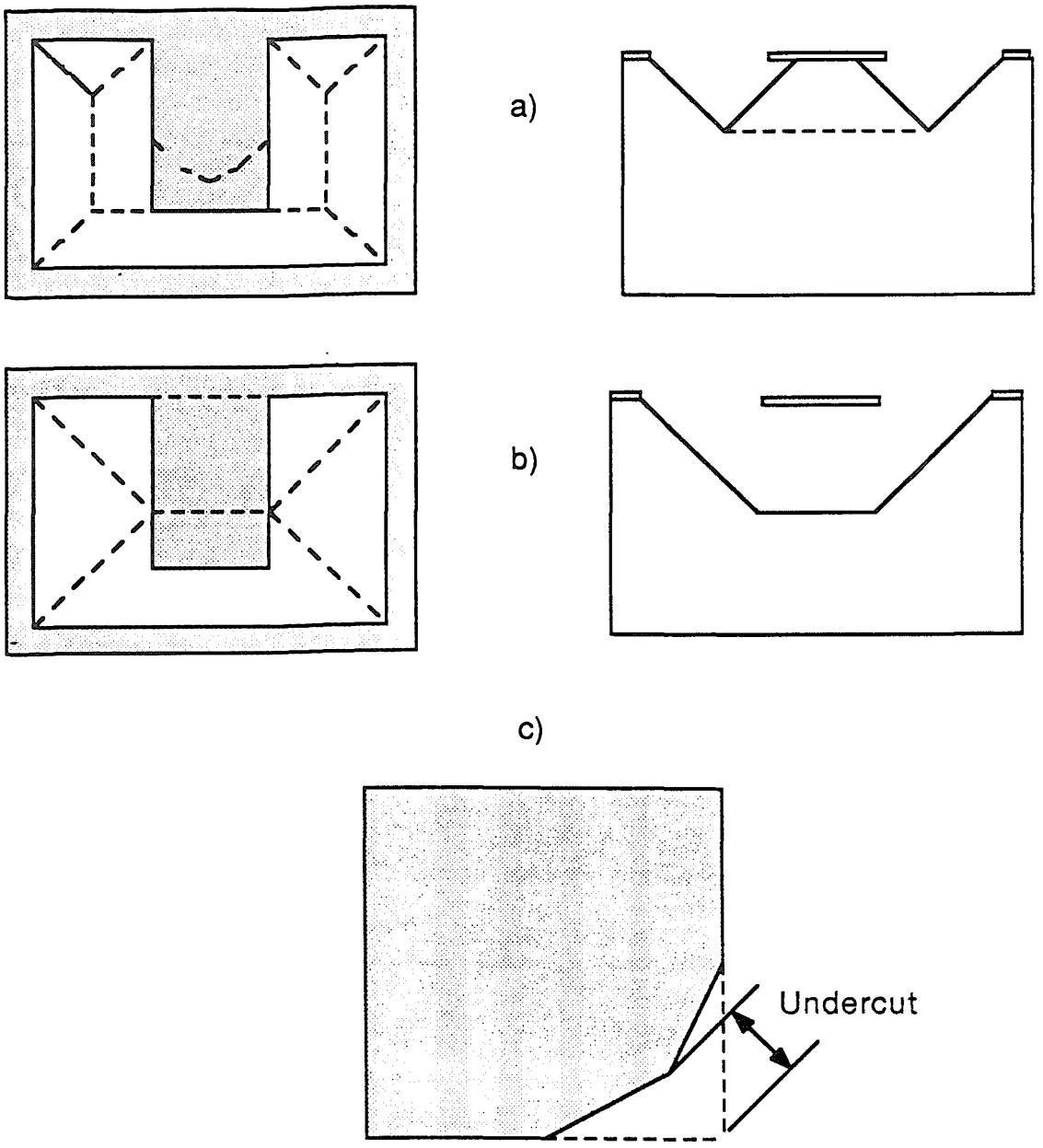

Figure 3.4. Etching of a cantilever in (100) silicon using EDP. (a) Etch not complete showing partial undercut of the cantilever (b) Etch complete and cantilever is free standing over a pyramidal pit bounded by (111) planes. (c) Undercut of a corner using EDP and (100) silicon.

the insulating layer adhere well to the substrate [12]. Parylene C [13] is a vapor deposited polymer with low water vapor permeability [14]. Various devices insulated with Parylene C have survived for a matter of months. However, the adhesion to gold is poor; Parylene coatings are susceptible to mechanical stress; a dedicated deposition system is required; and the films are difficult to pattern. Silicone rubber is a polymer that has been used successfully for passivating lead wires in saline for several years [15]. Polyurethane, is stiffer, with a higher tear strength than silicon rubber [16], but which is susceptible to stress cracking. Polysiloxane resin *Dow Corning* DC648 has been used for up to 2 months [16]-[19]. Patterns were defined by laser deinsulation of the electrode sites, a technique that is inferior to photolithography.

There are a large number of polymers with desirable properties that are easily patterned, without requiring expensive deposition systems. Layers can be spun on, with layer thickness determined by viscosity and spin speed. Positive photoresists such as *Shipley* 1350J have been used successfully for days [20], but scratch resistance is poor, and after several days adhesion is a problem and insulation is compromised. Negative photoresists such as KTFR and KTI732 (KTI Chemicals, Sunnyvale) have been used to insulate electrode leads for up to 3 months [21,22]. Dupont pyralin 2555 is a polyimide that has been used for 25 days in saline using adhesion promoter VM-651 [23]. We have found adhesion to be better with an aluminum oxide adhesion layer. A thin aluminum oxide layer is applied to the wafer either by using *Hitachi PIQ-Coupler-3* or by evaporating 30Å of aluminum. The thin layer of aluminum oxidizes at the temperatures necessary to cure the polyimide, becoming transparent and nonconductive. Pyralin 2555 is not photosensitive, and must be patterned with a photoresist such as 1350J. Fabrication time is reduced by using a negative

photosensitive polyimide, *MRK Selectilux HTR 3–50.* Using a 30Å thick layer of aluminum oxide both *Selectilux* and pyralin 2555 insulated dishes have been used for up to 3 months without deterioration of the insulation. None of these insulating layers are very scratch resistant, and their adhesion is poor in etches such as EDP.

Other dielectrics such as silicon dioxide and silicon nitride can be used for insulations. These films can be deposited via several different techniques, with film quality being very process dependent. Many dielectrics can be deposited by evaporation to form thin films [28]–[29]. A source is heated with either an electron beam or a resistor, it vaporizes, and then transverses the space between the source and the substrate to condense and form a thin film on the substrate. Since evaporations are typically conducted at low pressures (about 1×10^{-6} torr) from essentially point sources, film deposition is very directional, resulting in nonconformal films with poor step coverage.

At high temperatures in either steam or O_2 thermal SiO_2 can be grown on silicon [14]–[15]. This is a very high quality oxide, being attacked very slowly by etches such as EDP, and having been used as an insulting layer in saline environments [11]. However, the usefulness of such oxides is limited, since they must be grown at very high temperatures on bare silicon surfaces.

Insulating oxide films can be electrolytically deposited [11],[24]–[25]. Tantalum pentoxide is the most promising of these, having been shown to be stable *in vivo* and insoluble in saline. However, tantalum has disadvantages: it cannot be thermally evaporated due to the very high temperatures required ($> 3000°C$), so that e-beam evaporation is necessary; and it is not possible to directly wire bond to tantalum.

Sputtering can also be used to deposit dielectrics [30]–[34]. An RF power

source is used to accelerate ions, usually Ar^+, towards a target. These ions strike the target and dislodge primarily neutral target atoms which condense to form thin films. Sputtering has many advantages over other deposition techniques: a wide variety of materials can be deposited including insulators, alloys, and refractory materials; adhesion is generally good; and substrate deposition temperatures are low. When using an inert carrier gas such as argon the material to be deposited must be available in sheet form. It is also possible to deposit a compound made up of the target material reacted with the sputtering gas. For example oxides such as SiO_2 are formed by sputtering with a silicon target with a sputtering gas that is a mixture of oxygen and argon, and nitrides such as Si_3N_4 are formed using either NH_3 or N_2 as the active gases. While film quality and step coverage is typically better than that of evaporated films, dielectrics deposited by chemical vapor deposition (CVD) are generally superior.

CVD coatings are in general of high quality, and etch resistant, with good step coverage [29], [35]–[36]. In this process gases at a certain temperature react to form a solid. For example at 400°C

$$3\,SiH_{4(g)} + 4\,O_{2(g)} \rightarrow SiO_{2(s)} + 12H_{2(g)}.$$

While CVD SiO_2 can be deposited at temperatures low enough to be compatible with metals such as gold, such layers tend to have poor step coverage and pinhole defects are a problem due to particles loosely adhering to the reactor walls [29]. Such CVD SiO_2 layers have been used to insulate electrodes for several weeks [37]. At 700°C–1150°C and atmospheric pressure ammonia and monosilane react to form silicon nitride

$$3\,SiH_{4(g)} + 4\,NH_{3(g)} \rightarrow Si_3N_{4(s)} + 12H_{2(g)}.$$

Silicon nitride layers produced in this manner are excellent diffusion barriers to water and sodium, and have been used to encapsulate an MOS capacitor im-

mersed in saline for one year with no change in device characteristics [11]. Film uniformity and step coverage due to gas streaming in CVD films produced at atmospheric pressure can be improved by depositing at low pressures (LPCVD). However, the high temperatures required for film deposition are undesirable: differences in thermal expansion coefficients result in large stresses, impurities diffuse, materials can form undesirable alloys, and metals such as gold and aluminum cannot be used. Such fabrication difficulties can be overcome using metals such as tantalum, and very large stresses due to thermal expansion mismatch by depositing alternating layers with thermal expansion coefficients chosen to give the desired stress [38]. However, this complicates fabrication considerably, and it is difficult to reliably have two very large stresses (greater than 1×10^{10} dynes/cm^2) cancel each other.

Using a plasma, rather than thermal energy, to provide the activation energy for reactions facilitates deposition of high quality films at low temperatures [36],[39]-[41]. An RF discharge accelerates electrons which excite ions and neutral particles through collisions which react to form a solid on the substrate surface. The electrons and ions are not in thermal equilibrium, with the electrons being at much higher temperatures than ions, neutral particles, and the substrate. The reaction is very complicated, and the resulting films are amorphous and contain large amounts of hydrogen. Consequently PECVD silicon nitride films are less resistant to etches than CVD nitride produced at 900°C. None the less, PECVD Si_3N_4 layers provides excellent scratch resistance, good step coverage, and are an effective barrier to water and sodium diffusion. In addition silicon oxinitride can be deposited by reacting silane with a combination of ammonia and nitrous oxide. This allows excellent control over the stress in the deposited layer. Since PECVD films can be deposited at temperatures down to

200°C dielectrics deposited in this manner are compatible with any metallization layer.

PECVD silicon oxinitride was chosen as the insulating layer for the diving-board electrode based upon: machine availability, slow etch rates in EDP, low deposition temperatures, superior adhesion and insulting properties, and ability to control the stress. PECVD of thin films is a complicated process with many variables: temperature, relative flow rates of the different gases, power density and frequency, and pressure. Film properties such as stress, growth rate, refractive index, uniformity, and adhesion are machine dependent.

PECVD silicon-oxynitride films are deposited in a *Pacific Western Systems* 450 Vertical Parallel Plate Plasma Reactor as shown in Figure 3.5 [42]. Substrates are held vertically in a graphite boat to reduce contamination from particles falling from the reactor walls. Graphite is used as the electrically conductive boat due to its low thermal expansion coefficient and low reactivity. A custom graphite boat can hold 4″ wafers, 3″ wafers, 2″ wafers, and substrates as small as 1″ × 1″. The reactor is a vacuum sealed quartz tube contained within a three-zone furnace capable of attaining temperatures up to 500°C. RF power to the boat consists of pulses of 440 KHz with a pulse separation of 8 msec and a variable duration depending on the desired average power level.

Depositions are typically performed at 1-2 Torr with total gas flow rates in the range 1000-2000 sccm. A roots blower pump [43] backed by a vane pump is used to move such large volumes at low pressures. High flow capacity particulate filters and dilution of process gas with nitrogen protect the pumps from damage. Pressure is maintained using a *Vacuum General Controller* that compares the desired pressure to the actual pressure and adjusts a throttle valve between the reaction chamber and the vacuum system accordingly. Pressure is detected

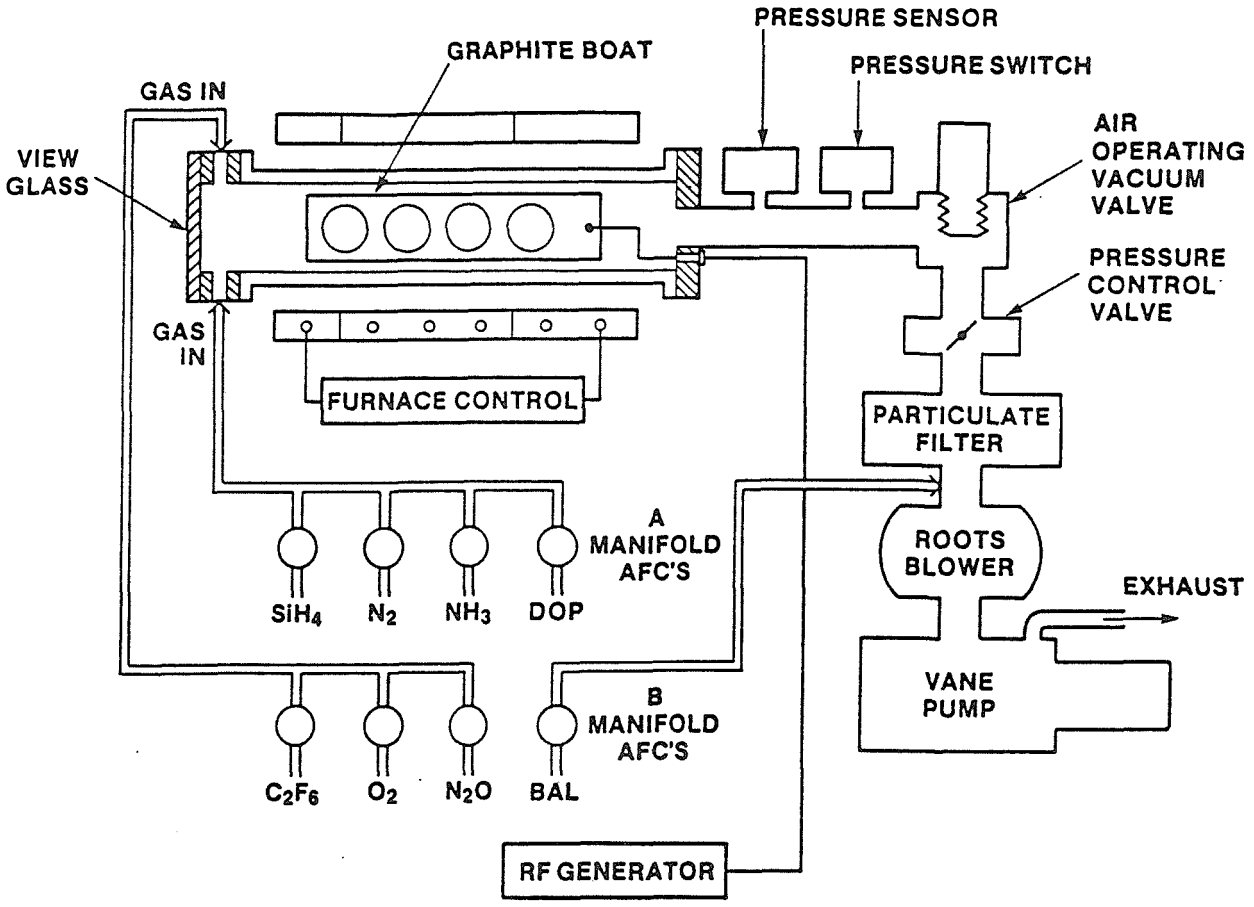

Figure 3.5. Schematic diagram of PWS 450 used in deposition of PECVD silicon-oxynitride layers.

by a capacitance manometer (*MKS Baratron*) that gives an absolute pressure insensitive to the chemical composition of the gas.

The flow rates of eight gases are controlled by automatic flow controllers. Typically SiH_4, NH_3, and N_2O, are reacted to form SiN_xO_y. Nitrogen is used to backfill the system, and CF_4 and O_2 are used to clean the system.

3.4 Electrode Fabrication

The diving-board electrode is made by a five-mask process as shown in Figure 3.6 (see Appendix for detailed procedure). The first mask defines the

cup structure. The outer rim of this cup forms the seal with the cell, and the cup must be deep enough to keep the metal surface away from the surface of the cell. The silicon is etched to a depth of 3 μm using an isotropic silicon etch: 100 HNO_3 /100 CH_3COOH /15 HF [5]. Once this cup structure is defined it is necessary to use a thick photoresist with good step coverage; a 3 μm thick layer of *Shipley* 1400–37 photoresist is compatible with 3 μm cup structures and 2 μm line widths.

The second mask defines a pedestal to which the wire bond is attached, and which is glued to the bottom of the culture dish. While the pedestal should be mechanically strong, it cannot be thicker than a cell, 10 μm–50 μm. The height is determined by a boron etch-stop process [44]–[46]; therefore working with very thin substrates is unnecessary. A 1 μm thick thermal oxide layer is grown and then patterned with buffered HF to define the intended pedestal area. This is followed by boron diffusion for 10 hours at 1170°C in a 5% O_2 / 95% N_2 atmosphere that heavily dopes the substrate in what is to be the pedestal region to a concentration exceeding $5 \times 10^{19} cm^{-3}$ to a depth of 10 μm. The boron-glass layer on the surface of the wafer is removed by oxidizing for one hour at 1100°C in dry O_2 and etching with buffered HF.

A 1000 Å thermal oxide is grown at 1000°C in steam for 10 minutes, and the third mask defines the contact hole in this layer. In addition to being important for its insulating properties, this thin oxide is important because it touches the cell. This surface is a high quality glass, which seems important for high resistance seals comparable to those of patch pipettes.

Next 100 Å of chrome, 800 Å of gold, 100 Å of chrome are successively evaporated on the wafer, and mask four defines the metal pattern. The top layer of chrome is etched with *Transene Chromium Mask Etchant* for 15 seconds; the

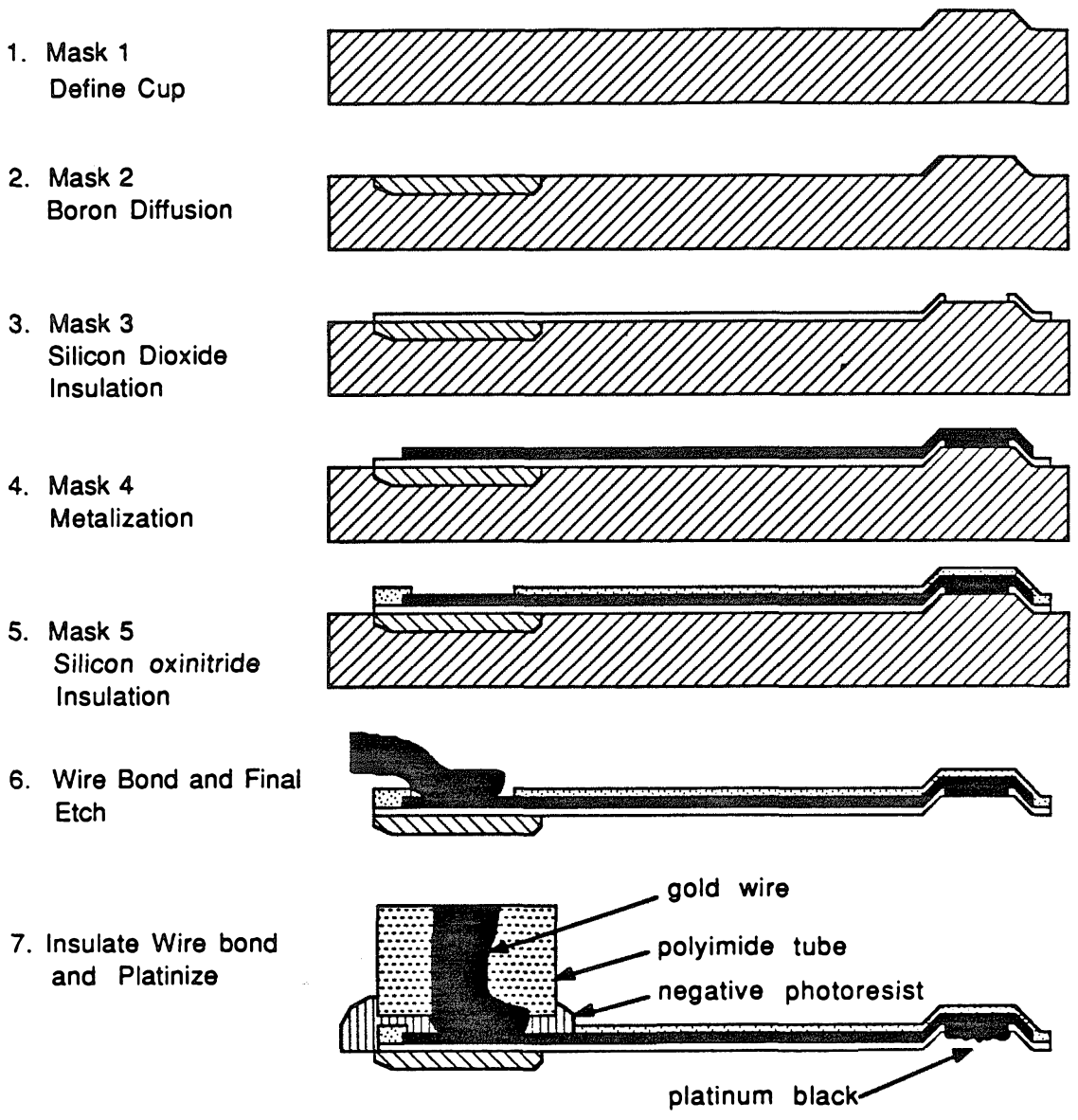

Figure 3.6. Fabrication procedure for the diving-board electrode.

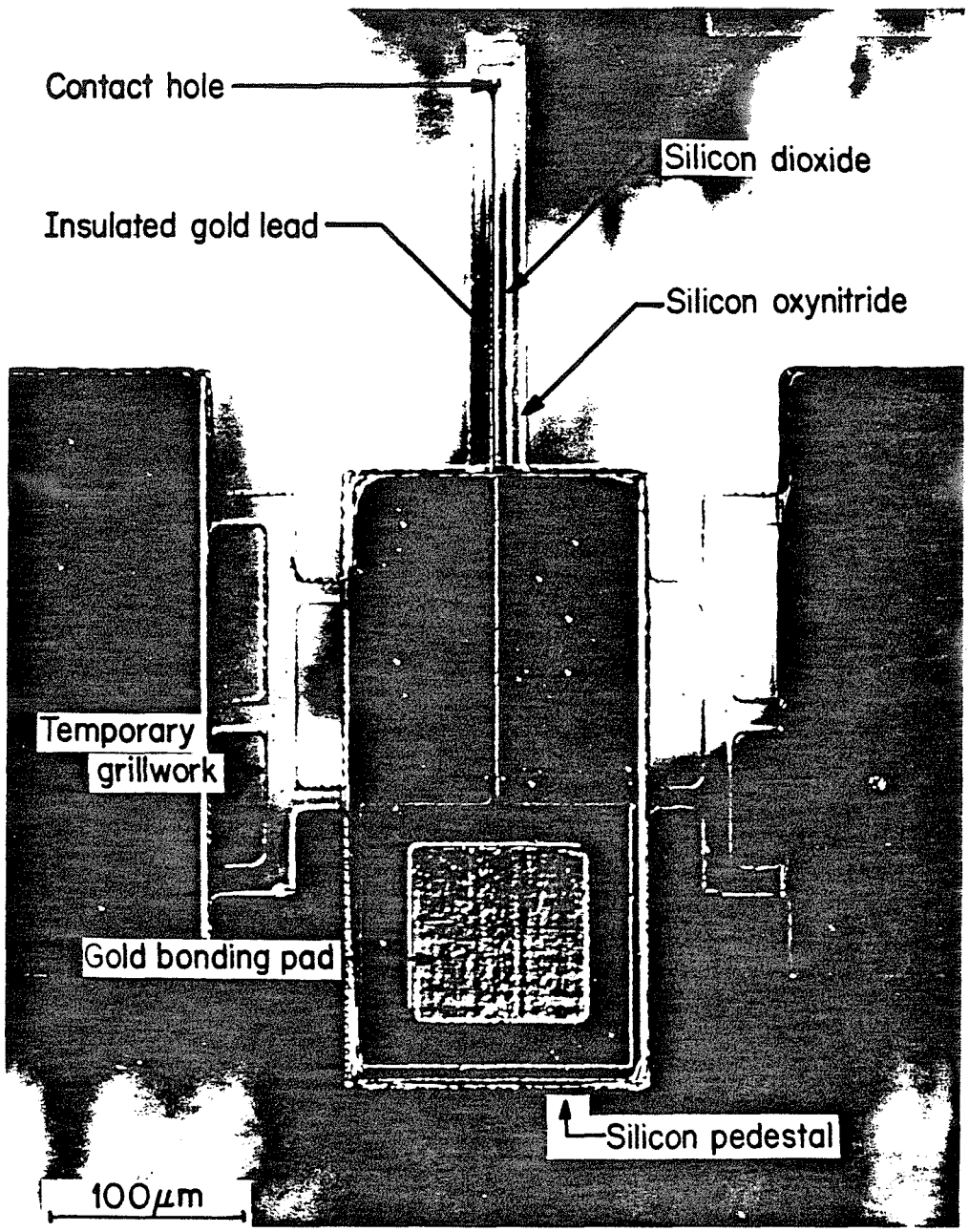

Figure 3.7. Diving board electrode after removal from EDP. There would normally be a 25 μm diameter wire bonded to the gold pad at the back of the pedestal.

gold is removed in 30 seconds in *Transene TFA Gold Etchant* that has been diluted 1:4 with water [47]; followed by another 15 seconds in the chrome etch.

Then 1 μm of silicon oxinitride is deposited by PECVD to form the top insulating layer [48], [49]. This layer determines the mechanical properties of the diving board, as well as defining tabs that later hold the electrodes in place, to protect them from damage. The final mask patterns this top insulating layer, which is etched in a 85% CF_4/15% O_2 plasma [50]. A 7 μm thick layer of *Shipley* AZ4770 photoresist is used for this step to insure protection of the cap region during the plasma etch.

The wafer is scribed and broken into 4 mm $\times$ 20 mm pieces, each of which is glued to a piece of glass. Then a wire bond is made from a large gold bonding pad on the piece of glass to each of about 40 devices. The bonds are made of gold so that they will survive the next etching step. Now the wafer is ready to be etched in an ethylenediamine, pyrocatechol, and water (EDP) solution [6], [7]. This etch attacks different silicon planes at different rates, but etches $\langle 111 \rangle$ planes very slowly. Furthermore it does not attack regions that are doped with boron to levels in excess of $5 \times 10^{19} \mathrm{cm}^{-3}$. After three hours in EDP at 100°C the undoped silicon is completely etched from beneath each electrode. Figure 3.7 show the device after the EDP etch. Each electrode is temporarily held to the substrate by a silicon-oxinitride grill.

Next each device is separated from the wafer and the wire bond is insulated. Each lead wire is manually loaded into a polyimide tube (*Polymicro Technologies* i.d. 120 μm, o.d. 150 μm) and the wire bond is insulated by painting with negative photoresist. This polyimide tube can be held by tweezers and manipulated into place without compromising the insulation. The final step is to electroplate the electrode at the bottom of the diving board with platinum black, to produce a

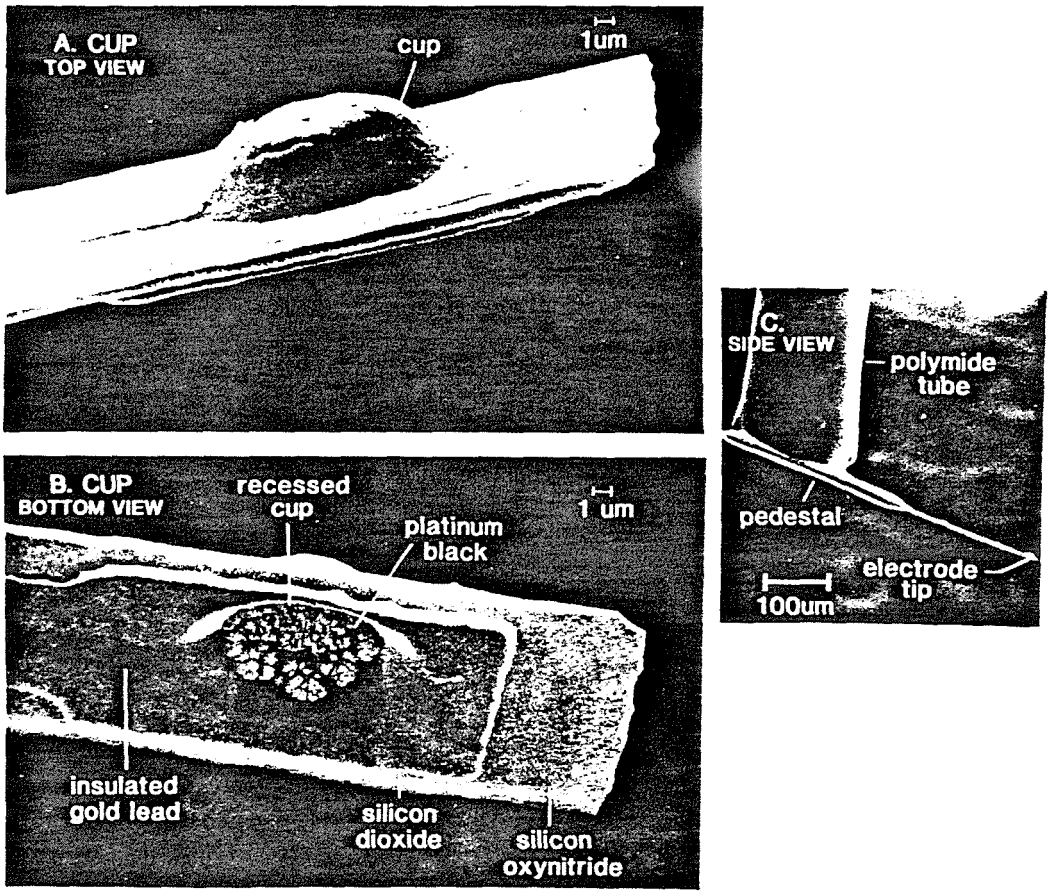

Figure 3.8. A finished diving-board electrode. (a) top view of the cup structure that is to fit above the neuron. (b) bottom view of the cup structure. (c) overview of the electrode.

low impedance contact to the electrolyte [51]. By electroplating with a current of 2 nA (about 10 mA/cm^2) for 15 seconds the electrode impedance at 1 kHz drops from 25 MΩ to below 1 MΩ, while the platinum remains thin enough that it does not interfere with the seal.

Figure 3.8 shows scanning electron micrographs of the cup structure, and an overview of a finished electrode. It takes an average of about 45 minutes to fabricate and test each device. Defective electrodes are eliminated on the basis of optical observations and impedance measurements made before platinization. Satisfactory electrodes can be reused several times.

3.5 Mechanical Properties of Diving-Board Electrode

In addition to considering the electrical properties of the diving-board electrode, it is necessary to take into account its mechanical properties. A relatively flat diving board is necessary to make it possible to simultaneously contact the pedestal with the bottom of the culture dish and the electrode tip with the neuron, and to make the force exerted by the electrode on the cell downward without a lateral force that would tend to force the cell out from beneath the diving board.

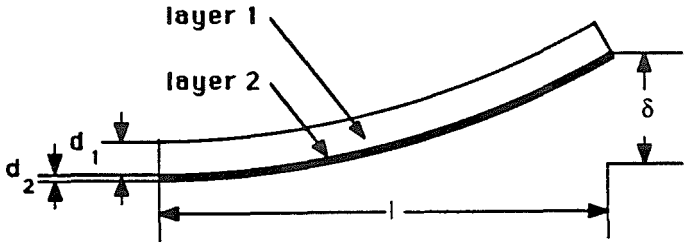

Figure 3.9. Bending due to stress in a two-layer cantilever.

However, there are stresses in each layer which may bend the diving board. This is illustrated in Figure 9, which shows a cantilever of length l that is composed of two layers of thickness d_1 and d_2. The Young's modulus of the thick layer is given by Y_1, and the Poisson's ratio is ν_1. A stress σ in layer 2 bends the beam an amount δ. For small deflections and $d_1 \gg d_2$ [52], we can write

$$\delta = \frac{3l^2(1-\nu_1)\sigma d_2}{Y_1 d_1^2}. \tag{1}$$

In our electrodes, the thick layer is silicon oxinitride, 200 μm long and 1 μm thick. Young's modulus, Y_1, 1×10^9 dynes/cm^2 [53] and the Poisson ratio ν_1 is 0.2. If $d_2 = 0.2\,\mu$m a stress typical of insulating dielectrics of $\sigma = 5 \times 10^{12}$ dynes/cm^2, would cause an unacceptably large beam deflection of 100 μm. If the stress is compressive it will cause the cantilever to bend up as in the diagram, while if the stress is tensile the cantilever will bend down.

The present fabrication technique minimizes the deflection of the cantilever in two ways. First, the silicon-oxinitride layer is made very rigid compared to the other two layers by making it much thicker than the gold and the oxide layer, and by making the surface areas of the gold and the silicon dioxide layers small compared to the surface area of the oxinitride layer. Second, the stress of the silicon oxinitride layer is empirically adjusted to minimize the beam deflection.

Consider the three layer structure of the diving board as represented in Figure 3.10. Layer 1 is silicon oxinitride, layer 2 is gold, and layer 3 is silicon dioxide. The stresses of the films on the silicon substrate are σ_1, σ_2, and σ_3. When the cantilever has been freed from the substrate, layer 1, which is much thicker than the other two layers, relaxes to a stress–free state, $\sigma_1^* = 0$. The stresses in the other two layers become $\sigma_2^* = \sigma_2 - (Y_2/Y_1)\sigma_1$ and $\sigma_3^* = \sigma_3 - (Y_3/Y_1)\sigma_1$ for $d_1 \gg d_2$ and $d_1 \gg d_3$, and $\nu_1 \approx \nu_2 \approx \nu_3$. The surface areas of

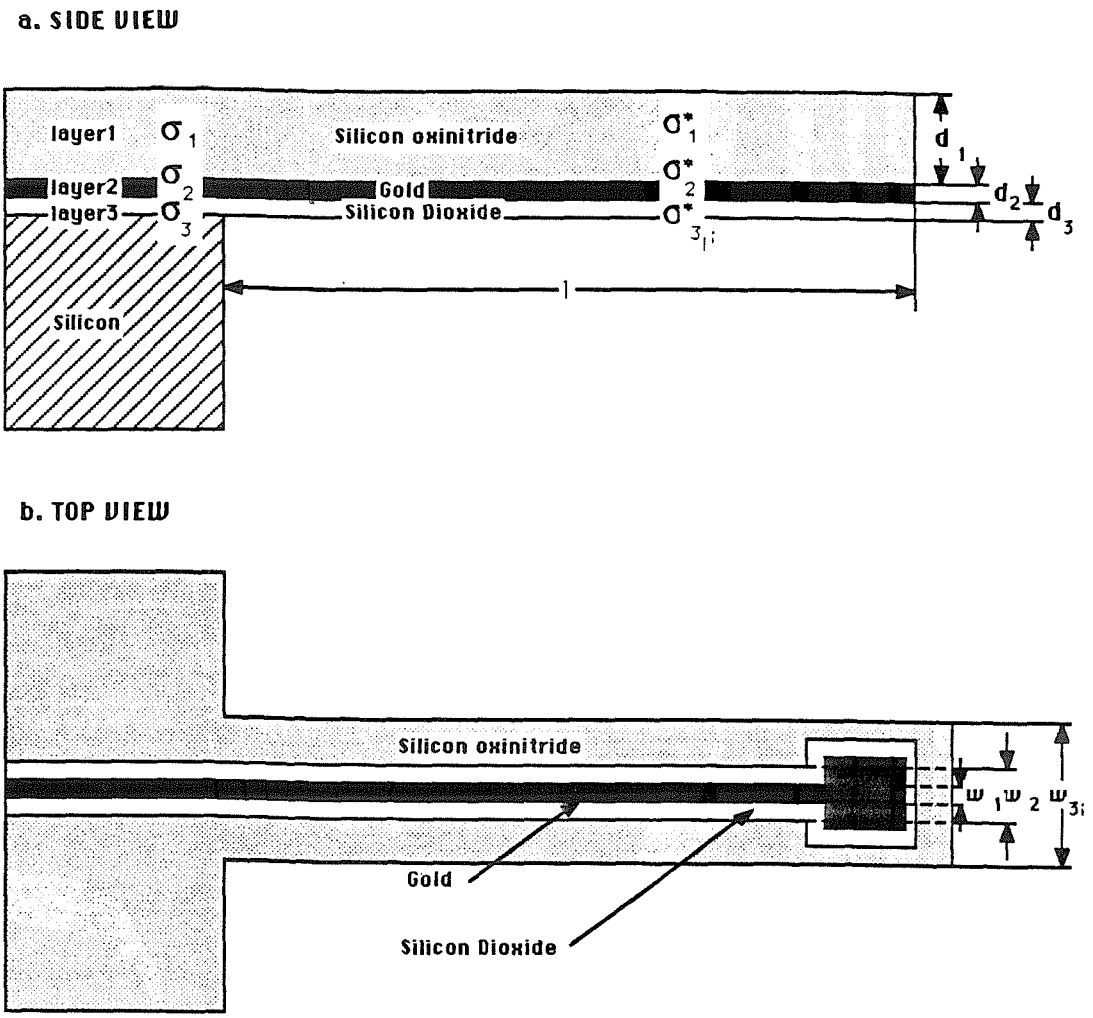

Figure 3.10. (a) Side view of three layer cantilever. (b) Top view of three layer cantilever.

layer 2 and layer 3 relative to layer 1 are given by $f_2 = w_2/w_1$ and $f_3 = w_3/w_1$. The beam deflection is given by:

$$\delta = \frac{3l^2(1-\nu_1)}{Y_1 d_1^2}\left(\sigma_2^* d_2 f_2 + \sigma_3^* d_3 f_3\right) = \delta_2 + \delta_3 \qquad (2)$$

So that if it is possible to vary the stress in any one of the layers sufficiently to have $\delta_2 = -\delta_3$ then the cantilever can be made flat.

It is difficult to change the stress in the gold and silicon-dioxide films in our electrodes, but we can vary the stress in the silicon-oxinitride films by adjusting the ratio of oxygen to nitrogen in the film. This is done by varying the flow rates of N_2O and NH_3 during the PECVD process (Figure 3.11). By depositing the silicon oxinitride layer at 350°C at a pressure of 1.5 torr, with flow rates of $NH_3/N_2O/SiH_4$ being 750/1150/250 $[N_2O]/[N_2O+NH_3]$=0.67), the deposited layer had a tensile stress of 1.4×10^9 dynes/cm^2 and the resulting diving-board electrodes are flat to a few microns.

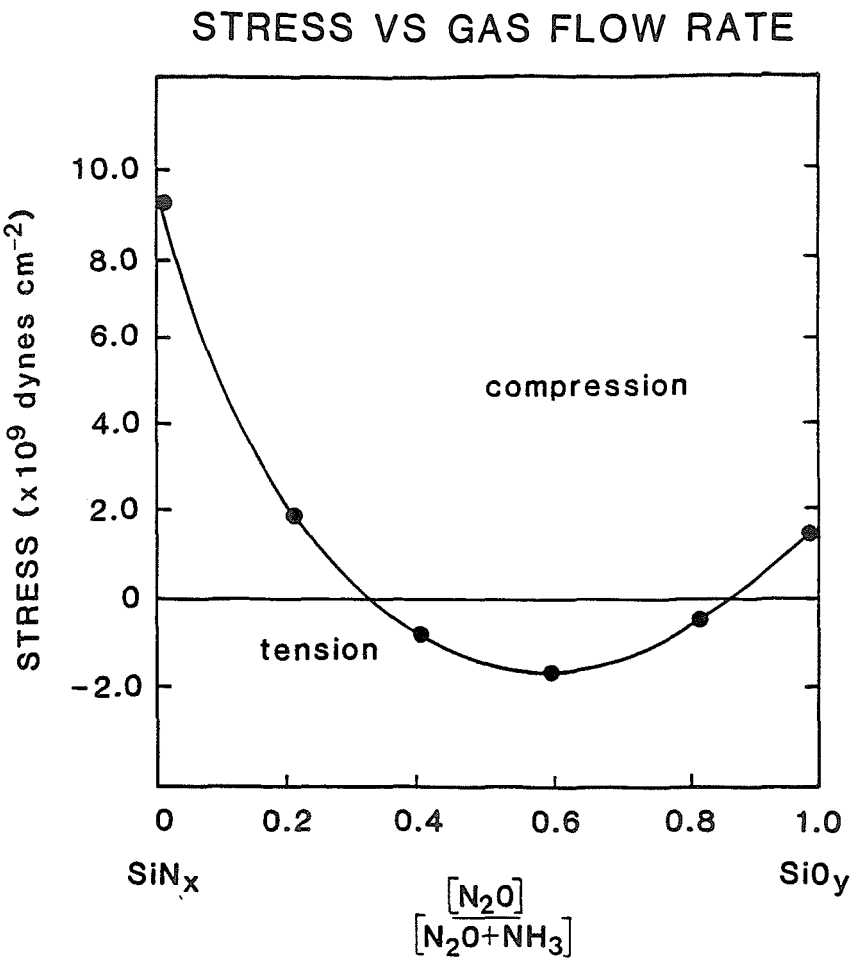

Figure 3.11. Controlling the stress in oxinitride films by varying the flow rates of N_2O and NH_3 [54]. The films are deposited at 350°C on silicon. The x-axis is the ratio of the N_2O flow rate to the total combined flow rate of N_2O and NH_3. When the ratio is zero the film is silicon nitride, and when the ratio is one the film is silicon dioxide.

References

[1] K. E. Peterson, "Silicon as a mechanical material", *Proc. IEEE*, vol. 70, no. 5, pp. 420–457, 1982.

[2] J. B. Angell, S. C. Terry, and P. W. Barth, "Silicon micromechanical devices," *Scientific American*, pp. 44-55, April 1983.

[3] K. D. Wise, "Silicon micromachining and its application to high performance integrated sensors," *Micromachining and Micropackaging of Transducers*, eds. C. D. Fung, P. W. Chueng, W. E. Ko, and D. G. Fleming, Elsevier Science Publishing Inc., New York, 1985.

[4] C. D. Fung, P. W. Chueng, W. E. Ko, and D. G. Fleming, eds., *Micromachining and Micropackaging of Transducers*, Elsevier Science Publishing Inc., New York, 1985.

[5] B. Schwartz and H. Robbins, "Chemical etching of silicon, IV. The system HF, HNO_3, $HC_2H_3O_2$, *J. Electrochem. Soc.*, vol. 106, p. 505, 1959.

[6] R. M. Finne, and D. L. Klein *J.Electrochem. Soc.*, "A water-amine-complexing agent system for etching silicon," vol. 114, pp.965–970, Sept. 1967.

[7] A. Reisman, M. Berkenblit, S. A. Chan, F. B. Kaufman, and D. C. Green, "The controlled etching of silicon in catalyzed ethylenediamine-pyrocatechol-water solutions," *J. Electrochem. Soc.*, vol. 126, no. 8, pp.1406–1415, 1979.

[8] D. L. Kendell, and G. R. de Gruel, "Orientations of the third kind: the coming of age of (110) silicon," *Micromachining and Micropackaging of Transducers*, eds. C. D. Fung, P. W. Chueng, W. E. Ko, and D. G. Fleming, Elsevier Science Publishing Inc., New York, 1985.

[9] E. Bassous, "Fabrication of novel three-dimensional microstructures by the anisotropic etching of (100) and (110) silicon," *IEEE Trans. Electron. Devices*, vol. ed-25, no. 10, pp. 1178–1184, Oct. 1978.

[10] K. E. Bean, "Anisotropic etching of silicon," *IEEE Trans. Electron. Devices*, vol. ed-25, no. 10, pp. 1185–1193, Oct. 1978.

[11] L. Bowman, and J. D. Meindl, "The packaging of implantable integrated sensors," in *IEEE Trans. Biomed. Eng.*, vol. BME-33, no. 2, Feb. 1986, pp. 248-255.

[12] P. E. K. Donaldson, "Experimental visual prosthesis," *IEEE Proc.*, vol. 120, pp. 281-298, Feb. 1973.

[13] Union Carbide Corp., Bound Brook, NJ.

[14] G. E. Loeb, M. J. Bak, M. Salcman, and E. M. Schmidt, "Parylene as a chronically stable, reproducible microelectrode insulator," IEEE Trans. Biomed. Eng., vol. BME-24, pp. 121-128, Mar. 1977.

[15] G. E. Loeb, C. L. Byers, S. J. Rebscher, D. E. Casey, M. M. Fong, R. A. Schindler, R. F. Gray, and M. M. Merzenich, "Design and fabrication of an experimental cochlear prosthesis,"*Med. Biol. Eng. Comput.*,vol.21, pp.241-254, May 1983.

[16] G. W. Gross, "Simultaneous single unit recording *in vitro* with a photoetched laser deinsulated gold multimicroelectrode surface," *IEEE Trans. Biomed.*

Eng., vol. 26, pp. 273-279, 1979.

[17] G. W. Gross, A. N. Williams, and J. H. Lucas, "Recording of spontaneous activity with photoetched microelectrode surfaces from spinal cord neurons in culture," *J. Neurosc. Methods*, vol. 5, pp. 13–22, 1982.

[18] G. W. Gross, W. Wen, and J. Lin, "Transparent indium-tin oxide electrode patterns for extracellular, multisite recording in neuronal cultures," *J. Neurosci. Methods* vol. 15, pp. 243-252, 1985.

[19] M. H. Droge, G. W. Gross, M. H. Hightower, and L. E. Czisny, "Multielectrode analysis of coordinated, multisite, rhythmic bursting in cultured CNS monolayer networks," *J. Neurosci.*, vol. 6, no. 6, June 1986.

[20] C. A. Thomas, Jr., P. A. Springer, G. E. Loeb, Y. Berwald-Netter, and L. M. Okun, "A miniature microelectrode array to monitor the bioelectric activity of cultured cells," *Exp. Cell Res.*, vol. 74, pp. 61–66, 1972.

[21] M. Kupperstein, and D. A. Whittington, "A practical 24 channel microelectrode for neural recording *in vivo*, *IEEE Trans. Biomed. Eng.*, vol. BME-28, no 3, March 1981.

[22] D. A. Israel, W. H. Barry, D. J. Edell, and R. G. Mark, "An array of microelectrodes to stimulate and record from cardiac cells in culture," *Am. J. Physio.*, vol. 247, pp. H669–H674, 1984.

[23] J. L. Novak, B. C. Wheeler, "Recording from the *Aplysia* abdominal ganglion with a planar microelectrode array," *IEEE Trans. Biomed. Eng.*, vol. BME-33, no. 2, Feb. 1986.

[24] F. A. Lowenheim, "Deposition of inorganic thin films from solution," in *Thin Film Processes*, ed. J. L. Vossen, and W. Kern, Academic Press, New York, 1978, pp. 209-255.

[25] P. E. K. Donaldson, "The stability of tantalum pentoxide films *in vivo*," *Med. Biol. Eng.*, vol. 12, pp. 131-135, Jan. 1974.

[26] L. E. Katz,"Oxidation," in *VLSI Technology*, ed. S. M. Sze, p. 194, 1983.

[27] A. S. Grove, *Physics and Technology of Semiconductor Devices*, Wiley, New York, 1967.

[28] R. Glang, "Vacuum evaporation," in *Handbook of Thin Film Technology*, ed. L. I. Maissel and R. Glang, McGraw-Hill Book Company, New York, pp. 1-1–1-300, 1970.

[29] A. C. Adams,"Dielectric and polysilicon film deposition," in *VLSI Technology*, ed. S. M. Sze, pp. 93-129, 1983.

[30] L. Maissel, "Application of sputtering to the deposition of films," in *Handbook of Thin Film Technology*, ed. L. I. Maissel and R. Glang, McGraw-Hill Book Company, New York, pp. 4-1–4-44, 1970.

[31] J. L. Vossen, J. J. Cuomo, "Glow Discharge Sputter Deposition," in *Thin Film Processes*, ed. J. L. Vossen, and W. Kern, Academic Press, New York, 1978, pp. 12-62.

[32] J. A. Thornton, and A. S. Penfield, "Cylindrical Magnetron Sputtering," in *Thin Film Processes*, ed. J. L. Vossen, and W. Kern, Academic Press, New York, 1978, pp. 76-110.

[33] D. B. Fraser, " The sputter and S-Gun magnetrons,"in *Thin Film Processes*, ed. J. L. Vossen, and W. Kern, Academic Press, New York, 1978, pp. 115-128.

[34] R. K. Waits, "Planar Magnetron Sputtering," in *Thin Film Processes*, ed. J. L. Vossen, and W. Kern, Academic Press, New York, 1978, pp. 131-170.

[35] W. Kern and V. S. Ban, "Chemical vapour deposition of inorganic thin films," in *Thin Film Processes*, ed. J. L. Vossen, and W. Kern, Academic Press, New York, 1978, pp. 258-320.

[36] T. Sugano, *Applications of plasma processes to VLSI technology*, John Wiley & Sons Inc., New York, 1985.

[37] J. Pine, "Recording action potentials from cultured neurons with extracellular microcircuit electrodes," *J. Neurosc. Methods*, vol. 2, pp. 19–31, 1980.

[38] K. Najafi, K. D. Wise, and T. Mochizuki, "A high-yield IC-compatible multichannel recording array,"*IEEE Trans. Electron. Devices*, vol. ed-32, no. 7, pp. 1206-1211, July 1985.

[39] J. R. Hollahan, and R. S. Rosler, "Plasma deposition of inorganic thin films," in *Thin Film Processes*, ed. J. L. Vossen, and W. Kern, Academic Press, New York, 1978, pp. 335-358.

[40] H. Yasuda, "Glow discharge polymerization," in *Thin Film Processes*, ed. J. L. Vossen, and W. Kern, Academic Press, New York, 1978, pp. 361-396.

[41] A. R. Reinberg, "Plasma deposition of inorganic thin films," *Ann. Rev. Mater. Sci.*, vol. 9, pp. 341-72, 1979.

[42] W. R. Snow, "PWS 450 COYOTE: A vertical parallel plate plasma reactor for silicon nitride deposition," Pacific Western Systems Application Note, March 1981.

[43] R. Glang, "High-vacuum technology," in *Handbook of Thin Film Technology*, ed. L. I. Maissel and R. Glang, McGraw-Hill Book Company, New York, pp. 2-7–2-8, 1970.

[44] Sohio Carborundum PDS Planar Diffusion Sources: Technical Information, 1986.

[45] D. Rupprecht, and J. Stach, "Oxidized boron nitride wafers as an *in-situ* boron dopant for silicon diffusions," *J. Electrochem. Soc.*, vol. 120, no. 9, pp. 1266–1271, 1973.

[46] K. Najafi, K. D. Wise, and T. Mochizuki, "A high-yield IC-compatible multichannel recording array,"*IEEE Trans. Electron. Devices*, vol. ed-32, no. 7, July 1985.

[47] R. Glang and L. V. Gregor, "Generation of patterns in thin films," in *Handbook of Thin Film Technology*, ed. L. I. Maissel and R. Glang, McGraw-Hill Book Company, New York, p. 7–37, 1970.

[48] C. M. Melliar–Smith and C. J. Mogab, "Plasma assisted etching techniques for pattern deliniation" in *Thin Film Processes*, ed. J. L. Vossen and W. Kern, Academic Press, New York, pp. 497–552, 1978.

[49] R. C. Gesteland, B. Howland, J. Y. Lettvin, and W. M. Pitts, "Comments on microelectrodes," *Proc. IRE*, vol. 47, pp. 1856–1862, 1959.

[50] D. S. Campbell, "Mechanical properties of thin films," in *Handbook of Thin Film Technology*, ed. L. I. Maissel and R. Glang, McGraw-Hill Book Company, New York, p. 12–29, 1970.

[51] K. E. Peterson and C. R. Guarnieri, "Young's modulus measurements of thin films using micromechanics," *J. Appl. Phys.*, vol. 50, pp. 6761–6766, 1979.

[52] Figure provided courtesy of W. R. Snow and V. Dunton of *Pacific Western Systems.*

Chapter 4

Stimulating and Recording with Current-Clamped Loose-Patch Electrodes

4.1 Equivalent Circuit

The operation of the diving-board electrode is very much like that of a loose-patch electrode [6]. Figure 4.1(a) shows a schematic of an electrode in contact with a cell and an electrical equivalent circuit. The shunt resistance R_{sh} is greater than 1 G Ω and shunt capacitance C_{sh} is approximately 10 pF, so that for a low seal-resistance the shunt impedance can be ignored. The electrode impedance Z_e depends upon the type of electrode used. In the case of a glass loose-patch electrode it is essentially resistive, and varies between 100KΩ and 1MΩ. For the metal diving-board electrode, Z_e the impedance varies as the area of the exposed metal and is primarily capacitive. It is desirable to have a low electrode-impedance for three reasons. First, it facilitates measuring the seal resistance. Second, for recording, a low impedance electrode reduces the Johnson noise and increases the signal-to-noise ratio. Third, when stimulating, a low impedance electrode helps avoid the problem of gas evolution.

The patch region beneath the electrode in Figure 4.1 is made up of a layer of membrane with a capacitance estimated by assuming a membrane capacitance of approximately 1μF/cm^2; therefore C_{m1} is 1pF for a 100 μm^2 patch. Spanning this membrane are n different channel types with electrochemical driving forces $V_1 ... V_n$. The resistances $R_1 ... R_n$ corresponding to the each particular channel type are voltage and time dependent. The net resistance depends upon the channel densities, which is in general nonuniform over the cell and unknown in the patch region. The whole-cell impedance Z_{m2} is also voltage and time

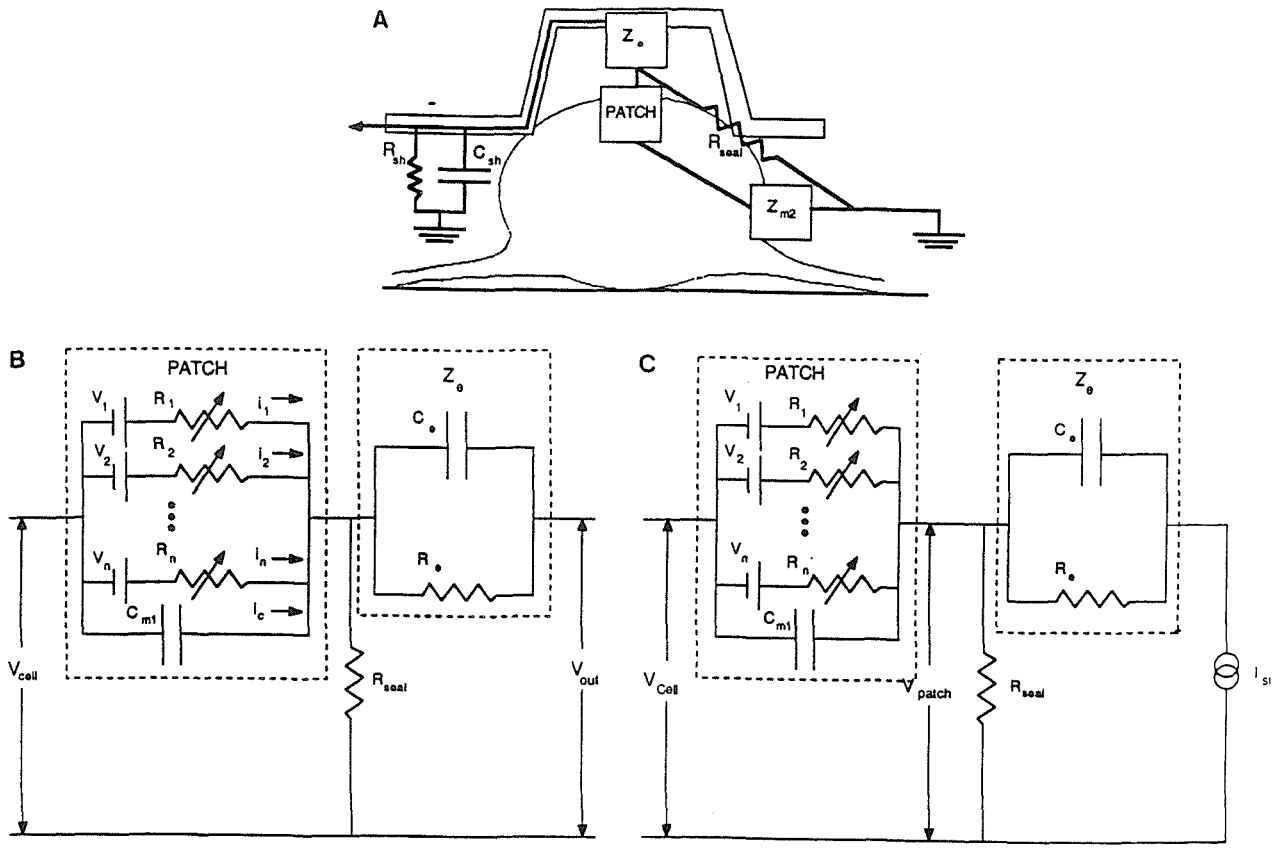

Figure 4.1. (a) Schematic diagram of an electrode in contact with a cell and an approximate equivalent circuit for (b) recording and (c) stimulating.

dependent. At the resting potential of the cell Z_{m2} can be approximated by a capacitor and a resistor in parallel. For *Helisoma* neurons B19 and B5 the resistance is typically about 50 MΩ and the capacitance 500 pF.

The seal resistance R_{seal} should be as large as possible. It is determined by the conductance of the thin film of tissue culture medium between the rim of the electrode and the cell. For *Helisoma* neurons seals of 1–5 MΩ were obtained.

4.2 Recording

Figure 4.1 (b) is an equivalent circuit of a diving-board electrode being used

to record from a neuron. $i_1 ... i_n$ are the currents passing through each particular type of channel, and i_c is the current through the membrane capacitance. The recorded voltage V_{out} is given by:

$$V_{out} = \left(i_c + \sum_{chan=1}^{N} i_{chan}\right) R_{seal} \tag{1}$$

$$V_{out} = \left(C_{m1} \frac{dV_{cell}}{dt} + \sum_{chan=1}^{N} \frac{(V_{cell} - V_{chan})}{R_{chan}}\right) R_{seal} \tag{2}$$

$$V_{out} = V_{cap} + V_{ionic} \tag{3}$$

$$V_{ionic} = V_{Na+} + V_{K+} + V_l + \sum_{chan=4}^{N} i_{chan} \tag{4}$$

Figure 4.2 shows qualitatively the relative contribution of different channels and the capacitive current to the signal recorded by the loose-patch electrode. V_{cap} is the differentiated intracellular voltage seen through the capacitance of the membrane under the electrode. For this signal to be large the action potential must be fast. For the rising phase of the action potential the value of dV_{cell}/dt is approximately 100 mV/msec for *Helisoma* B19 neurons, and 20mV/msec for *Helisoma* B5 neurons. Assuming a membrane area of 100 μm^2, and a seal resistance of 2 MΩ for *Helisoma* B19 neurons $V_{cap} \approx 200\mu$V, and for *Helisoma* B5 neurons $V_{cap} \approx 40\mu$V.

V_{Na+} is the voltage drop across the seal resistance due to current flowing through sodium channels in the patch. The sodium conductance g_{Na+} is voltage and time dependent, and the shape of this curve is given in Figure 4.2 (c). The shape of the contribution of current flowing through the sodium channels is given by, $g_{Na+}(V_{cell} - V_{Na+})$. The contribution per ion channel can be given by

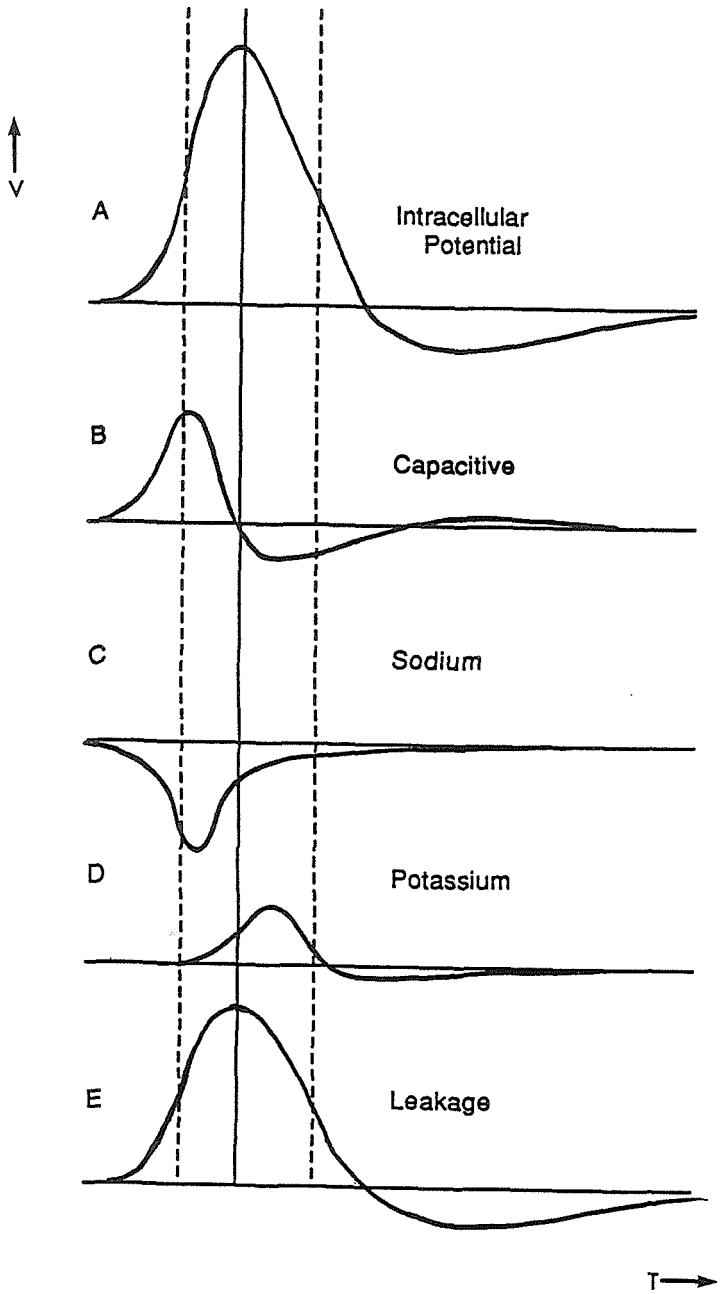

Figure 4.2. (a) intracellular potential (b) capacitive signal through cell membrane (c) signal through sodium channel (d) signal through potassium channel (e) signal through non-ion-selective leakage channels.

assuming a conductance of 10 pS per sodium channel and a maximum driving force of -50 mV, so the maximum voltage contribution per open sodium channel is about -1 μV for R_{seal}=2 MΩ.

V_{K+} is the voltage drop across the seal resistance due to current flowing through potassium channels in the patch. The sodium conductance g_{K+} is voltage and time dependant, and the shape of this curve is given in Figure 4.2 (d). The shape of the contribution of current flowing through the potassium channels is given by, $g_{K+}(V_{cell} - V_{K+})$. The contribution per ion channel can be given by assuming a conductance of 10 pS per potassium channel and a maximum driving force of +50 mV, so the maximum voltage contribution per open potassium channel is about +1 μV for R_{seal}=2 MΩ.

V_l is the voltage drop across the seal resistance due to current flow through . For a leakage resistance $R_l = 1$ GΩ $V_l = 100\,\mu$V. This signal is the intracellular signal attenuated by an amount $R_s/(R_s + R_l)$. By applying large current pulse to the patch electrode it is possible to temporarily make this signal very large by putting holes in the patch beneath the membrane and greatly decreasing the leakage resistance. Ideally one would like this signal to be as large as possible, so that patch recording would make it possible to record post synaptic potentials. This must be balanced with the fact that for seal resistances less than a gigaohm R_l can not be made too small or the cell will be severely damaged. For any given cell type an acceptable maximum leakage resistance $R_l + R_s$ that will not harm the cell can be empirically determined.

While the contributions of sodium channels, potassium channels, and non-selective holes has been shown explicitly, there is also a contribution from the other channels contained in the membrane, such as calcium channels and chloride channels. In general the capacitive contribution has been found to dominate,

except when the leakage resistance has been reduced by a high voltage pulse.

Figure 4.3 compares the intracellular potential, the derivative of the intracellular potential, and the recording from a glass loose-patch electrode. For the *Helisoma* B19 neuron of Figure 4.3(a) the signal is essentially a derivative, but the magnitude of the signal is larger by a factor of 10 than one would predict by using the measured derivative of the action potential, the measured seal resistance, and the predicted area of membrane beneath the patch electrode. This is a consequence of these neurons having a convoluted rather than a smooth membrane, resulting in a very much larger capacitance in the membrane beneath the patch, which in turn results in very much larger extracellular signals. In addition to the large capacitive signals smaller ionic signals were sometimes seen, as in Figure 4.3(b). The small negative signal superimposed on the capacitive signal during the rising phase of the action potential are presumably due to sodium channels contained in the patch beneath the membrane.

The signal-to-noise ratio can be determined by considering the noise contributions. The primary source of noise is Johnson noise

$$V_{noise}(rms) = \sqrt{4(R_{seal} + R_e)kTB}. \tag{6}$$

Where the R_{seal} is the seal resistance, R_e is the real part of the electrode impedance, k is Boltzmann's constant, T is the temperature, and B is the bandwidth in Hz. For a 1 kHz bandwidth, a seal resistance of 2MΩ, and an electrode with a real impedance $R_e = 500\text{k}\Omega$, the corresponding rms Johnson noise is 5μV. Therefore, for $R_{seal} = 2\,M\Omega$, $V_{cap}/V_{noise}(rms) \approx 50$ for *Helisoma* B19 action potentials, and $V_{cap}/V_{noise}(rms) \approx 10$ for Helisoma B5 action potentials.

Recording subthreshold signals will be difficult since the signals are typically small and slow. Furthermore signals are difficult to interpret since the

(a) *Helisoma* B19

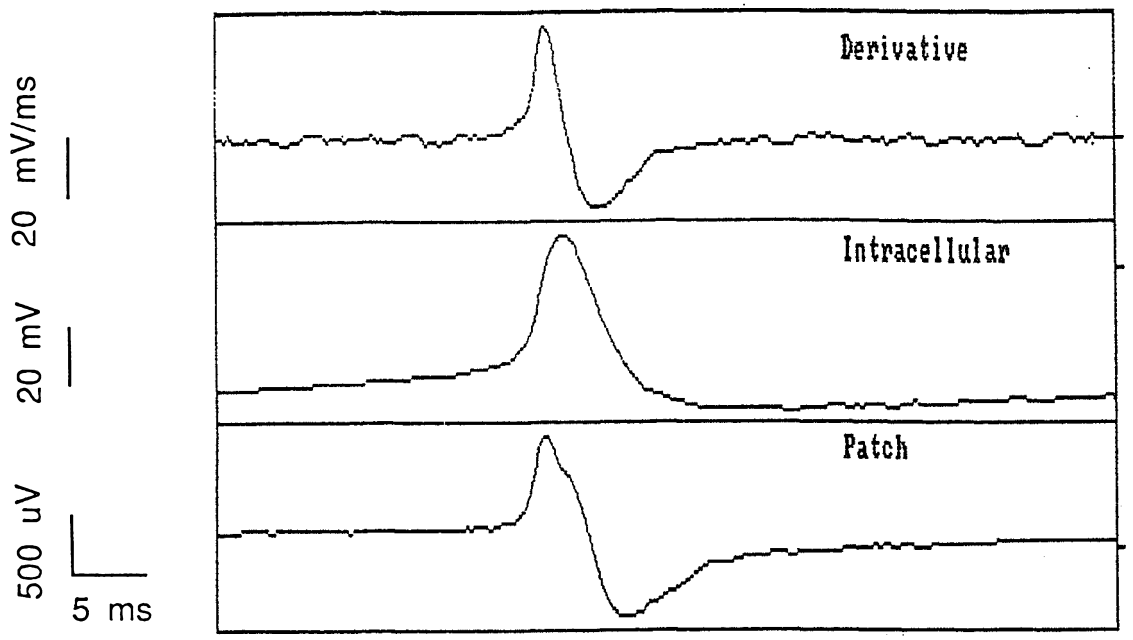

(b) *Helisoma* B5

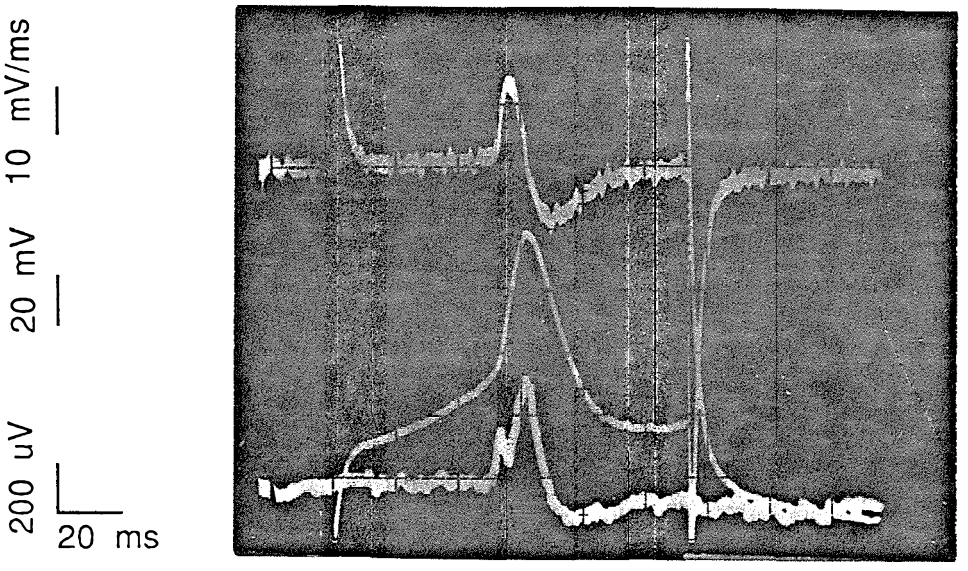

Figure 4.3. Neurons stimulated with a current pulse passed through an intracellular electrode (40–50 MΩ), and the response of the cell recorded with the intracellular electrode, the derivative of the intracellular signal, and the loose-patch electrode (diameter ≈ 10 μm). (a) *Helisoma* B19 neuron (R_{seal} = 3.0 MΩ, bandwidth 10 Hz–1 kHz). (b) A *Helisoma* B5 neuron (R_{seal} = 2.0 MΩ, bandwidth 10 Hz–1 kHz).

intracellular signal is distorted by passing through the patch membrane. In order to record subthreshold signals very good seals are required. If a gigaohm seal could be obtained then it would be practical to electrically break down the cell membrane beneath the cup and have essentially a chronic whole-cell patch recording. Diving-board electrodes have been used in this manner, but so far the seal resistances have not been large enough to prevent a deterioration of the resting potential of the cell.

4.3 Stimulation

The equivalent circuit for stimulation is shown in Figure 4.1(c). It is generally true that a membrane depolarization of approximately 15 mV will fire a neuron. As a current pulse is applied through the electrode most of the current passes out beneath the cup, with a small fraction passing into the cell through the patch and then out through the rest of the cell. For a stimulus current pulse I_{stim} the voltage applied to the patch is $V_{patch} = I_{stim} R_{seal}$ assuming $R_{seal} \ll Z_{m1}$. A positive current pulse thus hyperpolarizes the patch membrane, and depolarizes the rest of the cell membrane. For stimulus pulses short compared to the time constant of the cell (which is typically $\geq$ 5msec.) the internal voltage change is approximated by

$$\Delta V_{cell} = \frac{\Delta t(i)}{C_{m2}} \tag{6}$$

$$\Delta V_{cell} = \frac{\Delta t}{C_{m2}} \Big(i_c + \sum_{chan=1}^{N} i_{chan} \Big) \tag{7}$$

$$\Delta V_{cell} = \frac{\Delta t C_{m1}}{C_{m2}} \frac{dV_{patch}}{dt} + \frac{\Delta t}{C_{m2}} \Big(\sum_{chan=1}^{N} \frac{(V_{cell} - V_{patch} - V_{chan})}{R_{chan}} \Big). \tag{8}$$

Since channel type and density beneath the patch is not known it is difficult to predict the required stimulus current.

There are two constraints limiting the amount of current that can be used for stimulating. First, if a voltage of greater than about 1 V is applied to a metal electrode, gas is evolved that kills the cells. An electrode can be approximated by a capacitor with a capacitance C_e. A current pulse with amplitude I_{stim} and duration Δt results in an electrode potential $\Delta V_e = I_{stim} \times \Delta t / C_e$ which limits the total charge $I\Delta t$ useful for stimulating. Second, I_{stim} must be kept small enough that V_{patch} remains less than about 300 mV, or the membrane in the patch may be electrically broken down. This would damage the cell unless R_{seal} was much larger than the few megohms thus far achieved.

References

[1] A. Marty, and E. Neher, "Tight-Seal Whole-Cell Recording", in *Single Channel Recording*, ed. B. Sakmann, and E. Neher, Plenum Press, New York, pp. 107–121, 1983.

[2] C. A. Thomas, Jr., P. A. Springer, G. E. Loeb, Y. Berwald-Netter, and L. M. Okun, "A miniature microelectrode array to monitor the bioelectric activity of cultured cells," *Exp. Cell Res.*, vol. 74, pp. 61–66, 1972.

[3] G. W. Gross, A. N. Williams, and J. H. Lucas, "Recording of spontaneous activity with photoetched microelectrode surfaces from spinal cord neurons in culture," *J. Neurosc. Methods*, vol. 5, pp. 13–22, 1982.

[4] J. Pine, "Recording action potentials from cultured neurons with extracellular microcircuit electrodes," *J. Neurosc. Methods*, vol. 2, pp. 19–31, 1980.

[5] D. W. Tank, C. S. Cohan, and S. B. Kater, "Cell body capping of array electrodes improves measurements of extracellular voltages in micro–cultures of invertebrate neurons," *IEEE Conference on Synthetic Microstructures, Airlie, Virginia,* 1986.

[6] D. A. Israel, W. H. Barry, D. J. Edell, and R. G. Mark, "An array of microelectrodes to stimulate and record from cardiac cells in culture," *Am. J. Physio.*, vol. 247, pp. H669–H674, 1984.

[7] W. Stuhmer, W. M. Roberts, and W. Almers, "The loose patch clamp", in *Single Channel Recording*, ed. B. Sakmann, and E. Neher, Plenum Press, New York, pp. 123–132, 1983.

Chapter 5

Diving-Board Electrode Tests

5.1 Establishing the Chronic Connection

An underwater-setting biocompatible adhesive was required for gluing the diving-board to the bottom of the tissue culture dish. Various glues were screened for their ability to set and adhere under water. Of these many were not suitable due to their viscosity and the lack of a thinner that would allow a very small drop of glue to be applied. While several epoxies set and adhere under water, limited working times make them difficult to work with. *Electro-Lite Corporation 4481* is an adhesive that sets when exposed to ultraviolet light and adheres well under water to all plastics tested, but not to glass, or substrates coated with polylysine or collagen. The adhesive can be thinned with isopropyl alcohol facilitating formation of small drops.

Once a glue with the desired curing and adhesion characteristics was found, it was necessary to test the biocompatibility of the gluing procedure as shown in Figure 5.1. Twenty-four hours after plating a glue drop was placed by one of two *Helisoma* B19 neurons contained in the same dish. The adhesive was set using a 1 minute exposure to a mercury arc lamp through a 20X objective, using an iris to restrict the illumination to the glue drop. The cell continued to grow in the same manner as the control. The growth of neurons (n=10) tested in this manner was found to be no different than that of the controls. However, processes illuminated with levels of u.v. light necessary to set the glue quit growing within five minutes of illumination. Similar tests were performed with two-week old SCG neurons, which continued to look healthy for many days after the gluing process.

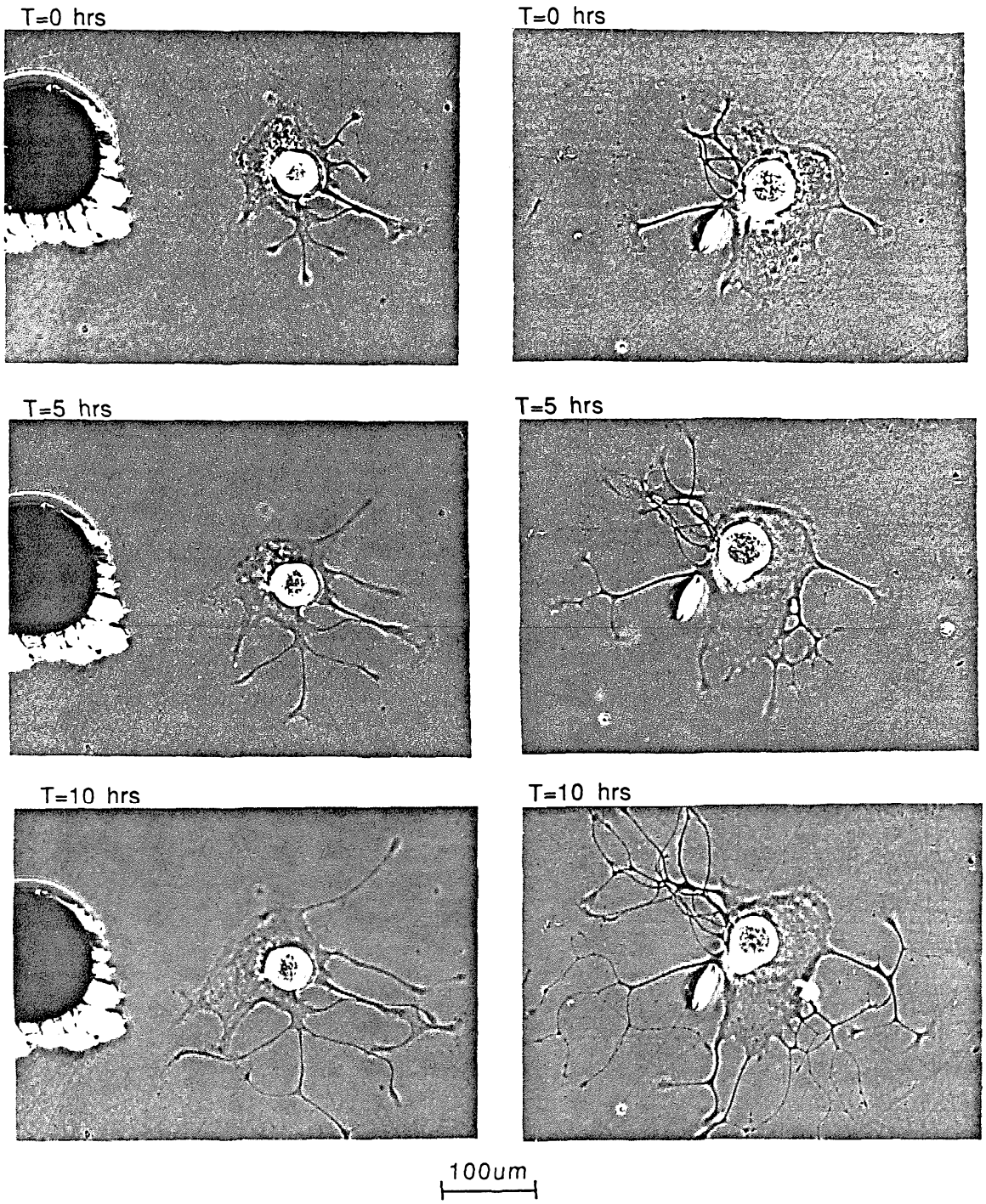

Figure 5.1. *Helisoma* B19 neurons. At $t = 0$ hours a drop of adhesive was placed near one neuron. Pictures taken at $t = 0$ hours, $t = 5$ hours, and $t = 10$ hours.

Intracellular penetrations were performed to check the electrophysiology of neurons with nearby drops of glue compared to controls. In no case did the gluing process have any effect on either *Helisoma* or SCG neurons.

The diving-board electrodes are manipulated into place while being viewed through an inverted microscope equipped with phase and epifluorescence optics. The polyimide handle of an electrode is held by fine forceps mounted in a holder that provides pressure to hold the electrode firmly until it has been glued to the bottom of the culture dishes. Then the pressure is reduced and the electrode is gently released, without damaging the glue joint. The holder is mounted in a special manipulator that is in turn mounted in a *Leitz* micromanipulator. In addition to the standard x, y, z degrees of freedom provided by the micromanipulator, this special manipulator provides θ, and ϕ control needed to make the diving board flat relative to the surface of the tissue culture dish.

Once the electrode has been made flat relative to the culture dish a metal needle is used to scratch the plastic in a region where the pedestal is to be glued. Then a 50 μm diameter drop of glue is applied to the bottom of the tissue culture dish through a 10 μm diameter glass electrode using pressure to control the drop size. Then the electrode is placed with the pedestal in contact with the glue and the diving-board tip in contact with the cell. When a seal resistance of several Megohms has been obtained the drop of glue is exposed to ultraviolet light from the mercury arc lamp of the epifluorescence illuminator.

Electrical contact to the electrode is maintained during manipulation and gluing so that the seal resistance can be monitored. The culture dish has wires extending to the interior through holes in the side. At the end of each wire is a flexible 25 μm gold wire-bond wire. When the electrode has been positioned near the cell a conductive graphite paint, *TV Tubecoat*, is used to connect the

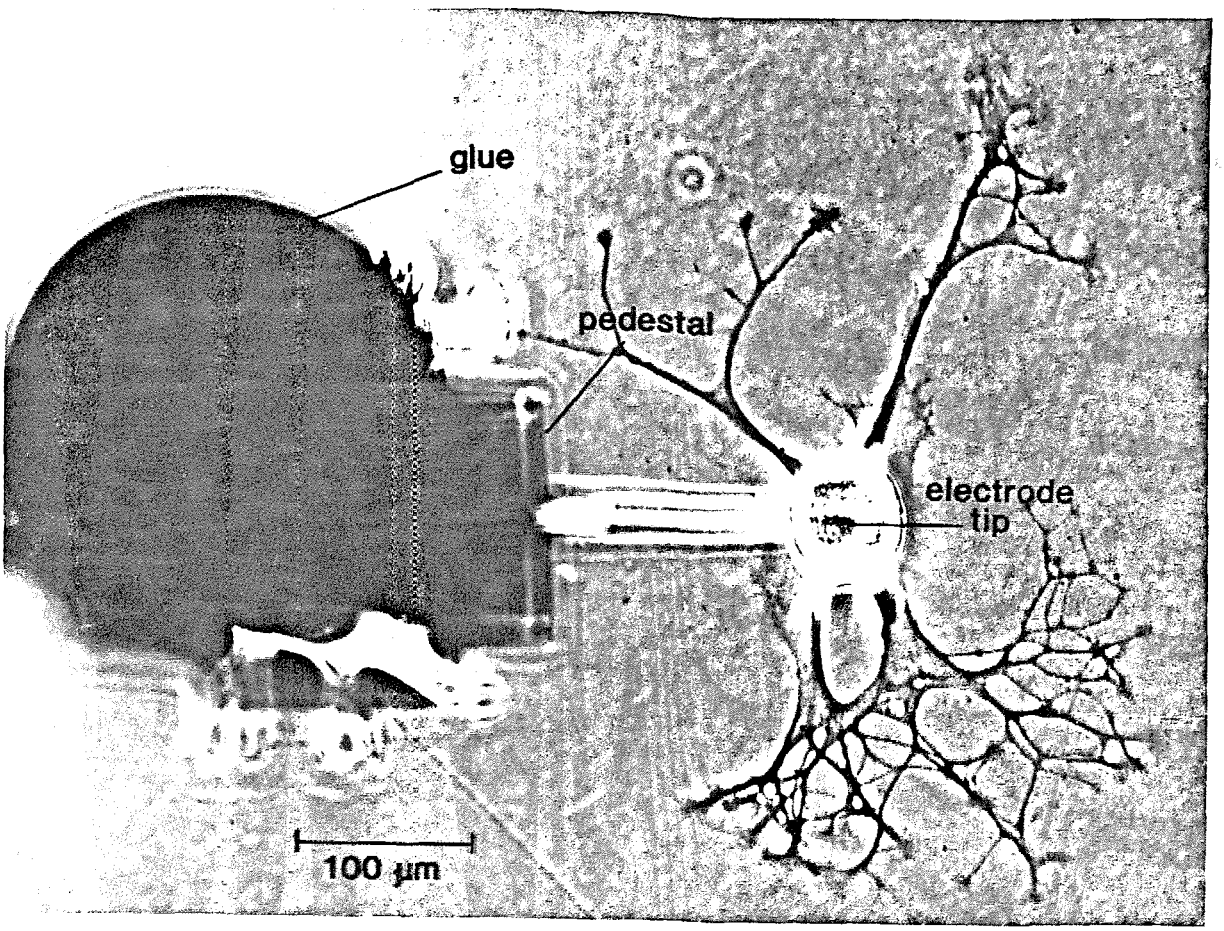

Figure 5.2. Diving board electrode in chronic electrical contact with a *Helisoma* B19 neuron. The pedestal is glued to the bottom of the culture dish and the electrode tip is in contact with the cell body.

wire from the diving board electrode to one of the wires connected to the side of the dish, which is in turn connected to external electronics. After the device has been glued it is possible to position another diving-board electrode. Once the electrodes are mounted, the lid is put back on the tissue culture dish and the diving-board electrodes are ready for long-term experiments. Figure 5.2 shows a diving-board electrode in contact with a cultured *Helisoma* neuron.

To understand device operation two-electrode experiments were performed. In preliminary experiments a 12 μm glass pipette was substituted for the diving-board electrode. An intracellular electrode and a patch pipette recording from the same cell. In this way it was possible to compare the intracellular response with the response of the patch pipette. Once stimulation and recording were accomplished, and understood with the patch pipette, a diving-board electrode was used. Other than the inherent electrical differences between liquid filled and metal electrodes, diving-board electrodes behave like glass patch-electrodes of the same tip diameter for both stimulation and recording.

5.2 Recording from Identified Helisoma Neurons

With the seals obtained it is possible to record action potentials with good signal-to-noise ratios, but in order to record subthreshold signals the seal resistance needs to be greatly improved. In the experiment of Figure 5.3 with diving board electrode mounted on top of a neuron an intracellular electrode was used to stimulate using a current pulse, and the diving-board electrode was used to record the resulting action potential. Signal-to-noise ratios for action potentials recorded from *Helisoma* B19 neurons were typically 20–100:1, and for *Helisoma* B5 neurons 4–10:1.

Diving-board electrodes have been used to record spontaneous activity from *Helisoma* B19 neurons for up to four days. Figure 5.4 (a) shows a diving-board electrode monitoring the spontaneous activity of a *Helisoma* B19 neuron for 2 days. Successive pictures at $t = 0$ hours, $t = 4$ hours, and $t = 24$ hours show normal cell growth. Figure 5.4 (b) is an example of the spontaneous activity recorded from this cell.

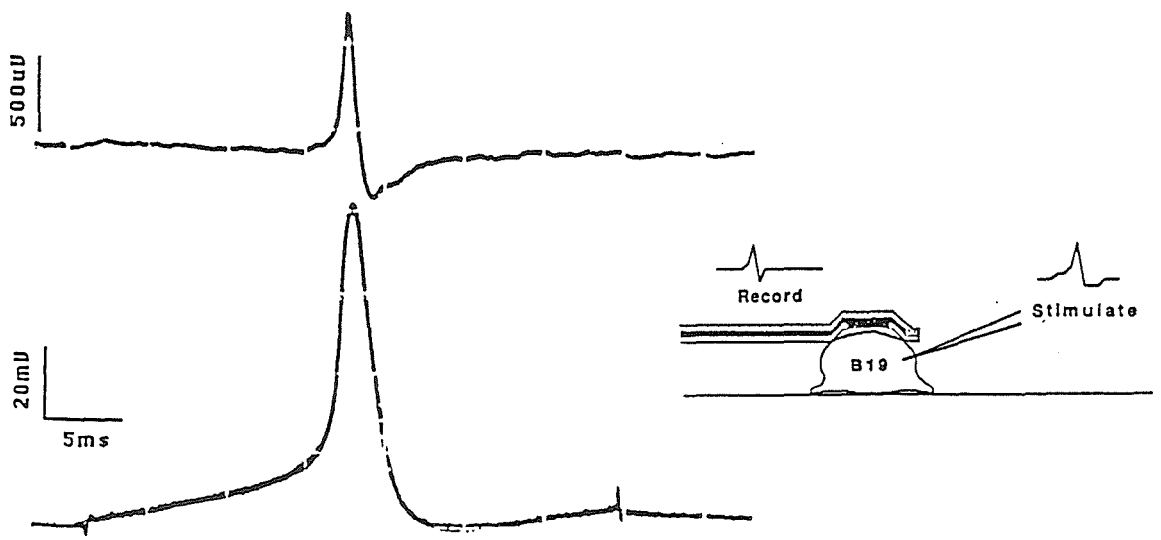

Figure 5.3. A *Helisoma* B19 neuron stimulated with a current pulse passed through an intracellular electrode, and the response of the cell recorded with the intracellular electrode, and the diving-board electrode ($R_{seal} = 4.0\,\mathrm{M}\Omega$, bandwidth 10 Hz–1 kHz).

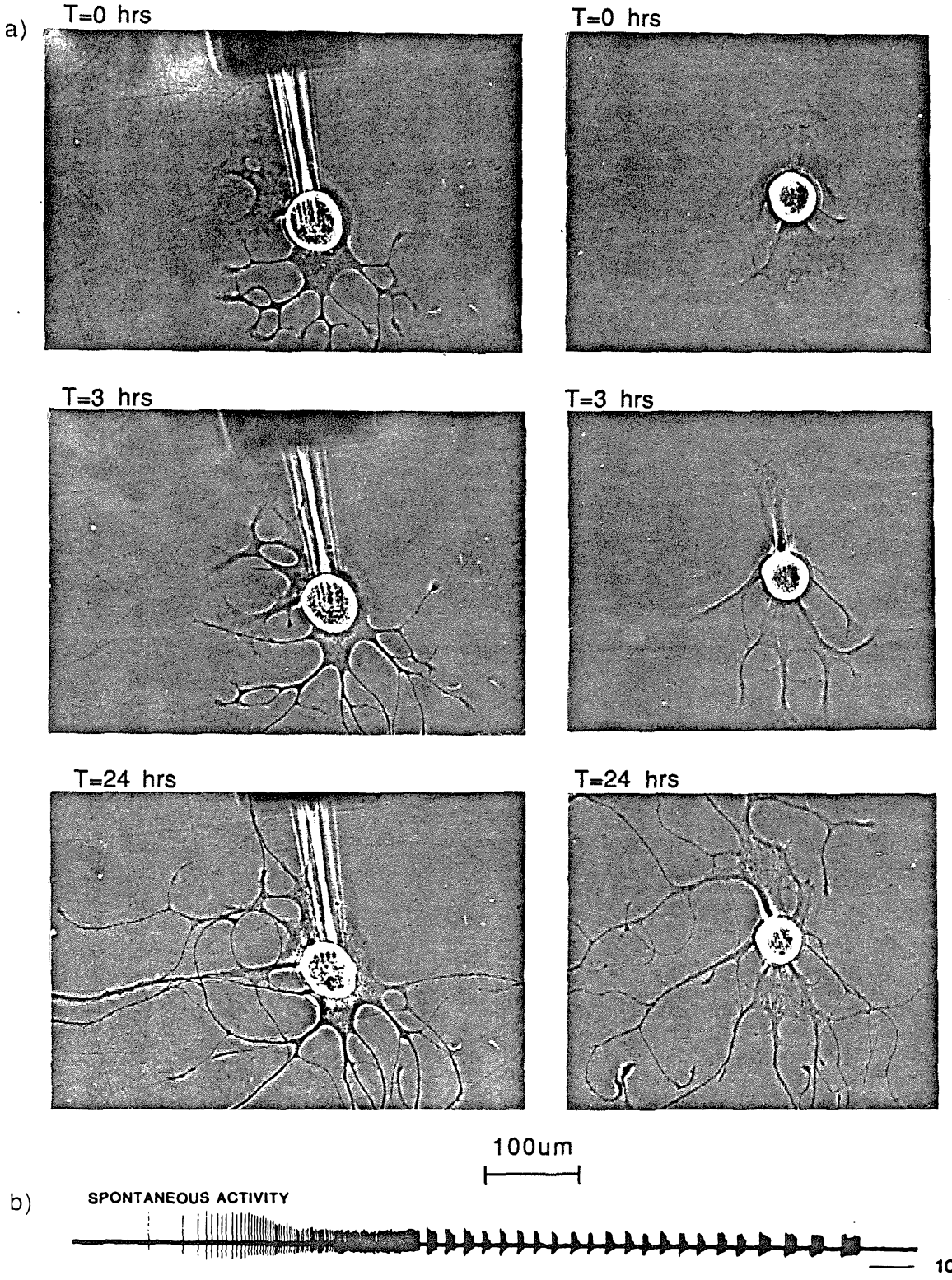

Figure 5.4.(a) Successive pictures of a diving-board being used to record from a *Helisoma* B19 neuron at $t = 0$ hours, $t = 4$ hours, and $t = 24$ hours. (b) An example of spontaneous activity recorded at $t = 2$ hours ($R_{seal} = 3\,\mathrm{M}\Omega$).

5.3 Stimulating Identified Helisoma Neurons

Diving-board electrodes have been used to stimulate *Helisoma* neurons. In the experiment of Figure 5.5 a current pulse passed through the diving-board electrode was used to stimulate the neurons while an intracellular electrode was used to monitor the potential of the cell.

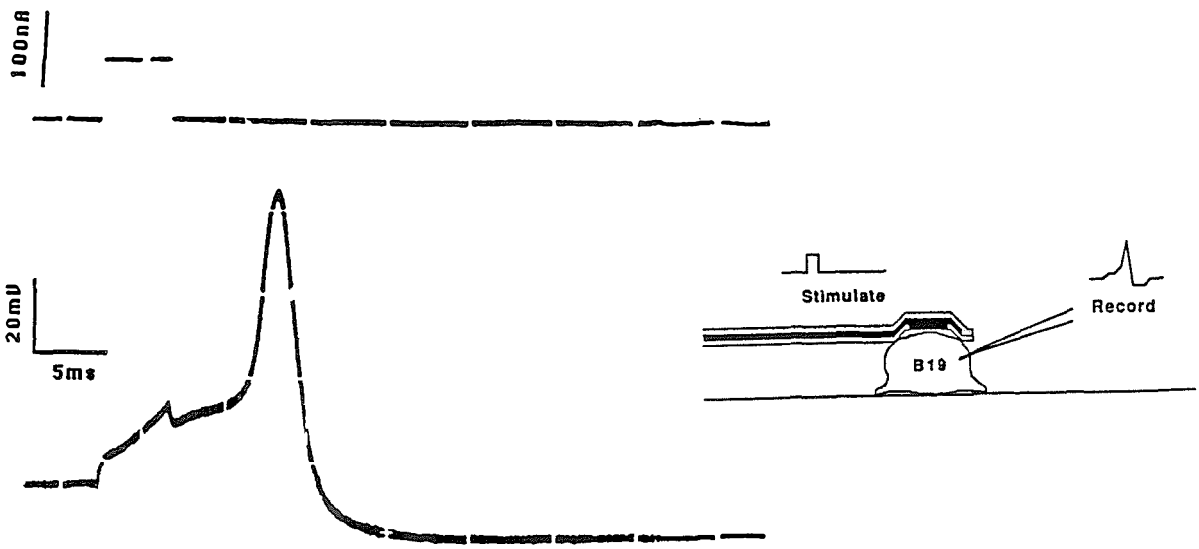

Figure 5.5. Stimulation of a *Helisoma* B19 neuron using a current pulse passed through a diving-board electrode to stimulate and recording using an intracellular electrode. ($I_{stim} = 90\,\text{nA}$, $\Delta t = 5\,\text{msec}$, $V_{patch} = 200\,\text{mV}$)

Helisoma cells have been stimulated intermittently for up to 4 days. Figure 5.6 shows a diving-board electrode that was placed on a cell at time $t =$ 0 hours. At 24 hours the cell was penetrated with an intracellular electrode to monitor the activity of the cell. Then the current pulses were passed through the diving board and the cell was stimulated at 1 Hz and 10 Hz. The intracellular electrode was then removed and the cell was stimulated at 1 Hz for 24 hours. At that time the cell was penetrated once again to verify that the cell was still being stimulated and that the threshold had not changed.

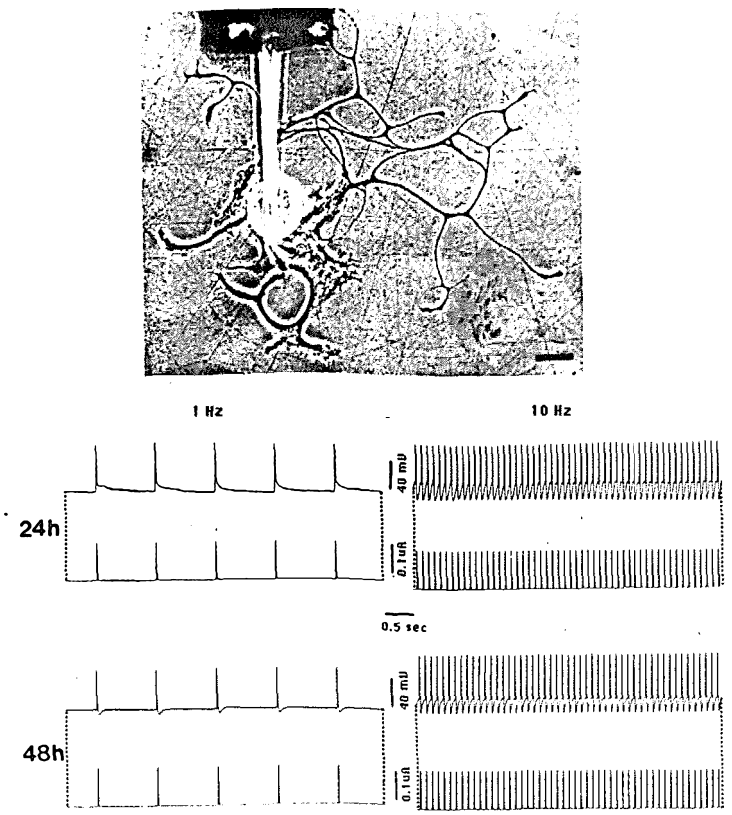

Figure 5.6. A diving-board electrode in electrical contact with a *Helisoma* B19 neuron. Calibration bar is 50 μm. (I_{stim} = 140 nA, Δt = 0.5 msec, V_{patch} = 170 mV) Twenty-four hours after the device was placed on the neuron an intracellular electrode was used to monitor the activity of the cell and current pulses passed through the electrode were used to stimulate the cell at 1 Hz and at 10 Hz. The stimulus current passed through the diving-board electrode is shown below the intracellular voltage record. The intracellular electrode was then removed while the diving board electrode continued to stimulate the cell at 1 Hz. At time t = 48 hours an intracellular electrode was used to verify that the stimulus threshold had not changed.

It is necessary to measure the evoked action potential to verify that the cell is being stimulated. While simultaneous intracellular recording has been used, a less invasive method is preferred. It is desirable to be able to measure the evoked action potential with the same diving-board electrode used to stimulate the cell. The primary difficulty is the large stimulus artifact, which is on the order of 200 mV, much larger than the recorded action potential, which is on the order of 100 μV. There are two ways of solving this problem. The first is to raise the stimulus pulse very slowly; at threshold a late action potential occurs many milliseconds after the stimulus pulse can be recorded. Once threshold has been determined the stimulus pulse can be increased by 10% to obtain reliable stimulation. In Figure 5.7 *Helisoma* B19 is stimulated by a diving-board electrode and the response of the late action potential is recorded by the same electrode. The second solution, which has not been done yet, is to remove the stimulus artifact by computer-processing the signal.

5.4 Preliminary Studies on Vertebrate Neurons

Preliminary studies have also been performed with dissociated rat superior cervical ganglion neurons (SCG's). Several factors make working with SCG's more difficult than with *Helisoma* neurons: they are smaller (a diameter of about 25 μm for SCG's compared to about 50 μm for *Helisoma* neurons); the extracellular solution resistivity is lower by about a factor of four resulting in lower seal resistances; and SCG's are in general more delicate than *Helisoma* neurons. Despite these difficulties it has been possible to stimulate SCG's, and to record action potentials with a signal-to-noise ratio of 10:1 ($R_{seal} = 0.4\,M\Omega$). Long-term stimulation and recording studies will be performed in the near future. The success of the diving-board electrodes on SCG's demonstrates their versatility, and indicates that they can be used with neurons 20 μm in diameter

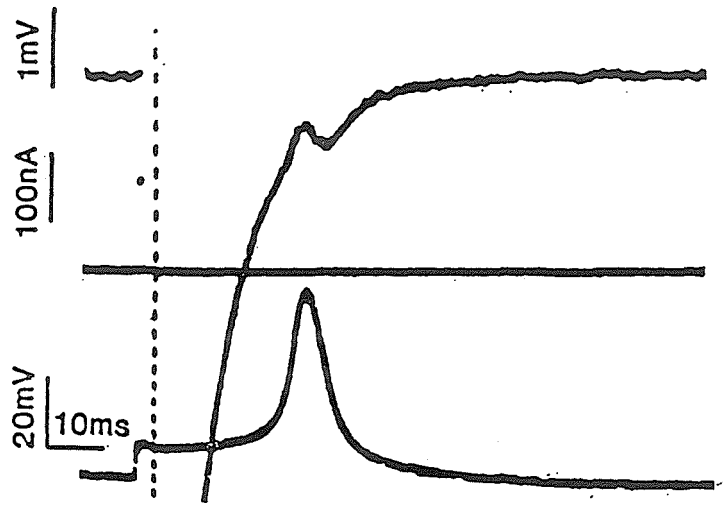

Figure 5.7. A *Helisoma* neuron B19 stimulated by a diving-board electrode. (I_{stim} = 100 nA, Δt = 0.2 msec, V_{patch} = 210 mV) Since the stimulus is near threshold the resulting action potential is many milliseconds after the stimulus pulse and it can be recorded on the diving-board electrode. (R_{seal} = 1.5 MΩ, bandwidth 100 Hz–1 kHz).

and larger. The devices can be scaled down for use with smaller neurons.

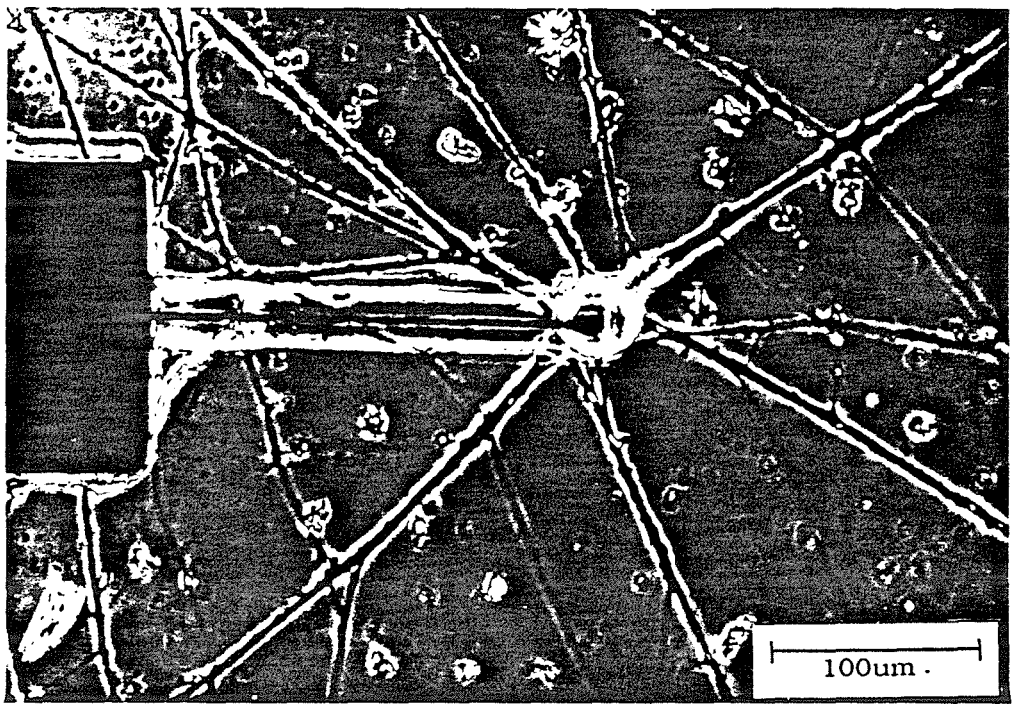

Figure 5.8. Diving-board electrode on a rat SCG neuron.

Chapter 6

Electrode Capping By Cultured Invertebrate Neurons

6.1 Introduction

Multielectrode dishes have been used to record from a variety of *in vitro* preparations [1]-[5]. In general it is possible to record small extracellular signals resulting from current flow associated with an action potential. However, it may be difficult to interpret these signals, since the signal-to-noise ratio is often poor, and it is not always possible to get a one-to-one electrode-neuron correspondence. It is also possible to stimulate neurons using these electrodes [2]. Such stimulation, in which a current pulse is passed through an electrode, relies on creating a voltage drop in the media sufficient to fire nearby axons and cell bodies. Such stimulation techniques suffer from the disadvantage that it is difficult to verify the stimulus using the extracellular array, therefore an independent means of stimulus verification such as voltage-sensitive dyes [6],[7] or intracellular recording is required. These problems are a result of the extracellular media (typically 50–400 Ω-cm) shunting the stimulus current and extracellular signals produced by the cell. For cultured vertebrate neurons there is no easy way to reliably overcome this problem.

However, it is possible to seal a dish electrode to a cultured invertebrate neuron in much the same manner as a loose-patch electrode. Figure 6.1 (a) is an example of a *Helisoma* neuron sealing over several electrodes. This results in a one-to-one electrode-neuron correspondence, facilitating recording action potentials from each neuron in a simple network, stimulating neurons, and recording action potential with the stimulating dish electrode.

(a)

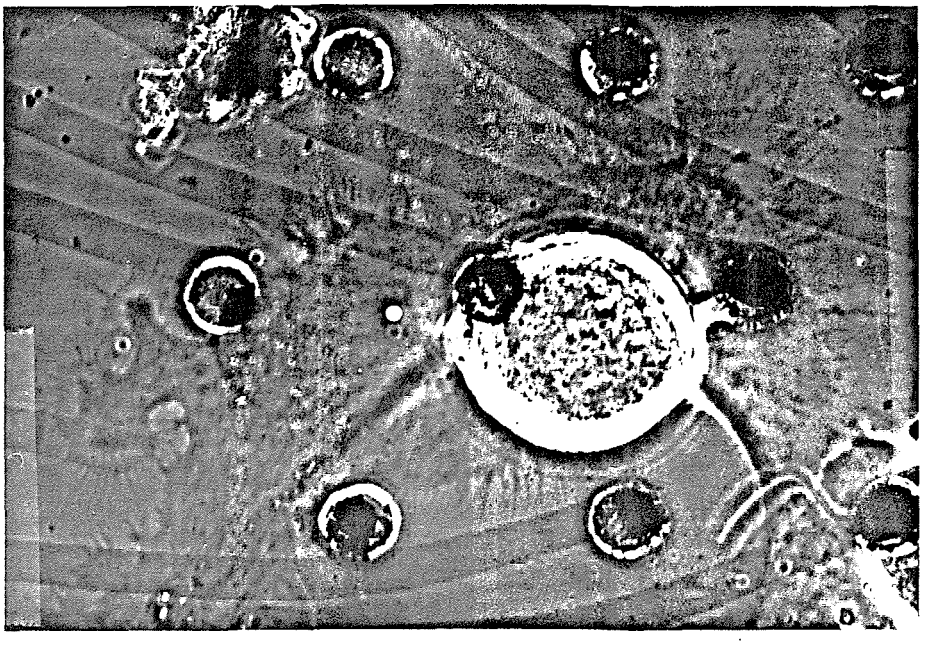

(b)

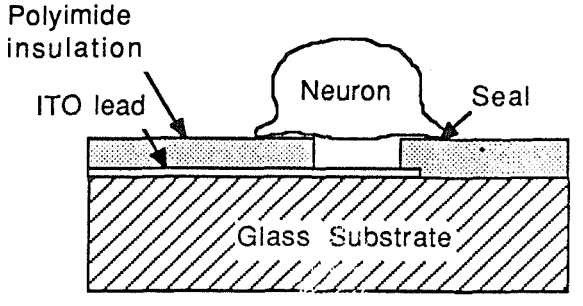

Figure 6.1. (a) *Helisoma* B19 neuron growing on a multielectrode dish. Loose-patch type recordings can be obtained from the electrodes completely covered by the neuron. (b) Schematic of a neuron sealing over a dish electrode.

6.2 Dish Fabrication

The multielectrode arrays are fabricated using conventional integrated circuit technology. Figure 6.2 (a) is a picture of a completed array. The electrode leads are indium-tin oxide (ITO) [3], [8]; the insulation is photosensitive polyimide; and the electrode tip is electroplated platinum black. The electrode pattern consists of a hexagonal array of 61 electrodes, 12 μm in diameter, separated by 70 μm.

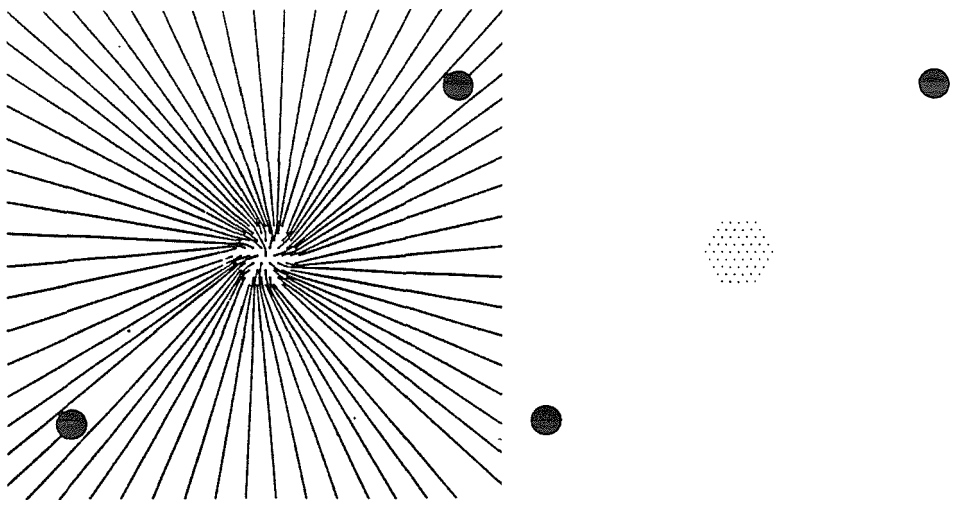

(a) (b)

Figure 6.2. Masks used in fabrication of microelectrode array. (a) Lead Mask (b) Insulation Mask.

Fabrication begins with a glass substrate (0.016″ thick), coated with a layer of ITO (1000Åthick, and with a sheet resistance of 100 Ω/square) obtained from Donnelly Corporation (Midland, MI). After cleaning, the leads are patterned using *Shipley* 1350J photoresist, with a 125 mJ/cm^2 exposure for the central pattern and a 800 mJ/cm^2 exposure for the peripheral part of the wafer to remove the thick edge bead that forms at the wafer edge when photoresist is spun on, that would result in shorted leads. The ITO is etched for 4 minutes in a freshly prepared solution of 50 H_2O/50 HCl/1 HNO_3 at 40°C. The photoresist is removed and a 30Å thick layer of aluminum is evaporated on to the wafer, resulting in a thin layer of aluminum oxide which is an effective adhesion promoter. Next photosensitive polyimide (*MRK Selectilux HTR 3–50*) is spun on at 5000 rpm for 30 seconds, soft baked for 5 minutes at 85°C, patterned with the electrode mask, developed, and cured for 12 hours at 200°C. To reduce the electrode impedances to less than 500 KΩ the electrodes are platinized in a solution of 1% chloroplatinic acid in 0.0025% HCl, plus 0.01% lead acetate, using a current

density of 20 mA/cm^2 for 10 seconds. Then the bottom of a small tissue culture dish with a 5 mm diameter hole is glued to the top of the substrate. Figure 6.3 (a) shows a completed ITO dish. It takes an average of about 1 hour to fabricate each dish, and they have been routinely reused several times, for a total time in saline of 60 days.

6.3 Dish Electronics

Figure 6.3 (b) shows a dish mounted in mounted in the interfacing printed-circuit board, which in turn mounts to the microscope stage. Sixty-three leads go to the inputs of eight eight-to-one multiplexers, with outputs designated as channels A–H. Each channel is amplified with a gain of 11, and is differential with respect to two large dish ground electrodes. A JFET switch connects each channel to an externally generated stimulus. Two 34-wire flat cables connect the printed circuit board to interface electronics, which generates five control signals for each channel. Figure 6.4 (a) shows one of eight identical channels, channel A. AEN enables multiplexer A; A0, A1, A2 selects the input to multiplexer A, and ASTIMON switches the STIMAIN signal on. The eight stimuli are turned on and off using two quad-JFET switches (Figure 6.4 (b)). Figure 6.4 (c) shows the reference amplifier.

Electrodes are addressed as in Figure 6.4 (c). By sending the correct control voltages any one of electrodes A–H can be accessed, making it possible to record and stimulate simultaneously using eight electrodes. A control box is used having eight switches that set the binary code to address the multiplexers A–H, and eight switches for stimulus enable A–H (Figure 6.4 (e)).

6.4 Experimental Procedure

Identified neurons were plated on polylysine coated multielectrode dishes.

(a)

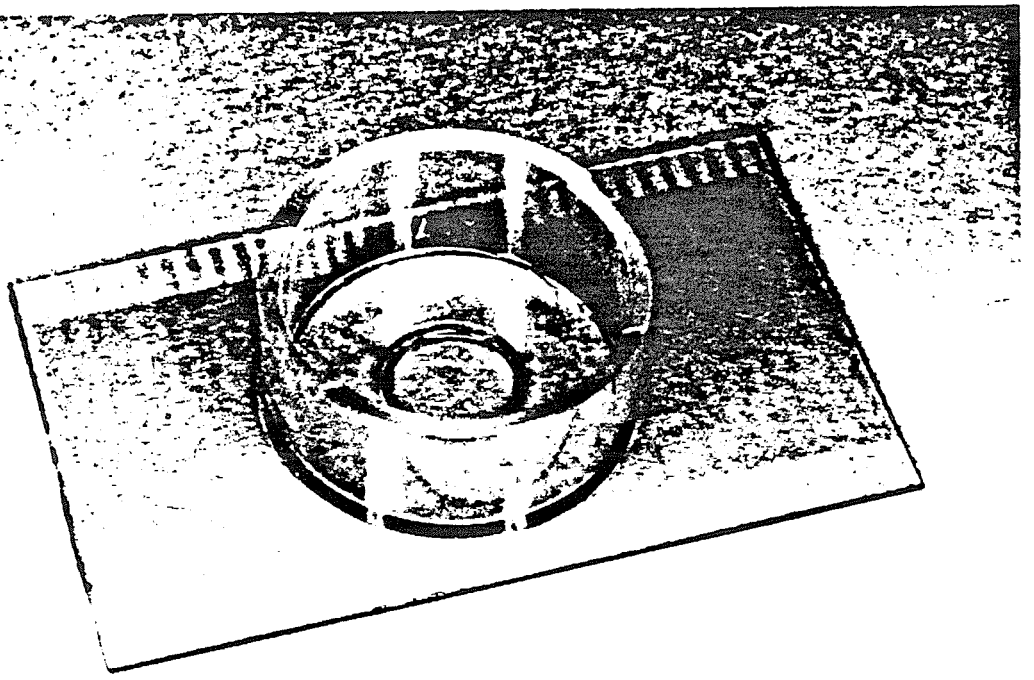

(b)

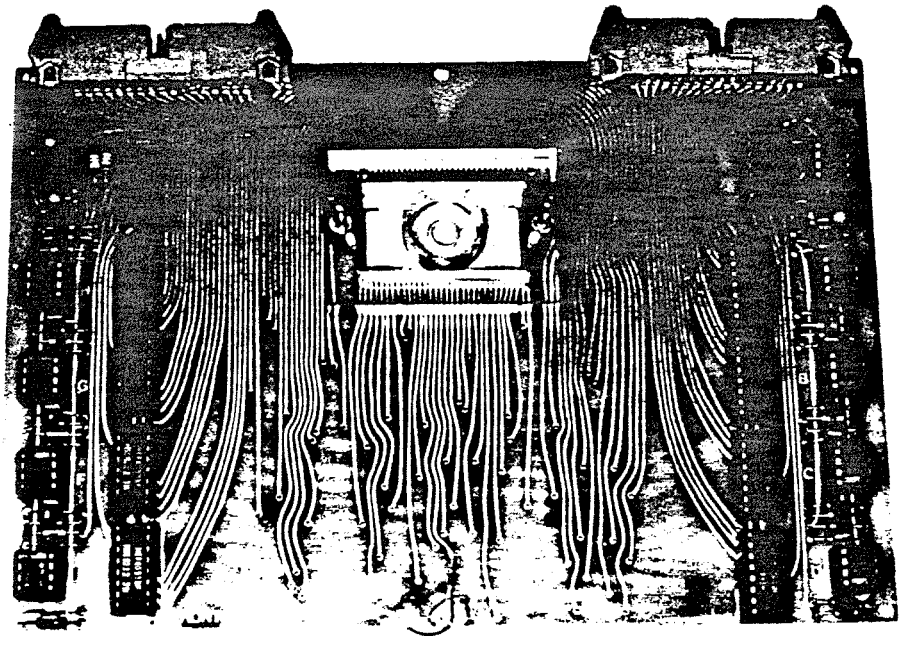

Figure 6.3. (a) Completed multielectrode culture dish. (b) Dish mounted on a circuit board.

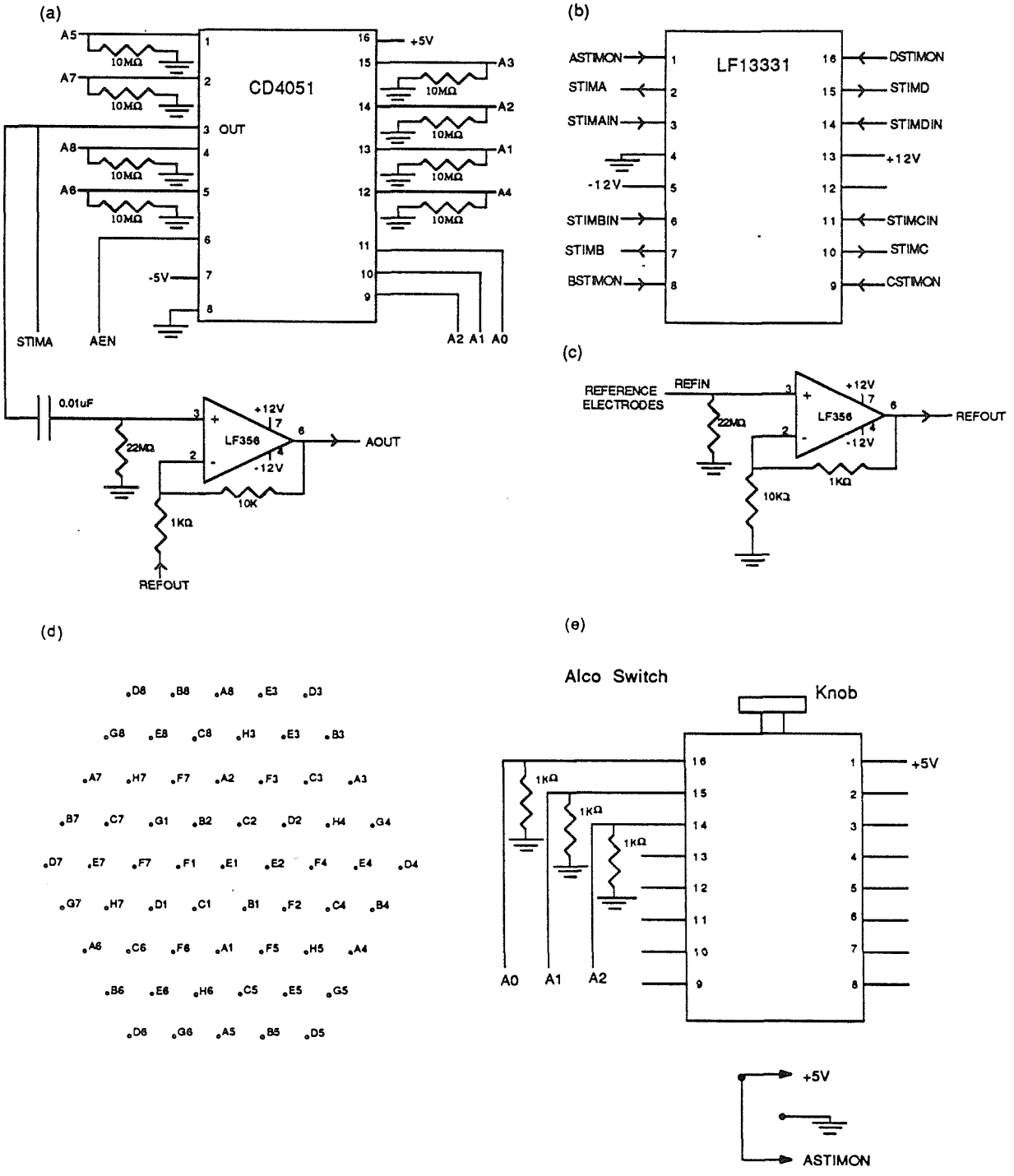

Figure 6.4. (a) Channel A (b) Stimulus Switches (c) Reference Electrodes (d) Dish addresses (e) Control box circuitry

Cell bodies moved an average of about 100 μm after plating, making neuron placement on a specific electrodes extremely difficult. However, by using an array with electrodes spaced 70 μm apart it was possible to have virtually every neuron sealed to an electrode. Cell growth dictated the seal resistance. When cells grew as in Figure 6.1, with a very large lamellipodia seals were obtained on several electrodes.

6.5 Recording

Dish electrodes have been used to record action potentials from *Helisoma* B19 neurons with signal-to-noise ratios of 100:1, and from B5 neurons with signal-to-noise ratios of 20:1. In Figure 6.5 is an example of spontaneous activity recorded using a multielectrode dish.

Using multielectrode dishes it is possible to record spontaneous activity from small networks of invertebrate neurons with good signal-to noise ratios and one-to-one electrode-neuron correspondence. In Figure 6.5 A is a *Helisoma* B5 neuron; B, and C are *Helisoma* B19 neurons. The action potentials recorded from *Helisoma* B5 neurons are in general much smaller than those recorded from *Helisoma* B19 neurons which have a much faster action potential. Dish recordings are primarily derivatives of the action potentials as seen through the capacitance of the cell membrane, with small ionic contributions. Multielectrode dishes have been used to monitor spontaneous activity for up to 13 days from *Helisoma* neurons.

By stimulating with an intracellular electrode and simultaneously recording with an intracellular electrode and a dish electrode the signals can be compared, and the frequency dependance can be determined as in Figure 6.6. Recording from a dish electrode under the soma of a *Helisoma* B19 neuron fired at 0.1 Hz the signal recorded by the dish electrode was essentially a derivative of the action

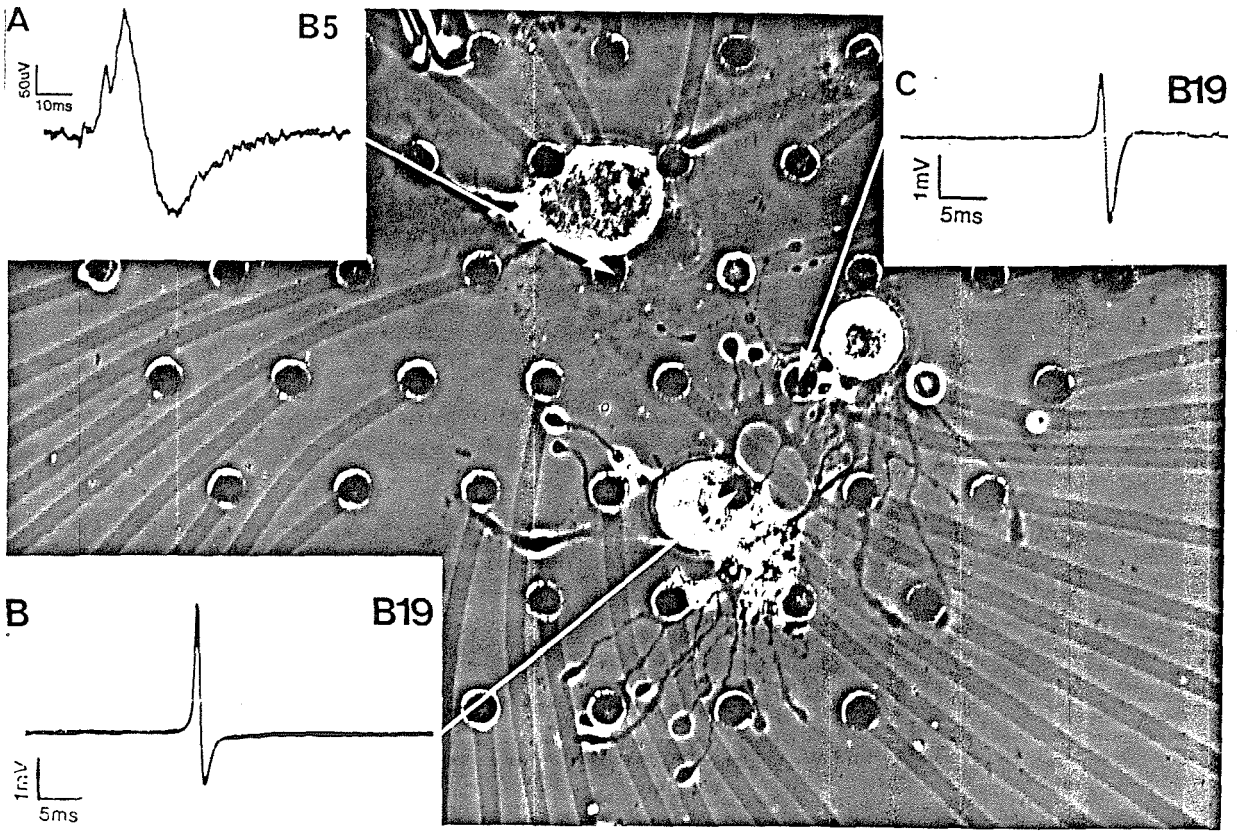

Figure 6.5. Spontaneous activity recorded from *Helisoma* neurons using a multielectrode array (bandwidth 10 Hz–1 kHz). The electrodes are 70 μm apart.

potential. As the frequency of stimulation increased to 10 Hz the signal recorded on the dish electrode changed in two ways: first the amplitude decreased due to action potential broadening; second, the signal had an ionic component in addition to the capacitive component. It would be possible to determine the channel type responsible for this ionic component using a patch pipette and different channel blockers, but these experiments have not been performed.

Experiments with multielectrode dishes also suggest ways in which recordings might be enhanced. If a cell is used to seal over processes or the entire cell body then extracellular signals similar to those obtained *in vivo* are possible. Figure 6.7 (a) shows two cells: cell A is a B19 neuron, and cell B is a B5 neuron.

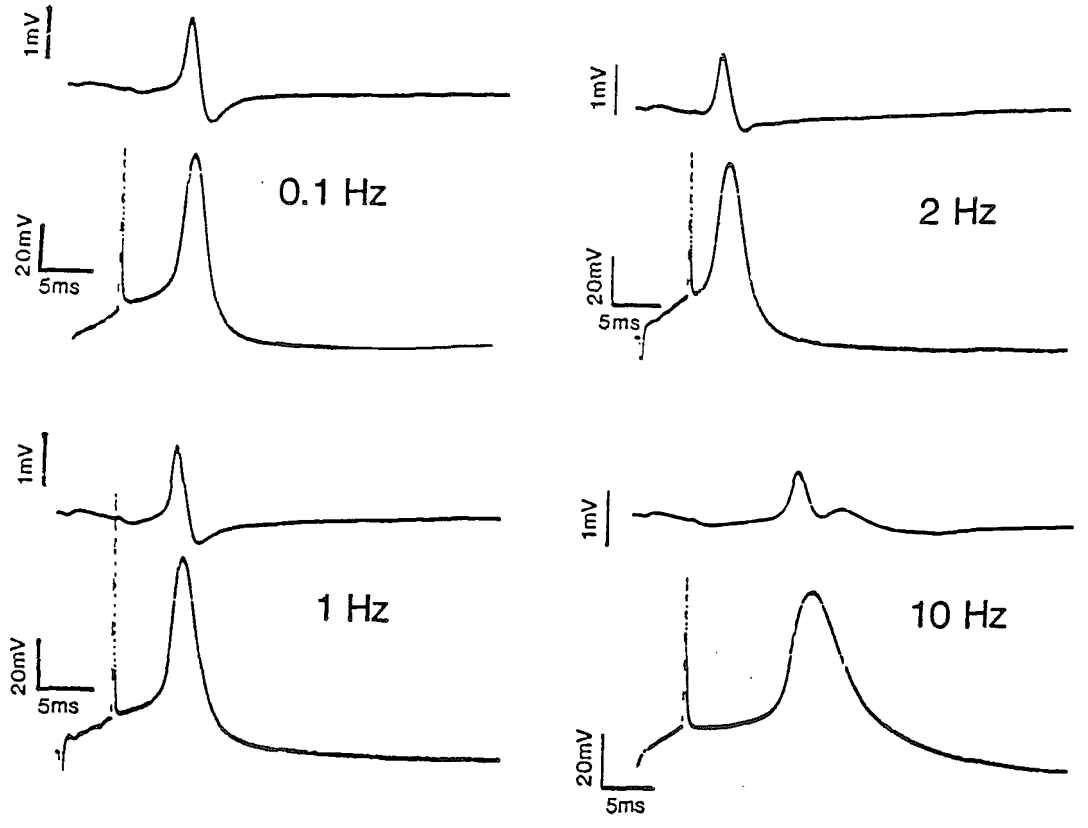

Figure 6.6. Simultaneous recording from dish electrode and intracellular electrode, with the neuron stimulated at 0.1 Hz, 1 Hz, 2 Hz, and 10 Hz (bandwidth 10 Hz–1 kHz).

Figure 6.7 (b) shows spontaneous activity recorded from dish electrodes 1 and 2. By stimulating cell A and cell B we see that the spontaneous activity previously recorded is not from cell B which is located directly over the electrode, but rather is from cell A. An axon stump from neuron A is located under neuron B. As a result the current flow associated with the action potential results in a much larger voltage drop. Figure 6.7 (b) shows signals recorded from a dish electrode that is not sealed and signals from an electrode with a neuron sealed over the axon stump, demonstrating the improvement in signal-to-noise ratios facilitated by obtaining a seal, over that obtained with an extracellular electrode.

These results suggest a technique that might be implemented to obtain im-

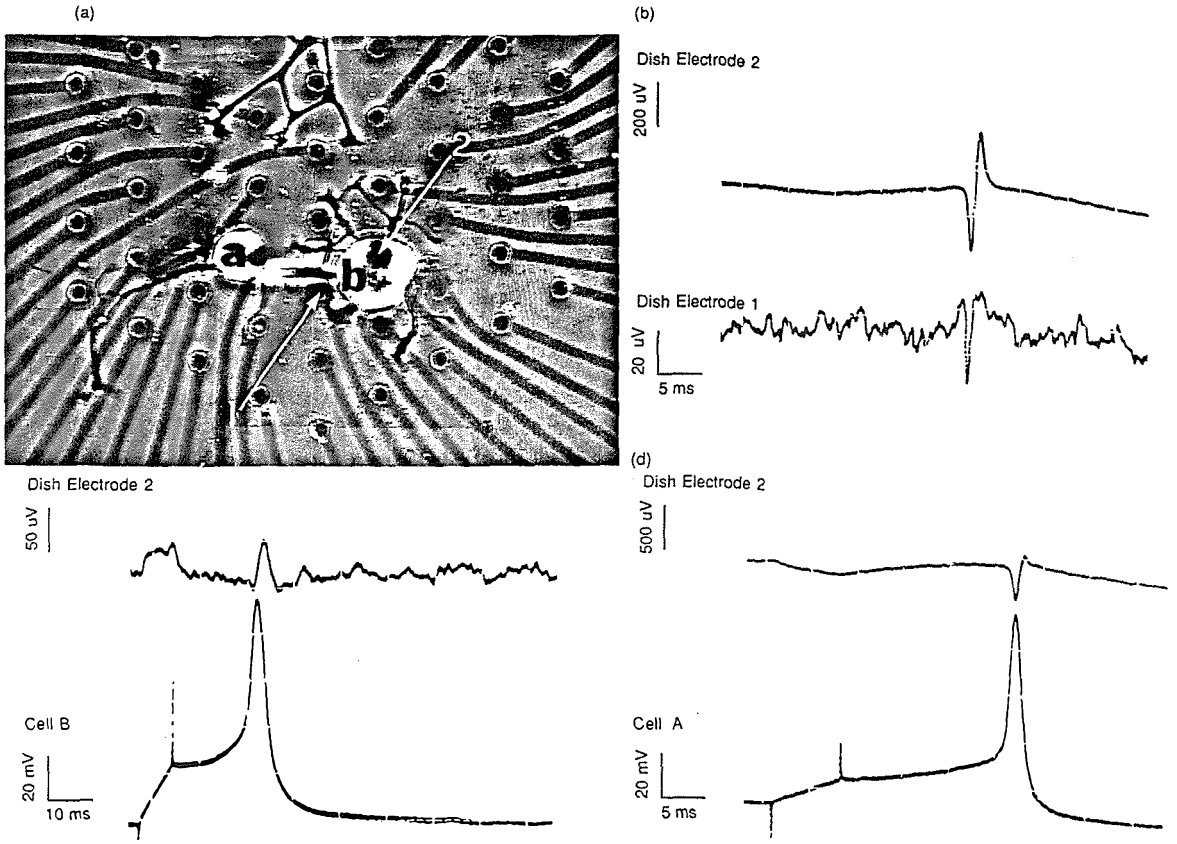

Figure 6.7. (a) Picture of cells growing on multielectrode array. (b) Spontaneous activity recorded by the multielectrode array. (c) Intracellular penetration of cell A. (d) Intracellular penetration of cell B (bandwidth 10 Hz–1 kHz).

proved recording. Once cells have grown out and formed connections a confluent layer of cells such as glia could be grown over the cells, sealing the electrodes, preventing bath electrolyte from shunting the signal, and allowing recordings processes as well as cell bodies. This method could be applied to smaller vertebrate cells, since the "sealing" need not be done by the neurons, but would be done by other cell types.

6.6 Stimulation

Neurons can be stimulated by passing current pulses through dish electrodes. The fact that the neuron is sealed to the electrode makes it possible to use the multielectrode array to stimulate a neuron, and to record the resulting action potential. In Figure 6.8(a) a dish electrode is used to stimulate a neuron and to record the resulting action potential. In Figure 6.8(b) a current pulse passed through a dish electrode is used to stimulate a neuron and another dish electrode is used to record the resulting activity. A large stimulus current is required to fire the cell because the stimulating electrode is not sealed beneath the cell. However, it would not be possible to record the resulting action potential were the neuron not sealed to the dish electrode.

Dish electrodes are promising for chronic stimulation experiments in which a means of noninvasively verifying stimulation is required. However it is important to monitor the seal resistance and adjust the stimulus current so that the breakdown voltage of the cell membrane is not exceeded. The procedure for long-term stimulation experiments is: (1) measure the seal resistance, (2) determine the firing threshold of the cell, (3) monitor the seal resistance and the resulting action potential throughout the experiment, (4) adjust the stimulus current to take into account changes in the seal resistance.

(a)

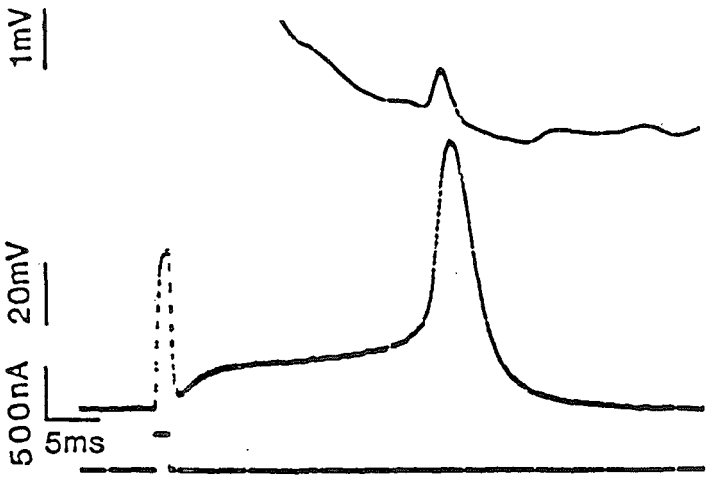

(b)

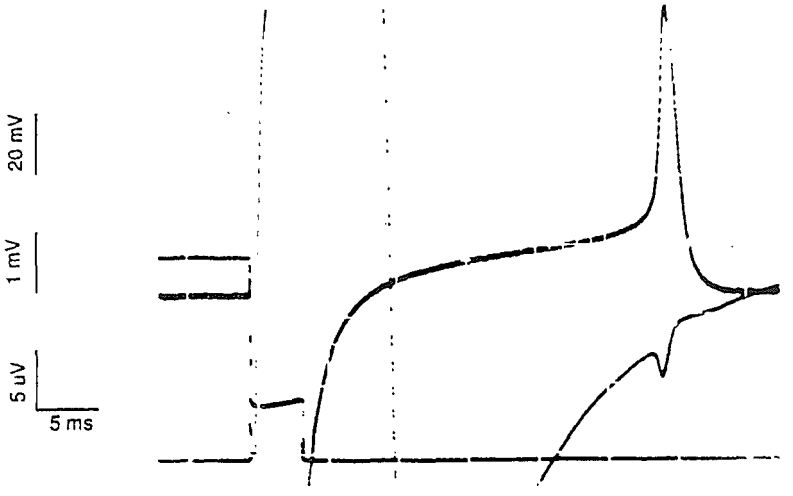

Figure 6.8. (a) A current pulse of duration 0.5 msec passed through a dish electrode stimulates a cell. The same dish electrode is used to record the resulting action potential, and an intracellular electrode is used to verify the response. (b) A current pulse passed through one dish electrode stimulates the cell, and another dish electrode is used to record the resulting action potential. An intracellular electrode is used to verify the response.

References

[1] C. A. Thomas, Jr., P. A. Springer, G. E. Loeb, Y. Berwald-Netter, and L. M. Okun, "A miniature microelectrode array to monitor the bioelectric activity of cultured cells," *Exp. Cell Res.*, vol. 74, pp. 61–66, 1972.

[2] J. Pine, "Recording action potentials from cultured neurons with extracellular microcircuit electrodes," *J. Neurosc. Methods*, vol. 2, pp. 19–31, 1980.

[3] G. W. Gross, A. N. Williams, and J. H. Lucas, "Recording of spontaneous activity with photoetched microelectrode surfaces from spinal cord neurons in culture," *J. Neurosc. Methods*, vol. 5, pp. 13–22, 1982.

[4] D. W. Tank, C. S. Cohan, and S. B. Kater, "Cell body capping of array electrodes improves measurements of extracellular voltages in micro–cultures of invertebrate neurons," *IEEE Conference on Synthetic Microstructures, Airlie, Virginia*, 1986.

[5] D. A. Israel, W. H. Barry, D. J. Edell, and R. G. Mark, "An array of microelectrodes to stimulate and record from cardiac cells in culture," *American Physiological Society*, pp. H669–H674, 1984.

[6] Rayburn,H., J. Gilbert, C-B .Chien, and J. Pine, Noninvasive techniques for long term monitoring of synaptic connectivity in cultures of superior ganglion cells, *Soc. of Neurosci. 14th Annual Meeting*, Abstract 171.1, 1984.

[7] Chien, C-B., W. D. Crank, J. Pine. Noninvasive techniques for measurement and long–term monitoring of synaptic connectivity in microcultures of sympathetic neurons, *Soc. of Neurosci. 17th Annual Meeting*, Abstract 393.14, 1987.

Chapter 7

Future Work

Using both the diving-board electrode and multielectrode dishes it is possible to establish a chronic two-way electrical connection to cultured neurons. There are many experiments that could be conducted with the devices in their present form, and by improving device performance the range of experiments would be increased significantly. Such integrated-circuit techniques will allow many experiments to be conducted that are difficult or impossible using what is now conventional technology.

7.1 Future Experiments with Diving-Board Electrodes

There are several obvious ways in which diving-board electrodes might be improved. By increasing the seal resistance, whole-cell intracellular connections could be obtained. Preliminary experiments should be performed using glass patch electrodes of the appropriate diameter, since diving-board electrodes are valuable and difficult to work with. The first step is to insure that the device and the cell surface are extremely clean. The next step is to treat the surface to make it "stickier". Once large seal resistances are obtained using glass electrodes without suction, diving-board electrodes can be used. Also, the manipulation and gluing procedure could be improved: the manipulator could be made smaller, with a better release mechanism; the contact between the electrode wire and the wire mounted to the dish could be made more reliably. Such improvements to the diving-board electrode should make it an attractive tool for researchers interested in long-term communication with cultured neurons.

Even without the ability to obtain intracellular connections, there are many experiments that can be done with diving-board electrodes that involve moni-

toring spontaneous activity and long-term stimulation. Dishes are easier to use, with performance comparable to diving-board electrodes, for large invertebrate neurons. This is not the case with vertebrate neurons: diving-board electrodes offer improved signal-to-noise, as well as the ability to record the evoked action potential with the stimulating electrode. Long-term electrical connections to cultured SCG neurons should be demonstrated, leading to long-term stimulation experiments on small systems of neurons.

7.2 Future Dish Experiments

Dish fabrication and dish electronics have progressed to the point where many experiments can be performed using cultured invertebrate neurons. Using multielectrode dishes facilitates stimulating either the processes or the cell body through a "sealed" electrode, and long-term recording of action potentials.

An example of experiments employing dishes is to study the collective behavior of small networks composed of identified *Aplysia* neurons. First, determine if stereotypical patterns of connections develop, and if so what the attributes of these connections are. Second, observe the effect of imposed activity on the system. Once the capability of long-term stimulation and recording has been established, connection strengths between neurons comprising a simple network can be mapped. Each cell in the culture will be stimulated by dish electrodes to fire an action potential, and the response of other neurons recorded with the array. Dish electrodes can also be used to monitor spontaneous activity of the nervous network. If dish electrodes fail to provide sufficient signal-to-noise ratios to resolve subthreshold signals voltage-sensitive dyes can be used to measure the resulting monosynaptic potentials from all the other cells. Using such dyes action potentials can be recorded without signal averaging with signal-to-noise ratios of 40:1 [2], indicating that subthreshold activity can be easily resolved.

Aplysia neurons are particularly suited to this study for four reasons. First, extensive work has been done using these neurons to study cellular mechanisms of learning [1]. Associative learning, activity–dependent facilitation, Hebbsian learning, sensitization, and habituation have all been studied in this preparation. Second, the neurons are large and technically easier to work with than vertebrate neurons. Third, preliminary results indicate that voltage sensitive dyes can be used to map the connection strengths of a system of such neurons, and extracellular electrodes can be used for long–term stimulation. Fourth, spontaneous activity can be continuously monitored, and the activity correlated with the connection strengths between the neurons.

Experiments similar to those proposed here are currently being performed using SCG's [3],[4]. These results indicate that mapping of small systems of neurons using voltage-sensitive dyes is an effective technique. Using cultured *Aplysia* neurons will provide several advantages over this vertebrate preparation including: larger signal-to-noise ratios using voltage sensitive dyes, the ability to easily record spontaneous activity using dish electrodes, the ability to stimulate the cell body and avoid complications associated with stimulating the processes, and more robust cells that are more convenient for conventional physiology.

7.3 Future In Vitro Applications of Microdevices

In addition to the diving-board electrode and multielectrode arrays, many types of devices could be fabricated and used for *in vitro* physiology using integrated circuit technology.

The dish structure could be modified to enhance electrode performance. One way is to confine neurons to wells as shown in Figure 7.1 (b). Neurons are placed in wells when they are young, growing to fill the well and seal to the electrode, with the forces exerted by the processes unable to pull the neuron

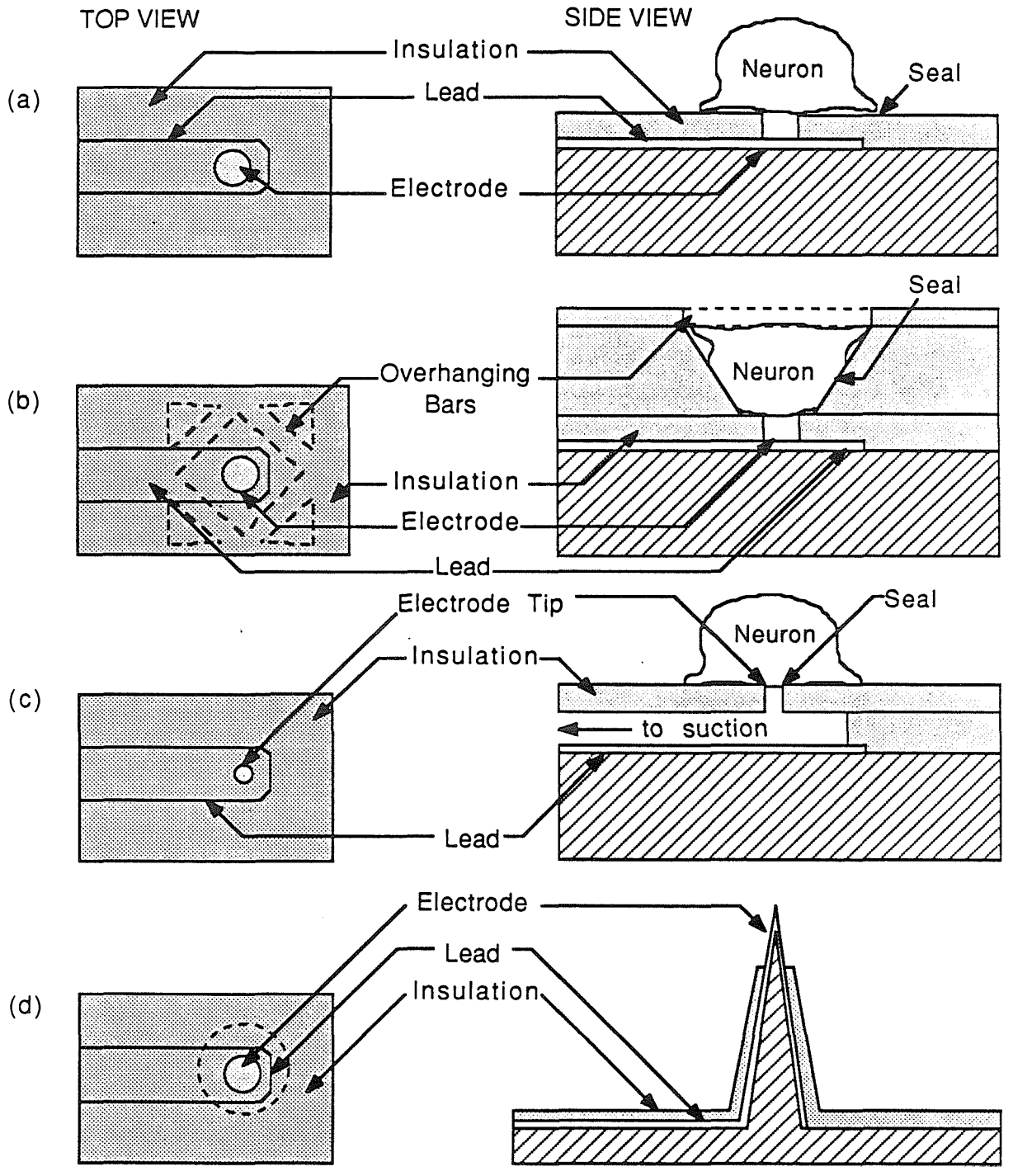

Figure 7.1. (a) Standard dish electrode (b) Cells in wells (c) Dish electrode capable of providing suction (d) spike electrodes to record from a slice.

away from intimate electrode contact [5],[6]. Techniques developed to improve seals to diving-board electrodes can be applied to well electrodes.

One serious limitation to both diving-board electrodes and dish-electrodes is the inability to provide suction to obtain a gigaohm seal. This problem could be overcome by building a special dish with hollow channels leading to the electrode sites as shown in Figure 7.1 (c). Suction could be applied through this tube, facilitating chronic whole-cell recording from many cells simultaneously. There are problems that must be overcome. First there is a conflicting surface requirement: while the surface to which the seal must be made should ideally be very clean, it is usually necessary to coat the dish with substances such as polylysine and collagen in order to get good outgrowth and healthy cells. Second, dializing the interior of the cell limits the duration of whole-cell recording. While appropriate choice of solution in the patch pipette helps to alleviate this problem, it doesn't solve the problem entirely. Once these problems are overcome such a device has great potential for providing more sensitive connections than can be obtained with conventional dishes.

Another application of the arrays is to stimulate and record from brain slices. Slices are typically prepared by dissecting out a brain, and cutting it into 500 μm thick sections, which are placed in tissue culture dishes. Such preparations offer the advantage of maintaining architecture found in the brain, while allowing manipulation of the biochemical environment and increased flexibility. While the prospect of using dishes to record from and to stimulate slices is attractive it is extremely difficult: cells within 50 μm of the surface are typically dead in slices, and anything of interest is located well away from the surface of the dish. What is needed is an array of electrodes sticking up into the slice, as is shown in Figure 7.1 (d) that could be manufactured using integrated circuit technology.

7.4 Impact of Integrated-Circuit Based Microdevices on Neurobiology

What would it take for these microdevices to have an impact on neurobiology, and to become a standard tool? First, their usefulness must be demonstrated. Second, the devices must be made available to the neurobiologists who want to use them.

Once fabrication and gluing procedures have been improved and further studies have been made demonstrating the general usefulness of the diving-board electrode, making this device widely available will be a problem, since the fabrication procedure requires equipment and expertise well beyond the limits of most neurobiology labs. Somehow the laboratory developing the technology must make the devices available. Since it takes about 80 hours to fabricate 100 devices it is unreasonable to expect one lab to supply devices to more than several other labs. One solution is to supply partially fabricated devices, and have fabrication completed in the labs where they are to be used. By supplying wafers after they have been wire bonded but before they have been etched, no special facilities would be required other than a fume hood for the EDP. In this way a fabrication facility could easily supply enough bonded wafers to meet the needs of many labs.

While multielectrode dishes have been used since 1972, and their usefulness has been demonstrated, technical barriers prevent widespread use: the devices are not generally available to researchers; and the electronics for recording from many electrodes simultaneously, while not particularly sophisticated, must be custom made. Only a few very "high tech" groups are prepared to invest the time, money, and resources to develop such a system.

Two ways to make this technology generally available are: to have such groups supply the dishes, with those wanting the dishes paying for them; or

else once a market is established to have private enterprise take over device and electronics production.

In the near future devices made utilizing integrated circuit technology will make considerable contributions to neurobiology.

References

[1] Abrams,T.W., "Cellular studies of an associative mechanism for classical conditioning in *Aplysia*," in *Model Neural Networks and Behavior*, A. S. Selverston ed., 1985.

[2] B. M. Salzberg, Private Communication, 1987.

[3] Rayburn,H., J. Gilbert, C-B .Chien, and J. Pine, "Noninvasive techniques for long term monitoring of synaptic connectivity in cultures of superior ganglion cells," *Soc. of Neurosci. 14th Annual Meeting*, Abstract 171.1, 1984.

[4] Chien, C-B., W. D. Crank, J. Pine. "Noninvasive techniques for measurement and long–term monitoring of synaptic connectivity in microcultures of sympathetic neurons," *Soc. of Neurosci. 17th Annual Meeting*, Abstract 393.14, 1987.

Appendix

Detailed Diving-Board Electrode Fabrication Procedure

Diving board electrodes are fabricated using integrated circuit technology, and micromachining. Figure A.1 shows the five masks used in the fabrication.

1. Clean wafers. Use < 100 > orientation silicon wafers with any doping but p^{++}.

a. 5 minute ultrasonic clean in trichloroethylene (TCE).
b. 5 minute ultrasonic clean in acetone.
c. 5 minute ultrasonic clean in ethanol.
d. 5 minutes in running water.
e. 5 minute clean in 3 parts sulfuric acid 1 part hydrogen peroxide (Piranha etch).
f. 5 minutes in running water.
g. 5 minutes in buffered HF.
h. Rinse in water and blow dry.

Wafers are cleaned in TCE, acetone, and in ethanol to remove organic contaminants. Then the surface of the wafer is oxidized in the sulfuric acid, hydrogen peroxide mixture. This surface oxide layer is removed in buffered HF, exposing fresh silicon. After briefly rinsing in water the wafer should be hydrophobic, indicating a very clean surface.

2. Cup

a. Grow 0.2 μm thick oxide: 15 minutes in steam 1100°C.
b. Take directly from furnace, allow to cool and spin on 1400–37 photoresist at 4000 rpm.
c. Pattern cup mask 85 mJ/cm^2.
d. Develop in *Shipley* 455 developer for 1 minute.
e. Hard bake for 30 minutes at 125°C.
f. 2 minute clean in O_2 plasma.

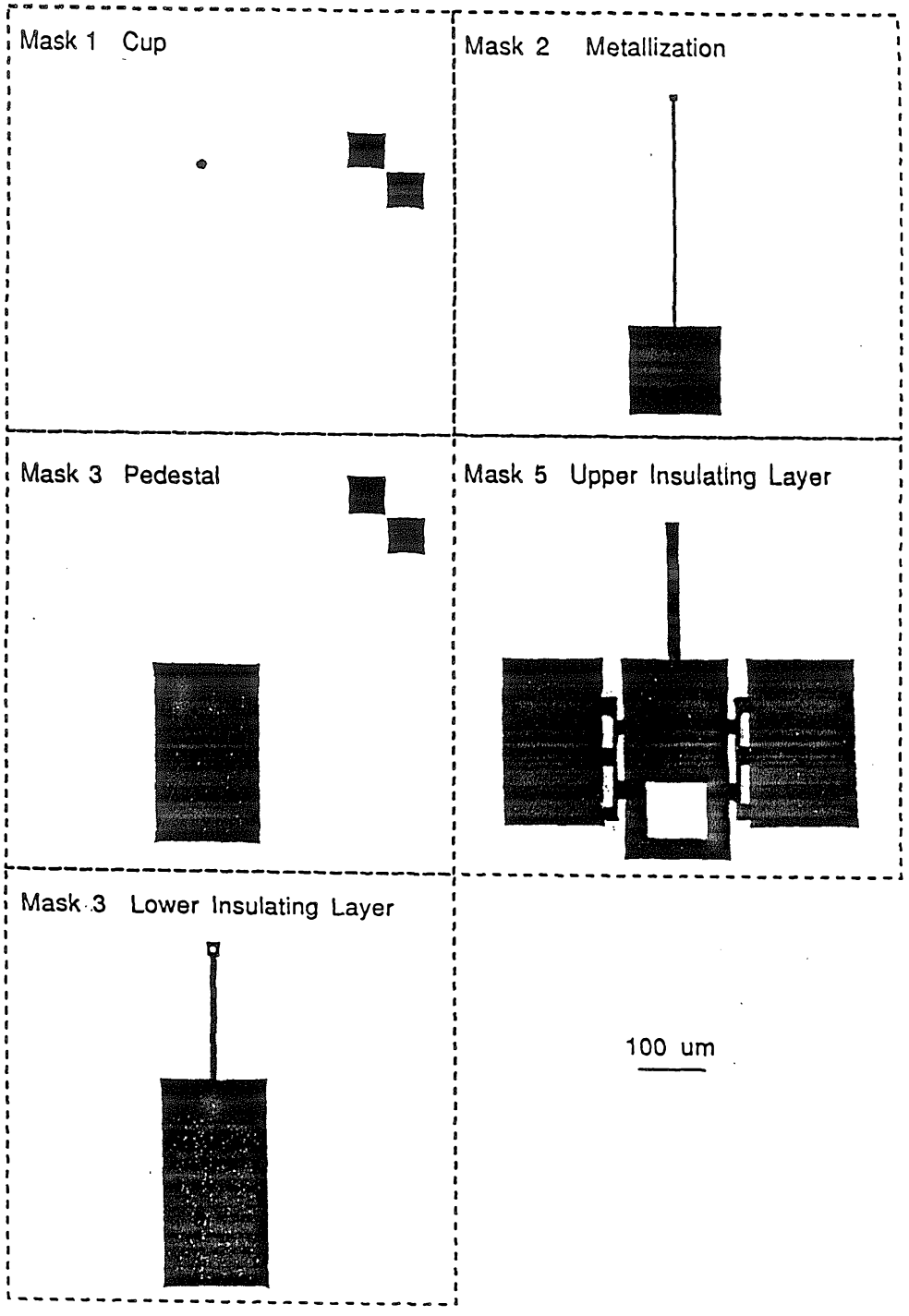

Figure A.1. The five masks used in the fabrication of diving board electrodes.

g. Etch in buffered HF for 3 minutes.

h. Remove photoresist in acetone, ethanol, water.

i. Etch for in 3 minutes in 100 parts HNO_3, 100 parts CH_3COOH, and 15 parts HF [1].

j. remove masking oxide: etch in buffered HF for 3 minutes.

k. As in Figure A.2 measure the diameter of the overhanging layer of oxide d_2 and the diameter of the silicon cup d_1 to determine the depth of the cup, $d_{cup} = (d_1 - d_2)/2$.

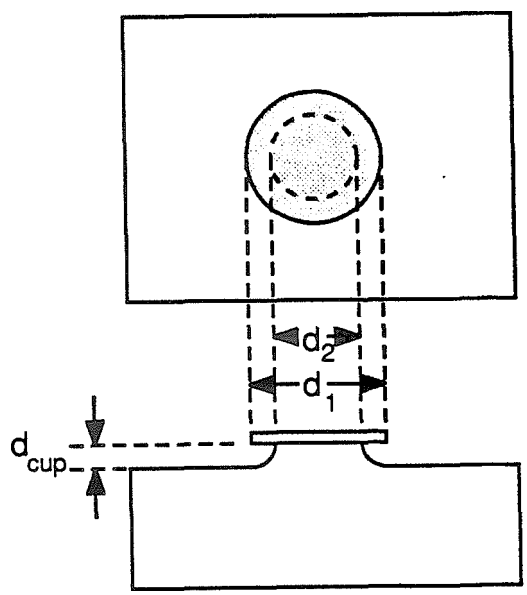

Figure A.2. Schematic view of the cup.

The cup is etched in silicon to a depth of 3 μm. An isotropic etch is used to make the resulting cup as circular as possible, with no sharp corners that would tend to reduce the seal resistance. It was necessary to use thermal SiO_2 [2,3] to mask the etch since no commonly available photoresist could stand up to any isotropic silicon etch well enough to etch a 3 μm deep cup. The oxide mask also made it easy to accurately determine the depth of the cup. By measuring the diameter of the masking oxide d_1 and the diameter of the top of the cup d_2 as in Figure A.2, the depth of the cup can be easily determined, $d_{cup} = (d_1 - d_2)/2$.

3. Pedestal.

a. Grow 1 μm thick oxide: 3 hours in steam 1100°C.
b. Spin on 1400-37 photoresist for 30 seconds at 4000 rpm.
c. Soft bake for 30 minutes at 85°C.
d. Pattern pedestal: 85 mJ/cm^2. Use the alignment marks to correctly orient the mask.
e. Develop in *Shipley* 455 developer for 1 minute.
f. Hard bake 30 minutes at 125°C.
g. Buffered HF etch for 12 min, rinse, and dry.
h. Dry in 130°C oven for 5 minutes.
i. Boron diffusion 16 hours 1180°C, O_2 100 sccm N_2 2000 sccm.
j. Boron Nitride Preparation: Clean and dry wafers as per data sheet [4], oxidize for 30 min at 1100°C. Set to desired temperature and gas flow and allow to stabilize for 12 hours before beginning diffusion. Take wafers out and set to 1100°C with oxygen at 200 sccm allow to stabilize and oxidize the surface for 1 hour.
k. Remove boron glass: 20 minutes buffered HF etch.

The pedestal is defined by a boron diffusion, since silicon doped to levels of greater than 5×10^{19} cm^{-3} is etched very slowly by EDP. The pedestal should be at least 10 μm thick, therefore a very deep boron diffusion is necessary. The diffusion is carried out at the highest temperature that is practically possible with a quartz furnace (1180°C) so that the diffusion coefficient of boron in silicon is as large as possible. Oxidized boron nitride wafers are used as the boron dopant [5]. Since boron diffuses much faster in heavily boron doped silicon [6] than in intrinsic silicon, a pedestal 12 μm thick requires a diffusion time of only 10 hours. By carrying out the diffusion at such high temperatures for such long periods of time the solid solubility of boron in silicon is exceeded; resulting in a distinctive surface. The depth of the diffusion can be estimated by measuring the distance to the faint line seen in the surface of the silicon, after the diffusion.

When doing a boron diffusion a layer of boron glass forms on the surface of the silicon. To remove this layer it must first be oxidized so that it can then removed in buffered HF along with the masking oxide.

4. Define lower insulating layer

a. Grow 1000 Å thick SiO_2 layer: 10 minutes 1000°C in steam.
b. Spin on 1400-37 photoresist for 30 seconds at 4000 rpm.
c. Soft bake for 30 minutes at 85°C.
d. Pattern pedestal: $85\,mJ/cm^2$.
e. Develop in *Shipley* 455 developer for 1 minute.
f. Etch for 2 minutes in buffered HF.
g. Remove photoresist: 5 minutes acetone, 5 minutes ethanol, 5 minutes running water, blow dry, and 2 minutes oxygen plasma.

The lower SiO_2 insulating layer is a high quality insulator that is etched at less than 100 Å/hour in EDP and provides a pinhole free, high quality glass surface with which to contact the cell. It is desirable to have as much of the top of the cup etched as possible to reduce the electrode impedance. This is simplified since the resist is thinner on the top of the cup so that only a very small exposure is required to completely etch the top of the cup. There is a limit on the thickness of this layer. As a layer of oxide is grown boron at the surface of the wafer tends to segregate into the oxide layer, reducing the concentration of boron in the surface layer of silicon. For long oxide growths the surface concentration of boron is low enough that the silicon is no longer protected from the EDP etch, and the pedestal is attacked.

5. Define conducting layer.

a. Evaporate 100 Å Cr, 800 Å Au, 100 Å Cr.
b. Pattern contact lead with 1400–37 photoresist.
c. Clean in O_2 plasma for 2 minutes.
d. Etch:*Transene chrome etch* 15sec, *Transene gold etch*:water(4:1) 30 sec, *Transene chrome etch* 15sec.
e. Remove photoresist and clean.

The conducting layer is defined with an etch since adhesion of the conducting layers was consistently better than with a liftoff. Since gold does not stick well to oxides chrome was used as an adhesion layer. The chrome oxidizes and sticks well to the silicon dioxide. If the gold is evaporated on to chrome that has not been oxidized it alloys and sticks. However, chrome oxidizes very easily so that the evaporation must be carried out at a low pressures (less than $2 \times 10^{-6} torr$).

Evaporation conditions are kept as similar as possible to keep the film stress and etching properties reproducible.

The chrome layers are etched in 9 parts cerric sulfate, 1 part HNO_3 [7], and the gold layer is etched in a solution of 400 g KI, 100 g I_2, and 400 ml of water diluted with water 1:4 [8].

6. Define top insulating layer.

a. Deposit 1.5 μm oxinitride: $NH_3/N_2O/SiH_4$ (flow rate 750/1150/250 sccm) are reacted at 300°C at a pressure of 2.0 torr and a power density of 11.7 mW/cm−2.
b. Spin on AZ 4770 photoresist for 30 seconds at 4000 rpm.
c. Soft bake for 100 minutes at 85°C.
d. Pattern pedestal: 400 mJ/cm^2.
e. Develop in AZ developer for 4 minutes.
c. Plasma etch: O_2/65 mtorr, CF_4/340 mtorr, net power 80 watts, for 70 minutes.
d. Remove photoresist and clean wafer.

The oxinitride layer is deposited using plasma enhanced chemical vapour deposition [9], [10]. This allows the deposition of a film with a well defined, selectable stress, at temperatures low enough to prevent undesirable alloying of the chrome with the gold. The silicon oxinitride layer is etched in the O_2, CF_4 plasma [11]. Etch completion can be determined by the rough surface of the etched silicon and the removal of the upper chrome layer on the bonding pad as seen in Figure A.3.

7. Make wire connections to each device.

a. Scribe the wafer and glue to a microscope slide, along with a gold pad for the other end of the wire bond. Use RTV and allow to cure for at least 24 hours before etching.
b. Wire bond with 25 μm gold wire: use *Westbond* ultrasonic wirebonder with power and time set to maximum. Only wire bond those devices that pass optical inspection.

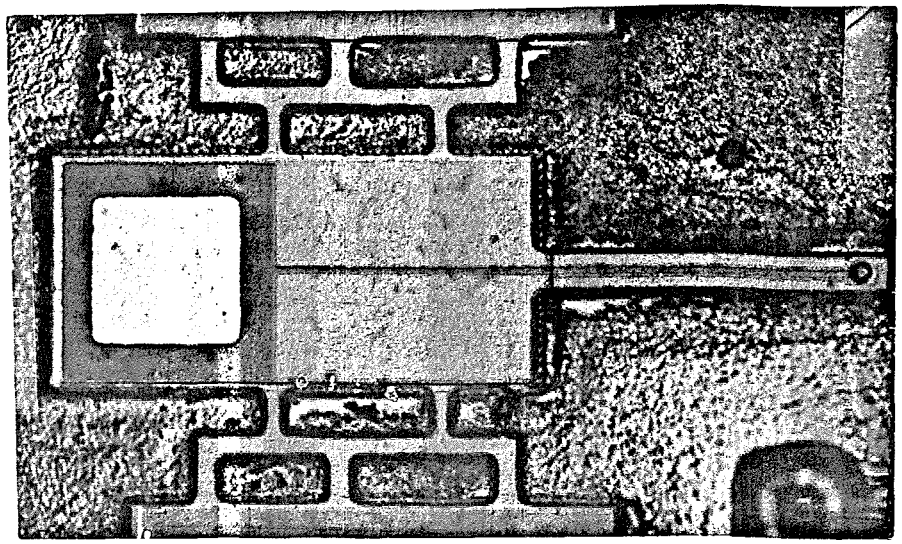

Figure A.3. Wafer after the oxinitride layer has been plasma etched.

Wire bonding is done with gold wire that will stand up to the EDP. The wire sticks well to clean gold, but sticks poorly or not at all to other surfaces.

8. Free the devices.

a. Dip in buffered HF diluted 3:1, and rinse in water.
b. EDP 100°C for 3 hours.
c. Rinse successively in clean beakers of water.
d. Dry in 85°C oven.
e. Inspect under optical microscope and discard any defective devices.

The wire-bonded wafers are cleaned of their native oxide and then the silicon is etched out from beneath each device [12,13]. At this point the devices are held to the wafer only by temporary grill work. Great care must be taken not to damage the devices. They must be cleaned in successive water baths.

9. Insulate the wire and wire bond.

a. prepare polyimide tube
b. using number 3 tweezers load each device into a tube, putting the wire through first, and then pulling the wire through from the other end.
c. bend the pedestal to make a 60 degree angle with the polyimide tube.
d. use a drop of negative photoresist to insulate the wire bond.

e. bake for at least 4 hours at 150°C

Special holders facilitate quick and easy loading of the polyimide tube and insulation of the wire bond. The polyimide tubes are temporarily held in place by photoresist.

10. Platinize and test.

a. Etch: *Transene chrome etch* 1 minute.
b. Measure electrode impedance.
c. Platinized in a solution of 1% chloroplatinic acid in 0.0025% HCl, plus 0.01% lead acetate, using a current density of $20\,\mathrm{mA/cm^2}$ for 10 seconds.
d. Measure electrode impedance.

For an exposed area of $20\,\mu\mathrm{m}^2$ the impedance in saline at 1000 kHz is 25 megohms [14]. This value can be reduced to about 500 kilohms, by electroplating with platinum.

References

[1] B. Schwartz and H. Robbins, "Chemical etching of silicon, IV. The system HF, HNO_3, $HC_2H_3O_2$, *J. Electrochem. Soc.*, vol. 106, p. 505, 1959.

[2] L. E. Katz,"Oxidation," in *VLSI Technology*, ed. S. M. Sze, p. 194, 1983.

[3] A. S. Grove, *Physics and Technology of Semiconductor Devices*, Wiley, New York, 1967.

[4] Sohio Carborundum PDS Planar Diffusion Sources: Technical Information, 1986.

[5] D. Rupprecht. and J. Stach, "Oxidized boron nitride wafers as an *in situ* boron dopant for silicon diffusions," *J. Electrochem. Soc.*, vol. 120, no. 9, pp. 1266–1271, 1973.

[6] J. Stack, and A. Turley, "Anomalous boron diffusion in silicon from planar boron nitride sources," *J. Electrochem. Soc.*, vol. 121, no. 5, pp. 722–724, 1974.

[7] R. Glang and L. V. Gregor, "Generation of patterns in thin films," in *Handbook of Thin Film Technology*, ed. L. I. Maissel and R. Glang, McGraw-Hill Book Company, New York, p. 7–36, 1970.

[8] R. Glang and L. V. Gregor, "Generation of patterns in thin films," in *Handbook of Thin Film Technology*, ed. L. I. Maissel and R. Glang, McGraw-Hill Book Company, New York, p. 7–37, 1970.

[9] W. R. Snow, "PWS 450 COYOTE: A vertical parallel plate plasma reactor for silicon nitride deposition," Pacific Western Systems Application Note, March 1981.

[10] T. Sugano, *Applications of plasma processes to VLSI technology*, John Wiley & Sons Inc., New York, 1985.

[11] C. M. Melliar–Smith and C. J. Mogab, "Plasma assisted etching techniques for pattern deliniation" in *Thin Film Processes*, ed. J. L. Vossen and W. Kern, Academic Press, New York, pp. 497–552, 1978.

[12] R. M. Finne, and D. L. Klein *J.Electrochem. Soc.*, "A water amine complexing agent system for etching silicon," vol. 114, pp.965–970, Sept. 1967.

[13] A. Reisman, M. Berkenblit, S. A. Chan, F. B. Kaufman, and D. C. Green, "The controlled etching of silicon in catalyzed ethylenediamine-pyrocatechol-water solutions," *J. Electrochem. Soc.*, vol. 126, no. 8, pp.1406–1415, 1979.

[14] R. C. Gesteland, B. Howland, J. Y. Lettvin, and W. M. Pitts, "Comments on microelectrodes," *Proc. IRE*, vol. 47, pp. 1856–1862, 1959.